UNIVERSITEIT VAN PRETORIA
UNIVERSITY OF PRETORIA
YUNIBESITHI YA PRETORIA

Characterisation and optimisation of the Zincor iron removal process

by

Johann Ockert Claassen

Submitted in partial fulfillment of the requirements of the degree

Master of Engineering

in the
Department of Materials Science and Metallurgical Engineering, University of Pretoria,
Pretoria, South Africa

February 2002

UNIVERSITEIT VAN PRETORIA
UNIVERSITY OF PRETORIA
YUNIBESITHI YA PRETORIA

Characterisation and optimisation of the Zincor iron removal process

by

Johann Ockert Claassen

Supervisor:
Prof. RF Sandenbergh
Department of Materials Science and Metallurgical Engineering, University of Pretoria
Pretoria

Abstract:

As one of the most abundant elements on earth, iron is nearly always present in metal concentrates. This is specifically true for zinc sulphide concentrates, which can contain up to 18% iron (marmatite). Today more than half of these concentrates are treated in hydrometallurgical- or combined hydrometallurgical-pyrometallurgical circuits. In hydrometallurgical circuits, iron is solubilised (either in a roast-leach-, a direct leach- or bacterial leach circuit) along with zinc and must be removed from the zinc-rich solution before the electrowinning- or solvent extraction step. Various iron removal processes were developed to address the iron problem in hydrometallurgical circuits. The better known of these include the jarosite-, goethite- and hematite processes also used in the zinc industry.

Zincor (Zinc Corporation of South Africa) patented an iron removal process (Zincor Process), which was generally considered to be very similar to the so-called "para-goethite" iron removal process used only in two other zinc smelters notably Porto Vesme (Italy) and Pasminco Hobart (Tasmania). However, since the Zincor Process was patented in 1976, various changes have been made such as a change from a batch parallel to a continuous series process, a change in precipitation pH-profile and the introduction of a pH controlled acid wash in the second tank.

The introduction of a weak acid leach step and vacuum belt filters at Zincor's residue treatment plant in the near future and an iron removal process that is not clearly understood, necessitated this further study of the Zincor iron removal process. The study has been conducted in three parts. The first part of the study has focused on the characterisation of the Zincor iron residue and the Zincor process. The second part of the study has been concerned

with the definition of an optimum operating window in terms of the filterability of the residue and the third part investigated the use of neutralisation reagents other than zinc calcine to control the pH during iron precipitation.

The distribution of iron in the Zincor iron precipitate, which usually contains between 35% and 40% iron, has been found to be as follows: approximately 45% as schwertmannite, 5% as ferrihydrite, 20% as jarosites, 25% as franklinite, trace amounts of pyrite as well as 5% of an unknown phase. This confirmed that goethite is not present in the Zincor iron residue and that iron is mainly removed in the form of amorphous intermediate iron phases such as schwertmannite and ferrihydrite. Of these two phases, schwertmannite was the least expected as most work up until now were done on samples taken from natural environments. The following description of the conditions that promote iron removal, mainly as schwertmannite, is viewed as an expansion of the available literature data, which was gathered at ambient conditions. In terms of the main operating parameters, optimum filterability was achieved under the following conditions: pH of 3.0, temperature as high as possible (70°C) and at least 25 kg/m^3 seeding. A retention time of at least 4 hours at a pH of 3.0 and 60°C was required, which decreased by more than 50% at a temperature of 70°C.

As these conditions mainly impact on the soluble zinc loss encountered during iron removal, an effort was made to further reduce the insoluble zinc loss, which is the inherent weakness in the Zincor process, and similar processes where zinc calcine is used for pH control, by investigating the use of alternative neutralisation reagents. This study showed that iron can be successfully removed with $Ca(OH)_2$, a basic zinc sulphate and zinc oxide mixture as well as chemically precipitated $CaCO_3$

produced in the paper and pulp industry. Of these alternatives, $CaCO_3$ appeared to be the most promising, with filtration rates an order of magnitude higher than the zinc oxide options (calcine and basic zinc sulphate mixture), due to better overall economics than with the use of $Ca(OH)_2$. Utilisation $CaCO_3$ as an alternative neutralisation agent might increase the overall zinc recovery figure at Zincor by up to 1.5%.

Based on the findings, it can be concluded that the Zincor process in its current form has a very distinct character compared to what was historically considered to be the very similar patented para-goethite iron removal process, as practiced at the Porto Vesme and the Pasminco Hobart hydrometallurgical zinc plants.

Keywords: hydrometallurgy, zinc, iron, precipitation, leach, silica, para-goethite, jarosite, schwertmannite, spectroscopy.

Acknowledgements:

I'm extremely grateful to the MD of Zincor, Ewald Meyer for the opportunity I was given to study the Zincor Process. It was mainly because of Ewald's vision and encouragement that momentum was never lost. I would also like to extend my gratitude to Zincor for the financial support I received and the permission granted to publish the results.

One of the most enjoyable parts of this study was to have met so many new people who all contributed to this work. This group of people included John Rennie and Gavin Howard who gave me a lot of technical support; Joao Fernandez and his team who always had time to do an excellent job with my samples; Leonie Reyneke who assisted with the XRD analysis; Dr. Tom van Moltke and his team, which included Robert Ehlers (XPS) and Carel Coetzee (SEM) who rendered a service of the highest quality; Linda Prinsloo (FT-IR Spectroscopy); Prof. Sylvia Paul (Raman Spectroscopy); Dr. Giovani Hearn and Dr. Antoine B-Mulaba (MES) who spent many hours to help solve the puzzle; Willem van der Merwe who assisted with supplying the equipment for the experimental work; Geoff Bernard who developed the control system for the mini-plant; Jaco Vermaak and Dirk Odendaal who did the Malvern particle analyses.I would especially like to thank Dr. Nanne Vegter who supplied me with a lot of literature and Prof. Roelf Sandenbergh, my mentor, for his valued support and inputs. With this work, I also want to recognize the work done by the pioneers of the Zincor process and the people who came after them for the role they have played to make it a success.

I would also like to take this opportunity to thank my family for their support and specifically my wife who stood by me over the past two years.

List of contents Page

1 INTRODUCTION

1.1 Iron in zinc hydrometallurgy

As one of the most abundant elements on earth, iron usually ends up in many beneficiated materials. This is also true in the zinc industry with zinc concentrates that can contain between 3% and 18% iron [Chen and Cabri, 1986]. Concentrates from various sources with varying iron contents are usually blended to make up the feed to the roasting section in the case where sphalerite is the main source of zinc. Under these conditions, the iron content typically varies between 2% and 10%. Table 1 shows typical values for iron in some of the concentrates treated at Zincor.

Table 1: Typical analyses of some Zincor concentrates [Internal Zincor Report, 2000].

ELEMENT/ CONCENTRATE	BLACK MOUNTAIN	IMCOR	PERING	MARANDA
	(%)	(%)	(%)	(%)
Zn	49.23	52.2	57.34	53.82
Cu	0.56	0.53	0.14	1.32
Cd	0.17	0.13	0.09	0.12
Pb	4.45	3.12	4.37	0.06
Fe	9.3	4.62	2.19	8.92
Ag	0.009	0.007	0.005	0.004
Co	0.044	0.0004	0.0006	0.014
Mn	0.66	0.38	0.10	0.04
Mg	0.05	0.77	0.46	0.09
S	30.1	28.84	30.45	32.37
SiO_2	2.77	1.82	0.56	1.76
Ca	0.07	1.37	0.77	0.1
Total	**97.41**	**93.79**	**96.48**	**98.62**

The iron is in most cases associated with pyrrhotite, pyrite and chalcopyrite as can be seen in Table 2.

Table 2: Proposed mineralogy of some Zincor concentrates [Internal Zincor Report, 2000].

MINERALS/ CONCENTRATES	BLACK MOUNTAIN	IMCOR	PERING	MARANDA
	Mass fraction	Mass fraction	Mass fraction	Mass fraction
ZnS	0.733	0.777	0.854	0.802
PbS	0.051	0.036	0.050	0.001
FeS	0.139	0.029	0.033	0.122
FeS_2	0.000	0.050	0.000	0.000
$CuFeS_2$	0.016	0.015	0.004	0.038
CdS	0.002	0.002	0.001	0.002
MnS	0.010	0.006	0.002	0.001
$CaMg(CO)_3$	0.003	0.038	0.023	0.004
SiO_2	0.028	0.018	0.006	0.018
Total	**0.982**	**0.971**	**0.972**	**0.987**

During the roasting process, these sulphide minerals are converted to oxide minerals, which can be leached under atmospheric conditions at a temperature of 50°C and a pH of between 1.0 and approximately 4.0 in a typical roast-leach-electrowinning circuit. The primary leach step, which is referred to as the neutral leach step, also solubilises all the other simple oxides.

The neutral leach residues however can contain large amounts of zinc [Filippou and Demopoulos, 1992] *i.e.* up to 20% in Zincor's case. This refractory zinc was found to be associated with a mineral called franklinite or zinc ferrite, which is a zinc spinel with the ideal formula ZnO. Fe_2O_3 that forms during the roasting process [Graydon and Kirk, 1988].

In order to improve the zinc recovery, it was found that zinc ferrite could be dissolved in solutions containing more than 100 g/l H_2SO_4 at temperatures ranging from 90°C to 95°C within 2 to 4 hours [Ramachandra *et al.*, 1976]. This procedure, however, not only

dissolves the zinc but also the iron associated with it. Any iron precipitated in the neutral leach step is re-dissolved at the same time to give a zinc-rich process solution containing between 15 g/l and 30 g/l iron, mostly in the ferric form. The iron is subsequently removed from the zinc-rich solution generally by precipitating it as an oxide or a hydroxy salt. These processes will be discussed in more detail in Section 1.5. Other techniques utilised to control iron in hydrometallurgy are discussed elsewhere [Ritcey, 1986].

The presence of iron in zinc concentrates therefore, not only necessitates the incorporation of at least two extra processing stages (hot acid leach and solution purification), but it ultimately determines the amount of zinc that can be recovered. Utilisation of calcine for pH control in some iron removal processes contributes towards the lower zinc recoveries obtained in these plants. The influence of the amount of iron in the calcine on the amount of zinc that can be extracted for some of the iron removal processes are shown in Figure 1.

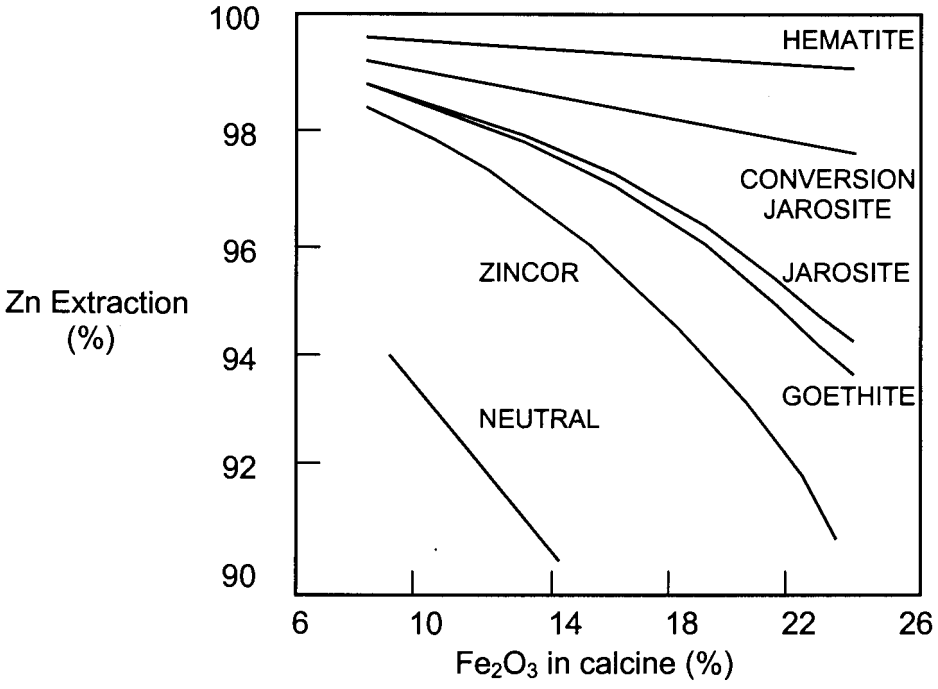

Figure 1: The influence of iron on zinc extraction for different iron removal processes [Van Niekerk and Begley, 1991].

Iron in hydrometallurgical zinc circuits also has positive effects specifically in terms of solution purification. It is known [Dutrizac, 1980] that the different iron precipitates contribute to the removal of significant amounts of impurities from the zinc-rich solution. This includes halides (fluoride and chloride) and cations such as arsenic, antimony, copper, nickel, manganese and cobalt. This phenomenon is generally used to great effect prior to the purification step during the precipitation of iron in the neutral leach stage. The incorporation of zinc in the crystal structure of jarosites, the adsorption of zinc species on the precipitate surface and the encapsulation of process solution by iron precipitates, however, can easily outweigh the above mentioned benefit.

Inclusion of halides and metal cations in the iron residue might also raise some concern from an environmental perspective and needs to be considered as part of the total iron removal process.

In recent times, direct leaching of concentrates at elevated temperatures and pressures as well as bacterial leaching [Takala, 1999; Hearne and Haegele, 1998] have gained momentum and might well become serious contenders in the hydrometallurgical zinc industry. In these processes zinc ferrites do not form, but significant amounts of iron are still solubilised that will require an efficient iron removal step.

From the above discussions, it must be clear that efficient removal of iron from the leach liquors is a critical step in the hydrometallurgical extraction of zinc from its ores.

1.2 Thermodynamics of iron removal

The production of crystalline iron precipitates is related to the thermodynamic and kinetic factors relevant to the dissolution and precipitation of iron species. Whereas the kinetics of a system specifically deals with the rate of the reactions, the thermodynamics defines the stability of the relevant species under a certain set of conditions. The conditions that determine the rate of the reactions and ultimately the stable product that forms are defined by, amongst other things, concentrations of various species in solution, pH, temperature and oxidation potential and their interrelationships.

In the paragraphs that follow, attention will be given to the stability of the relevant iron species (solution species and solid phases) under specific conditions before the factors that influence the rate of iron precipitation are enumerated.

A good starting point to form a basic understanding of the thermodynamics of iron removal is to study the relevant Pourbaix diagrams. These diagrams provide a convenient way to present the influence of electrochemical potential and pH on stability of species present in aqueous solutions. Pourbaix diagrams for the Zn – H_2O and Fe - H_2O systems are shown in Figures 2 and 3, respectively.

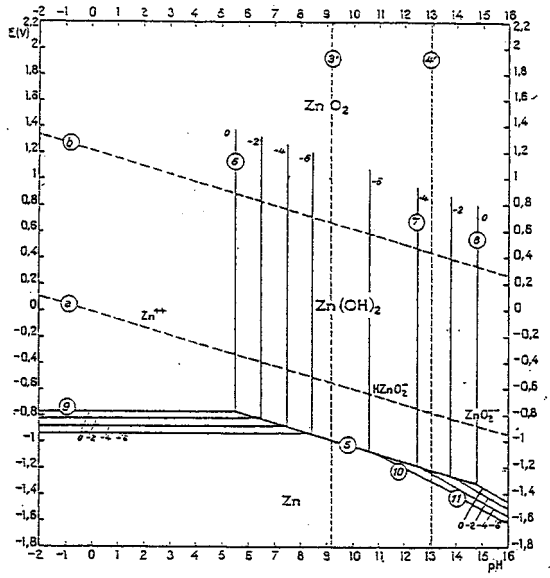

Figure 2: Potential/pH diagram of the Zn - H_2O system at 25°C [Pourbaix, 1974].

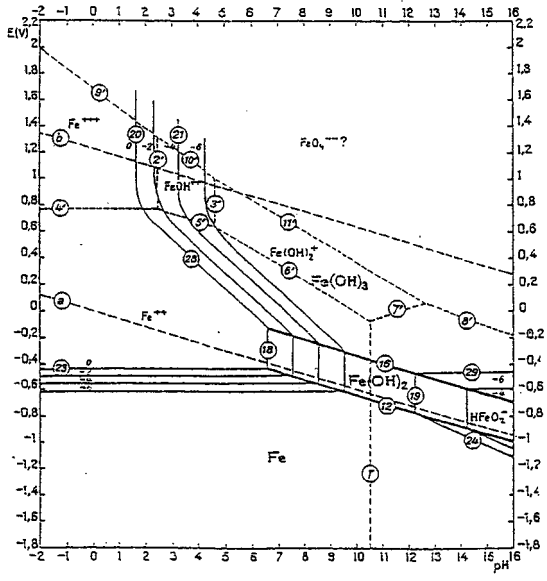

Figure 3: Potential/pH diagram of the Fe - H_2O system at 25°C [Pourbaix, 1974].

These two diagrams depict the simplest form of these diagrams as they only consider the respective metal ions in an aqueous environment. This is without a doubt an over-simplification when compared to the industrial conditions. It must be emphasised that these diagrams only apply to the metal water systems at equilibrium and do not indicate the influence of other species or metastable species or phases that may play an important role in practical processes.

Nonetheless, it sheds some light on a few basic concepts in iron removal. One of these concepts is that iron in its ferric form can be successfully separated from zinc bearing solutions by increasing the pH to approximately 2. It is therefore no surprise to see that most iron precipitates in the zinc industry are formed when hot iron solutions containing ferric iron are neutralised. Ferric iron, however, rarely occurs as such in aqueous solutions. Iron is usually present in the ferrous form, which is oxidised to the ferric form through the addition of air and/or manganese dioxide.

It is also evident from these figures that at the relatively low pH conditions encountered during iron precipitation in the zinc industry Zn^{2+}, Fe^{3+}, Fe^{2+} and the simple solution species $FeOH^{2+}$ and $Fe(OH)_2^{+}$ will be present. Another iron species, which predominates in more concentrated iron media (> 10^{-3}M ferric iron like in the HIS where no equilibrium solid iron phase is present), that was identified in synthetic solutions in the absence of sulphate, is $Fe_2(OH)_2^{4+}$, as indicated in Figure 4. These species, as well as others mentioned later, are believed to form the building blocks of the precipitates that eventually form [Dutrizac, 1980].

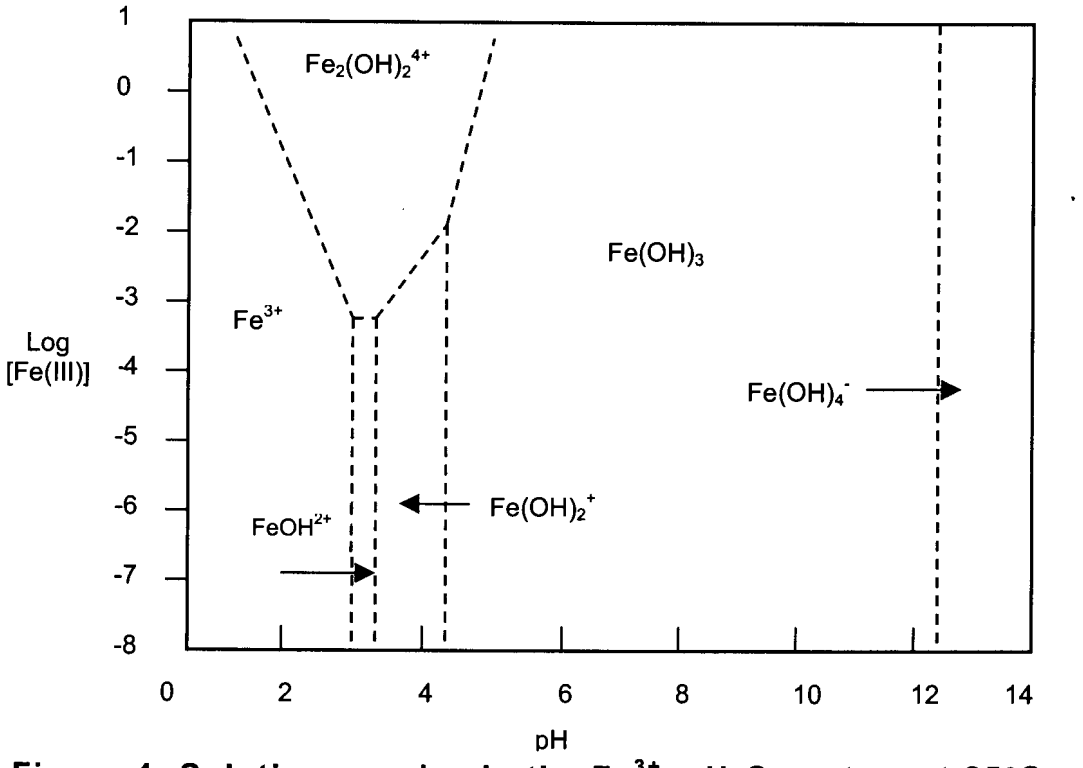

Figure 4: Solution species in the Fe^{3+} – H_2O system at 25°C [McAndrew *et al.*, 1975].

The region of interest to the zinc industry is at pH values between 1 and 4 and at ferric iron concentrations between 0.01 and 1M, where the dominant solution species were found to be Fe^{3+} and $Fe_2(OH)_2^{4+}$. These tests were conducted at ambient conditions and the question arises as to how an increase in temperature would influence the stability of these solution species. Sylva [1972] found that an increase in temperature improved the stability of $Fe_2(OH)_2^{4+}$ when the temperature was increased from 15°C - 51°C. When sulphate is added, these stability regions appear to change completely. A study by Ashurst and Hancock [1977] on dilute solutions containing ferric sulphate, showed that for the range of sulphate concentrations of relevance to the zinc industry (0.2 – 2.0M), the dominant species were Fe^{3+} and $FeSO_4^+$.

Other studies also indicated the presence of species such as $Fe(SO_4)_2^-$ [Magini, 1979] and bisulphate complexes [Lister and Rivington, 1975]. McAndrew *et al.* [1975] showed that the stability of bisulphate species increases with increasing temperature. This implies that bisulphate species might play an important role in iron removal processes in the zinc industry. The work by McAndrew assumed the absence of mixed hydroxyl – sulphate complexes, which might be an over-simplification in the light of the findings of Yakovlev *et al.* [1977] who indicated that species such as $Fe_2(OH)_2(SO_4)_2$ exist in sulphate solutions. These mixed species might well be the precursors of iron hydroxysulphate precipitates.

The role of some of the above mentioned charged species in iron precipitation is put into perspective when Stumm's surface adsorption theory [Stumm, 1992] is considered. At pH values below the pzc (point of zero charge), where the precipitated particles are positively charged, species such as $FeSO_4^+$ might well be more actively involved in iron precipitation. This would explain the formation of hydroxy salts at lower pH levels in the presence of sulphate. Furthermore, at pH levels above the pzc, OH^- in the form of $Fe(OH)_y^{3-y}$ is believed to be the more active species, which might explain the formation of iron hydroxide precipitates at higher pH levels.

The conditions required to stabilise the solid phases have been the topic of many publications [Posnjak and Merwin, 1922; Babcan, 1971; Kershaw and Pickering, 1980 and Cornell and Schwertmann, 1996]. Posnjak and his co-workers [1922] summarised the conditions required to precipitate iron from hot iron solutions (ferric iron) in the absence of alkali elements. Kershaw and Pickering [1980] later presented this work as follows (Figure 5):

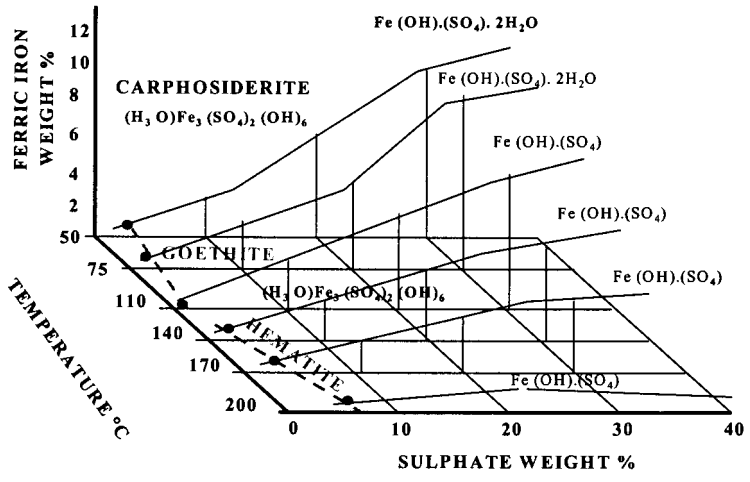

Figure 5: System $Fe_2(SO_4)_3 - H_2SO_4 - H_2O$: Polytherm 50°C to 200°C, 0 – 40% SO_4, ferric iron concentrations from 0 - 17% and in the absence of alkali elements [Kershaw and Pickering, 1980].

The figure shows that both goethite and hematite are formed from solutions when the ferric iron and sulphate concentrations are controlled at very low levels. It also shows that an increase in temperature favours hematite formation. It must again be emphasised that this figure as well as the one to follow by Babcan [1971] depict equilibrium phases and do not indicate the influence of other species or metastable species or phases that may play an important role in practical processes.

Currently, Zincor is operating its iron removal process at temperatures ranging between 50°C and 60°C with the ferric iron and sulphate (associated with sulphuric acid) concentrations maintained at approximately 0.1% (by mass) and 0.05% (by mass),

respectively. Under these conditions, it appears as though goethite might be present in Zincor's iron precipitate. This statement is confirmed when the work of Walter-Levy and Quemeneur [1964] is considered. Figure 6 shows (also see Figure 5) the iron compounds in equilibrium with ferric sulphate solution at 100°C in the presence of small amounts of acid and significant $ZnSO_4$ concentrations (1% Fe^{3+} ≡ 10 g/l). It appears that goethite starts forming at the lowest Fe^{3+} concentrations (0,1% - 0,2% Fe^{3+}), followed by $Fe_4(SO_4)(OH)_{10}$ (0,2% - 0,4% Fe^{3+}) and hydronium jarosite (>0,4% Fe^{3+}).

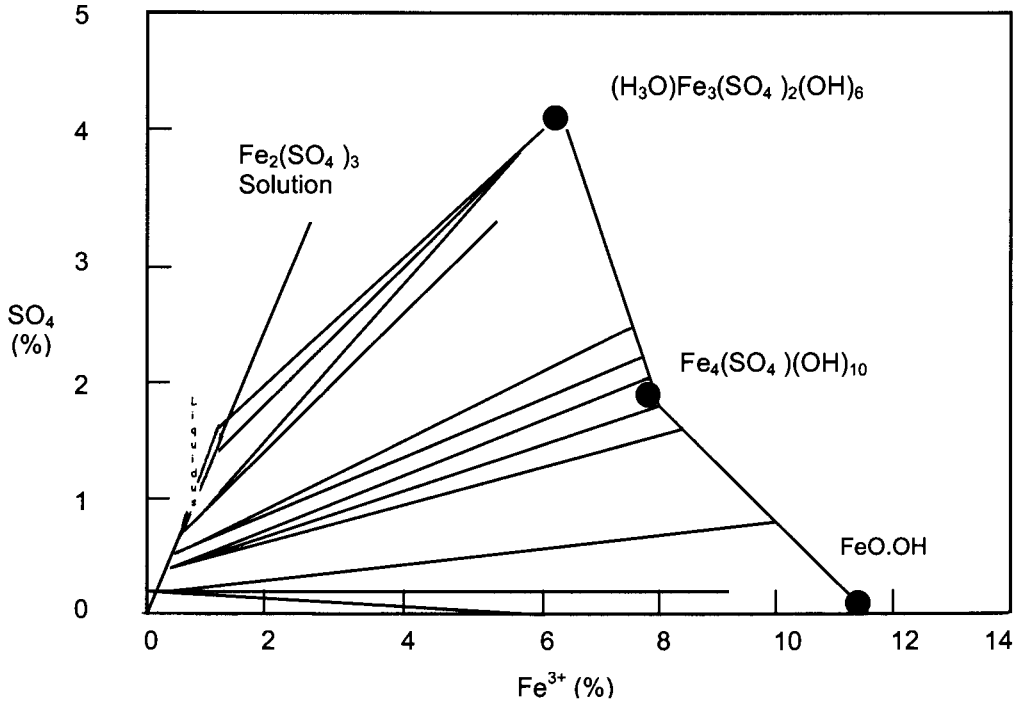

Figure 6: Part of the Fe_2O_3 – H_2O – SO_3 system at 100°C [Walter-Levy and Quemeneur, 1964].

A more convenient way of expressing these equilibrium iron phases would be in terms of temperature and pH as it remains the main operating parameters used to control an iron removal process. This was recognised by Babcan [1971] who used a 0.5M ferric sulphate

solution (approximately 14.4% sulphate by weight) as basis for his experiments (Figure 7).

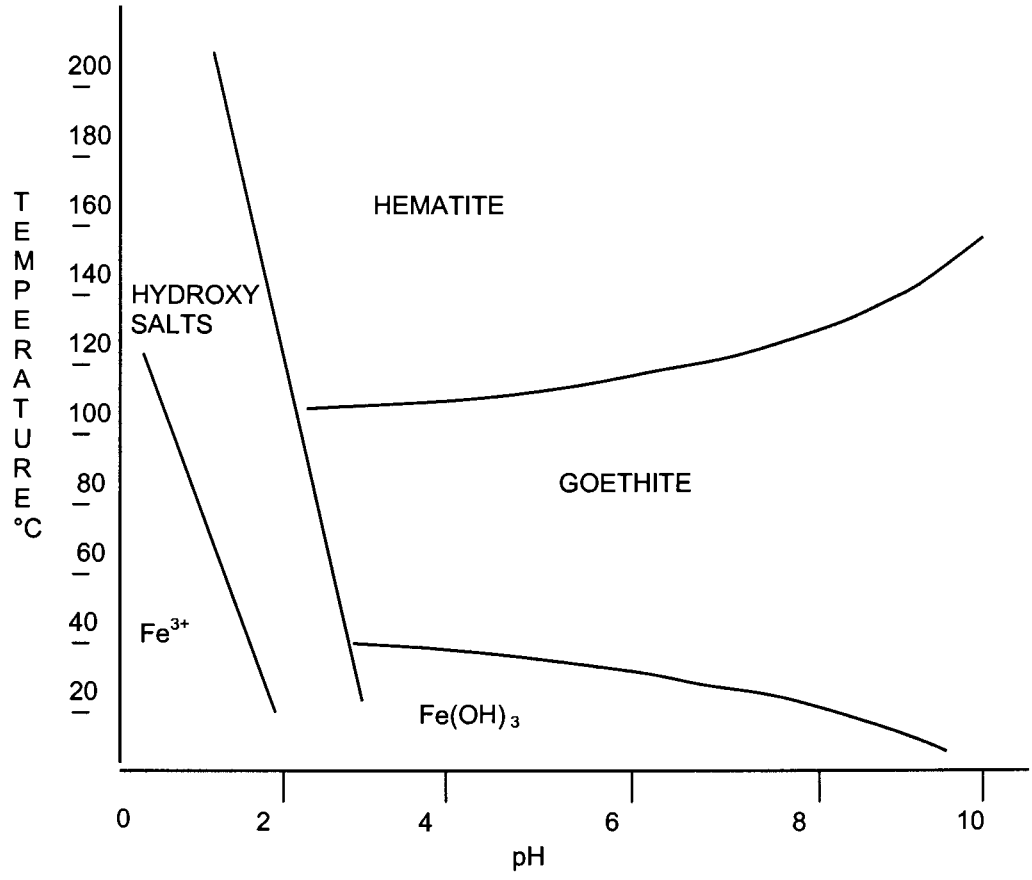

Figure 7: Conditions for the precipitation of iron oxide, oxide hydroxide, hydroxide and hydroxy salts (jarosites) from 0.5M ferric sulphate solutions [Babcan, 1971]

Figure 7 again suggests that goethite should be the main iron phase in Zincor's iron residue. It also shows that with a drop in pH the possibility of forming hydroxy salts (iron hydroxysulphates include jarosites) increases and that iron hydroxides might start to form with a drop in temperature.

The past decade, however, saw two very important findings that suggest that, under specific conditions, goethite might not be the stable iron phase in Zincor's iron residue. Both these findings involved the identification of intermediate iron phases or phases that are metastable towards goethite.

Brady *et al.* [1986] described the existence of an unidentified iron compound in mine drainage. The phase was characterised in more detail by Bigham *et al.* [1990] and subsequently named schwertmannite. By 1994 schwertmannite was identified [Bigham *et al.*, 1994] at over 40 sites in Europe, North America and Australia. It is very important to notice that all the samples in these studies were taken from natural environments associated with a source of iron and sulphate, *i.e.* mine drainage or effluents and pyritic deposits close to lakes and streams. Dutrizac [1999] attempted to identify schwertmannite in a sample taken from the weak acid leach stage of a typical roast-leach-electrowinning zinc circuit at Cominco's Trail Operations in British Columbia. Due to the very low abundance of what was suspected to be schwertmannite in the sample, the parties involved were unable to conclusively identify it. Prior to this, Bigham and his co-workers [Bigham *et al.*, 1996] studied the stability and solubility of schwertmannite and the phases associated with it in acidic sulphate waters. Their findings are summarised in Figure 8.

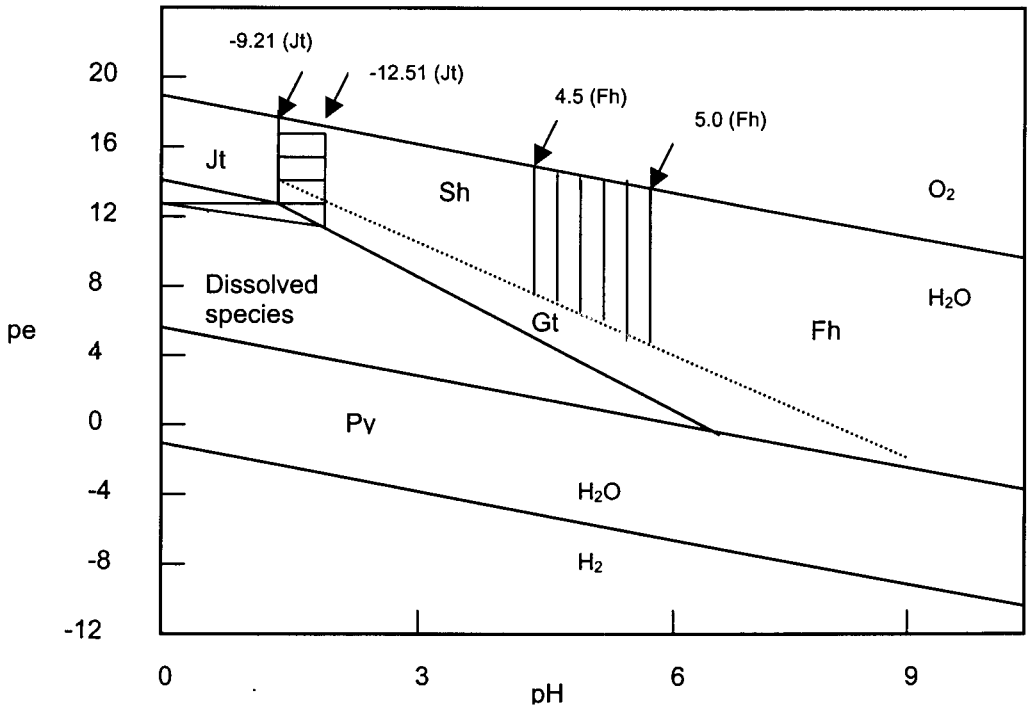

Figure 8: Diagram of pe-pH at 25°C where pe = Eh(mV)/59.2. Jt = K-jarosite, Sh = schwertmannite, Fh = ferrihydrite, Gt = goethite and Py = pyrite. Stability fields extended when different values of log $K_{Jt/Fh}$ were used. Single-hatched lines indicate expansion of K-jarosite (horizontal) and ferrihydrite (vertical) fields, respectively. Areas with dashed lines indicate fields of metastability [Bigham *et al.*, 1996].

It was found that schwertmannite is metastable with respect to goethite with goethite or hematite the final iron phase expected from this species. The study showed that the first traces of goethite were formed after approximately 65 hours when a schwertmannite sample was left in distilled water for a period of 5.5 years at ambient conditions.

The second important finding referred to previously is that the phases previously described as amorphous ferric hydroxide,

colloidal ferric hydroxide, $Fe(OH)_3$, etc. were recognised to be ferrihydrite [Jambor and Dutrizac, 1998]. In this paper it is also shown that ferrihydrite will transform to goethite in approximately 20 hours at ambient conditions. Even though most of the work related to schwertmannite specifically, as well as to ferrihydrite, were performed on samples taken from natural environments or done at ambient conditions, there is reason to believe that these phases also play an important role in iron removal at Zincor and probably in other hydrometallurgical processing circuits. The factors that influence the transformation of these phases to goethite, the properties of schwertmannite and ferrihydrite as well as their characterisation are discussed in more detail in Sections 2.3 and 2.4.

1.3 Kinetics of iron removal

The objective of this section is to touch on a few basic concepts viewed as important when dealing with the kinetics of iron removal. The ensuing paragraphs focus on some of the difficulties faced when attempting to define a suitable rate equation. Factors that influence the rate of iron removal as jarosite and goethite are also discussed.

It is very important to choose an experimental set-up that would best simulate the process under investigation. Traditionally, static tests (batch tests) were used as a means of determining a satisfactory rate equation as it simplifies the mathematical model. In these tests, the solution concentration of the species under investigation is typically determined as a function of time.

The problem with this, or any other experimental set-up for that matter, is that it might not reflect the mechanism of iron removal required even if the desired product is formed. The mechanism of iron removal refers to the exact sequence of steps involved in the reaction and as such requires knowledge of any intermediate substances that may exist between the reactants and the final product. The fact that the mechanisms of some iron removal processes are not fully understood (see Section 1.4), the generation of acid during iron precipitation as well as the formation of other iron phases (parallel reactions) during iron precipitation, complicate matters and hampers the understanding of iron precipitation rates.

When the precipitation of filterable iron phases (goethite and hematite) in the absence of alkali elements is considered for example, it is clear (refer Figures 5 & 6) that these phases only form

under specific conditions, *i.e.* at low ferric iron and sulphate concentrations (dilute solutions) and higher pH-values, which would be difficult to maintain in a batch test without complicating matters. Another option is to use a so-called dynamic test (flow test) to study the kinetics of the formation of these phases. In flow tests, the flow rate is kept constant and the volume change is measured as a function of time. Repeating the experiments at different flow rates would supply the information to draw up a rate equation. However, the dynamic flow test is not a solution to the problems mentioned above and it might even impose other challenges onto the system such as the development of pH-profiles in the reactor when a base is added.

Nonetheless, attempts have been made to determine a rate equation for the removal of iron as an alkali-jarosite by Wang *et al.* [1985] and Ciriello and Synnott [1996] by using batch tests. Wang *et al.* showed that for the reaction:

$$3Fe_2(SO_4)_3 + A_2SO_4 + 12H_2O = 2AFe_3(SO_4)_2(OH)_6 + H_2SO_4 \quad .....1$$

With $A = K^+, Na^+, NH_4^+$

The rate of iron removal according to the mass conservation law can be described by the following equation (determined at temperatures between 78°C and 98°C and with an excess amount of seed added):

$$-dC_{Fe(III)}/dt = k_1 C^2_{Fe(III)} \times C^{0.5}_{A2\,SO4} - k_{-1} C^{0.25}_{H2SO4} \quad .....2$$

The findings from Wang *et al.* [1985] may be summarised as follows:

- Alkali concentration: The rate of iron precipitation is proportional to the square root of the concentration of the alkaline species.

- Ferric iron concentration: Higher initial iron concentrations can result in higher final concentrations of the species in the solution. This, however, would only be true in batch systems when the pH is not controlled.

- Temperature: The study showed that iron removal increased dramatically when the temperature was raised above 85°C. This might indicate a change in the precipitation mechanism (parallel reactions possibly hydronium-jarosite formation) and should be carefully reviewed.

- Seeding: The addition of 25 – 150 g/l seed will shorten iron removal by several hours partly due to the elimination of the incubation time required to form a new phase when no seed is present. It is therefore expected that a factor representing the influence of seed addition on the rate of iron removal should be included in the rate equation.

- Acidity: An increase in the acidity of the solution will have a detrimental effect on the precipitation of jarosite according to reaction 1 and as indicated in the rate equation. Neutralisation of hot iron solution to acid levels of less than 10 g/l H_2SO_4 is required to initiate jarosite precipitation.

The formation and growth of goethite is controlled by a different mechanism [Dutrizac, 1980]. Some of the factors that influence the removal of iron as goethite include:

- pH: Operational pH values between 2.0 and 4.0 (promotes particle growth).

- Temperature: Temperatures of about 85°C give the optimum results.

- The presence of anions: It is believed that goethite precipitates from an anion-hydroxyl polymer. Anions with weak complexing properties for iron, such as sulphate, produce α- or γ - FeO.OH while anions such as Cl^- and F^- seem to give β - FeO.OH [Cornell and Schwertmann, 1996].

- Stirrer speed: Bryson [1986] suggested that smaller nuclei form on the surfaces of larger particles and that stirrer speed not only affects the nucleation and growth rate of goethite particles but also its settling and filtration properties. It appears as though an increase in stirrer speed can lead to the detachment of some of the smaller nuclei from the parent particle whereby growth is hindered.

The roles some of these parameters play in the removal of iron in the form of mainly amorphous iron phases (Zincor Process) are discussed in more detail in Section 2.4.3. Since the experimental setup and procedures used in this study to investigate the influence of these and other parameters on the filterability of a synthetic iron residue, were not specifically designed to compile a kinetic rate equation, only relative trends could be established. As such, the

relative changes in retention time required to obtain equivalent filtration rates when the various parameters were changed during iron removal, proved to be useful. In order to possibly further exploit the results obtained (see Section 2.4.3.2) and to compile a rate equation that is fit for design purposes, the kinetics of iron removal for the system under discussion would have to be investigated in more detail.

1.4 Precipitation mechanisms

As was discussed in the previous section, knowledge of the exact sequence in which reaction steps occur, assists in the understanding of the thermodynamics and kinetics of a chemical reaction. The practical implications of the intermediate phases that might form in a mineral processing environment are also identified.

In terms of iron oxide and oxyhydroxide formation, Dutrizac [1980] suggested that the polymeric growth of the early phases could occur via three methods. When excess base is rapidly added to the iron solution (OH/Fe $\geq$ 2.8 [Cornell and Schwertmann, 1996]), large gel colloids are usually formed via the formation of hydroxyl bridges. These colloids coagulate to form massive gel precipitates that are normally contaminated with metal species, sulphates and bonded water.

This process tends to be independent of changes in the temperature of the solution. However, when just enough base is continuously added to just neutralise the acid formed in the polymeric growth process, oxolated structures will form. These oxolated structures have the general formula $Fe_p^{III}O_r(OH)_s^{(3p-(2r+s)+}$ [Cornell and Schwertmann, 1996], which is formed from lower molecular weight species such as the dimer $Fe_2(OH)_4^{2+}$ mentioned earlier. Interaction between these species produces polymers, which aggregate to form large masses.

This process (hydrolysis) eventually lead to the formation of iron oxides such as goethite, lepidocrocite, akaganeite, ferrihydrite and hematite or mixtures of it. The time required for the precipitation of these species is a function of many factors, which include temperature, pH, nature of the anion present, initial $[Fe^{3+}]$ and seeding.

Cornell and Schwertmann [1996] also summarised the formation and transformation pathways of the most common oxides and oxy-hydroxides found in nature and many processing plants. Figure 9 shows the products of ferrous and ferric iron oxidation and protonation as well as the conditions required for the formation and transformation of the various phases.

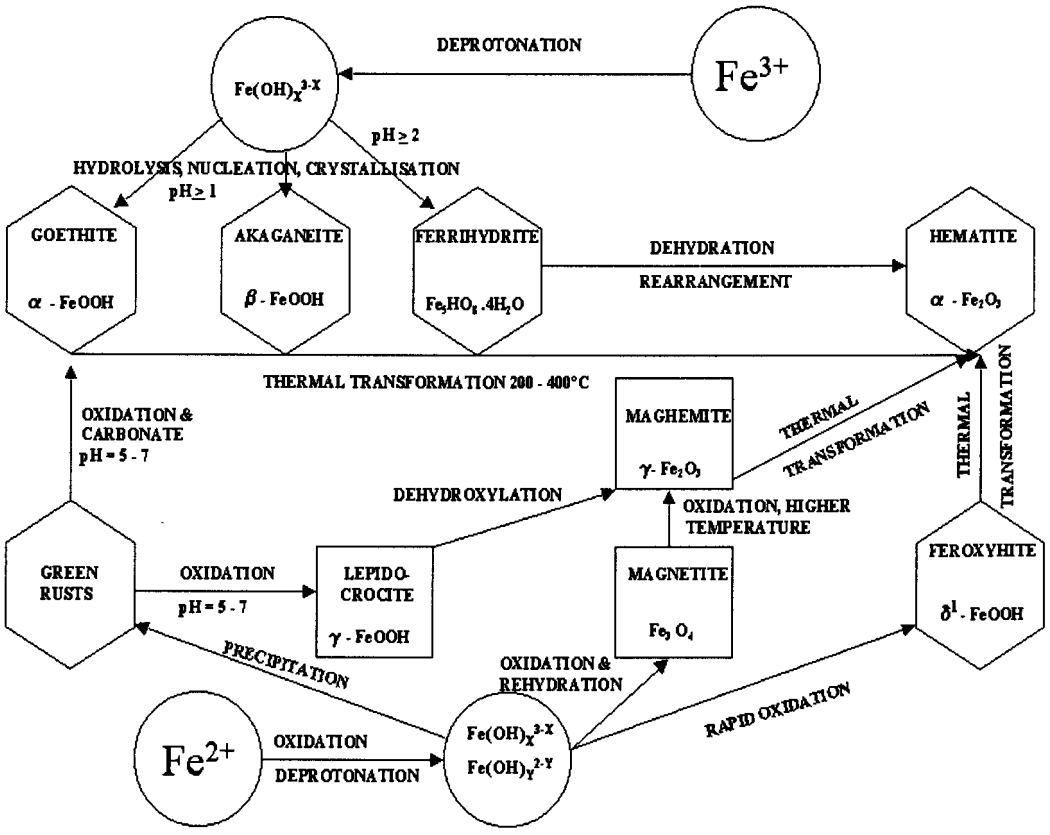

Figure 9: Diagram of the formation and transformation conditions of common iron oxides and oxy-hydroxides [Schwertmann & Cornell, 1991].

The role Cl^- can play in the formation of the β - FeO.OH polymorph would probably be taken by the sulphate ion (weaker complexing ion) in a zinc processing environment to form α- or γ - FeO.OH as was mentioned earlier. It is also interesting to note that ferrihydrite can form from ferric iron solutions at a pH as low as 2. This is contrary to the conditions depicted in Figure 8 where it was shown that ferrihydrite only starts forming at pH values above

approximately 4.5. The metastability of ferrihydrite towards goethite is also not shown in Figure 9 and must be kept in mind when analysing iron residues.

The schematic presentation shown in Figure 9 also doesn't take into account the influence of high sulphate concentrations. Sulphate concentrations between 0.2 and 2 M found in the zinc industry can lead to the formation of hydroxy salts and more specifically jarosites and schwertmannite when ferric iron is hydrolysed.

The precipitation pathway for hydroxy salts and more specific jarosite in this case is not well defined. It has been suggested [Dutrizac, 1980] that the OH^- bridges (Fe-OH-Fe) that form during the early phases of iron precipitation are opened by protons (importance of lower pH levels) to form the alunite type structure of the natural occurring mineral.

Some resemblance between the structures of schwertmannite and akaganeite was found [Bigham *et al.*, 1990; Dutrizac, 1999], which might indicate a similar precipitation pathway. This is an area where more work is needed to establish what role sulphate plays in stabilising the schwertmannite structure.

1.5 Iron removal processes

The removal of iron from the impure process solutions is not as straightforward as it might seem. Initial attempts to remove iron as a hydroxide resulted in poorly filterable, voluminous and gelatinous precipitates [Tainton and Leyson, 1924]. Solid separation and washing are improved if the precipitate is dense with a crystalline character. The size of the precipitates plays an important role in this respect. It is well established that the precipitate size is largely determined by the extent of supersaturation of the specific species at the time of precipitation. The higher the level of supersaturation, the higher the nucleation rate, which results in the precipitation of small particles. By using hot, dilute solutions, the level of supersaturation is kept as low as possible and crystalline precipitates of coarse particle size can form. The slow addition of reagents to the hot impure solution will normally ensure that the dilute solution conditions are maintained. This will then encourage a low rate of nucleation and favour precipitation by growth of the existing nuclei.

This principle is used in two of the processes developed to control and remove iron from zinc rich solutions *i.e.* the goethite and so-called para-goethite processes. The establishment of these processes in the zinc industry was preceeded by the development of the jarosite process. The advent of the jarosite process changed the complexity of the early treatment of the zinc containing neutral leach residues dramatically. It was the first iron removal process that allowed the production of a filterable residue on a commercial scale.

1.5.1 Jarosite Process

Jarosite is a natural occurring mineral with the chemical formula $KFe_3(SO_4)_2(OH)_6$. It forms part of the alunite family with the formula $AB_3(SO_4)_2(OH)_6$ where A might be H_3O^+ , Na^+, Rb^+, Ag^+, Tl^+, K^+, NH^+ , ½ Pb^{2+} or ½ Hg^{2+} and B might be Al^{2+}, Cu^{2+} or Fe^{3+}. Jarosite is the most common mineral, usually found in nature in association with goethite and hematite. Other jarosite type mine-rals include hydronium-jarosite $(H_3O)Fe_3(SO_4)_2(OH)_6$, ammonia-jarosite $(NH_4)Fe_3(SO_4)_2(OH)_6$, sodium-jarosite $NaFe_3(SO_4)_2(OH)_6$ and plumbo-jarosite $PbFe_6(SO_4)_4(OH)_{12}$ [Chen and Cabri, 1986].

The jarosite process is still the most widely used process in the zinc industry today. The first patents registered were those of Norzinc AS [Patent, 1965a], Asturiana de Zinc S.A. [Patent, 1964] and Electrolytic Zinc Company of Australasia Limited [Patent, 1965b]. Figure 10 shows a simplified jarosite flowsheet. Many changes have since been incorporated in some plants that include multiple stage leaching, lead-silver recovery, pre-neutralisation, acid wash, etc. Other versions of the process have also been described in the literature such as the Low - Contaminant – Jarosite Process [Pammenter *et al.*, 1986] and the Conversion Jarosite Process [Uusipaavalniemi and Karlman, 1996].

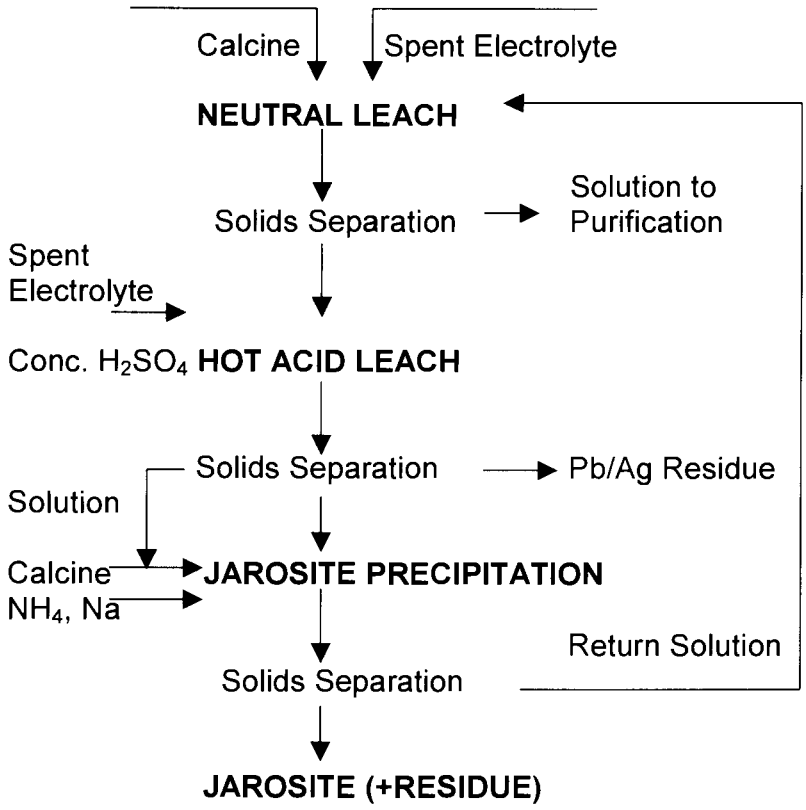

Figure 10: Simplified jarosite precipitation flowsheet [Arregui *et al.*, 1980].

In the jarosite process, the neutral leach residue is subjected to leaching at 85°C to 95°C in solutions containing more than 100 g/l H_2SO_4 for several hours to dissolve the zinc ferrites ($ZnO.Fe_2O_3$). Following the hot acid leach step, a cation (Na^+, K^+, NH_4^+, etc.) and calcine are added to precipitate iron as jarosite at a pH below 2. Up to 98% of the ferrites can be leached out and a zinc-rich solution containing between 1 g/l and 3 g/l iron can be produced.

In terms of the stabilities of the various jarosite species mentioned earlier, Wang *et al.* [1985] also showed that hydronium in hydronium-jarosite (see Figures 5 & 6) will be replaced by the alkali's in the following sequence K > NH_4 > Na. It was also

indicated that hydronium-jarosite formation below about 85°C was negligible. This is contrary to what Posnjak and Merwin [1922] found in their study where hydronium-jarosite (carphosiderite as it was called) was shown to be present at 50°C.

1.5.2 Goethite Process

Goethite is probably the most abundant form of iron oxide in soil, occurring in almost every soil type and climate region. The four polymorphs of FeO.OH that are known to exist in the natural environment are α-FeO.OH (goethite), β-FeO.OH (akaganeite), γ-FeO.OH (lepidocrocite) and σ-FeO.OH (feroxyhyte).

Of these minerals, goethite is the most common [Chen and Cabri, 1986]. The relative stability of goethite, under wet conditions at natural weathering conditions, is probably one of the reasons why it is more acceptable, in terms of the environmental requirements, for most locations in the zinc industry. It was also found that aluminium in the goethite structure further increases its stability (abundance of Al-substituted goethite in nature) under natural weathering conditions [Franz, 1978].

Goethite is commercially precipitated from zinc rich solutions by means of the Vieille Montagne Process [Patent, 1972] The process is presented in Figure 11.

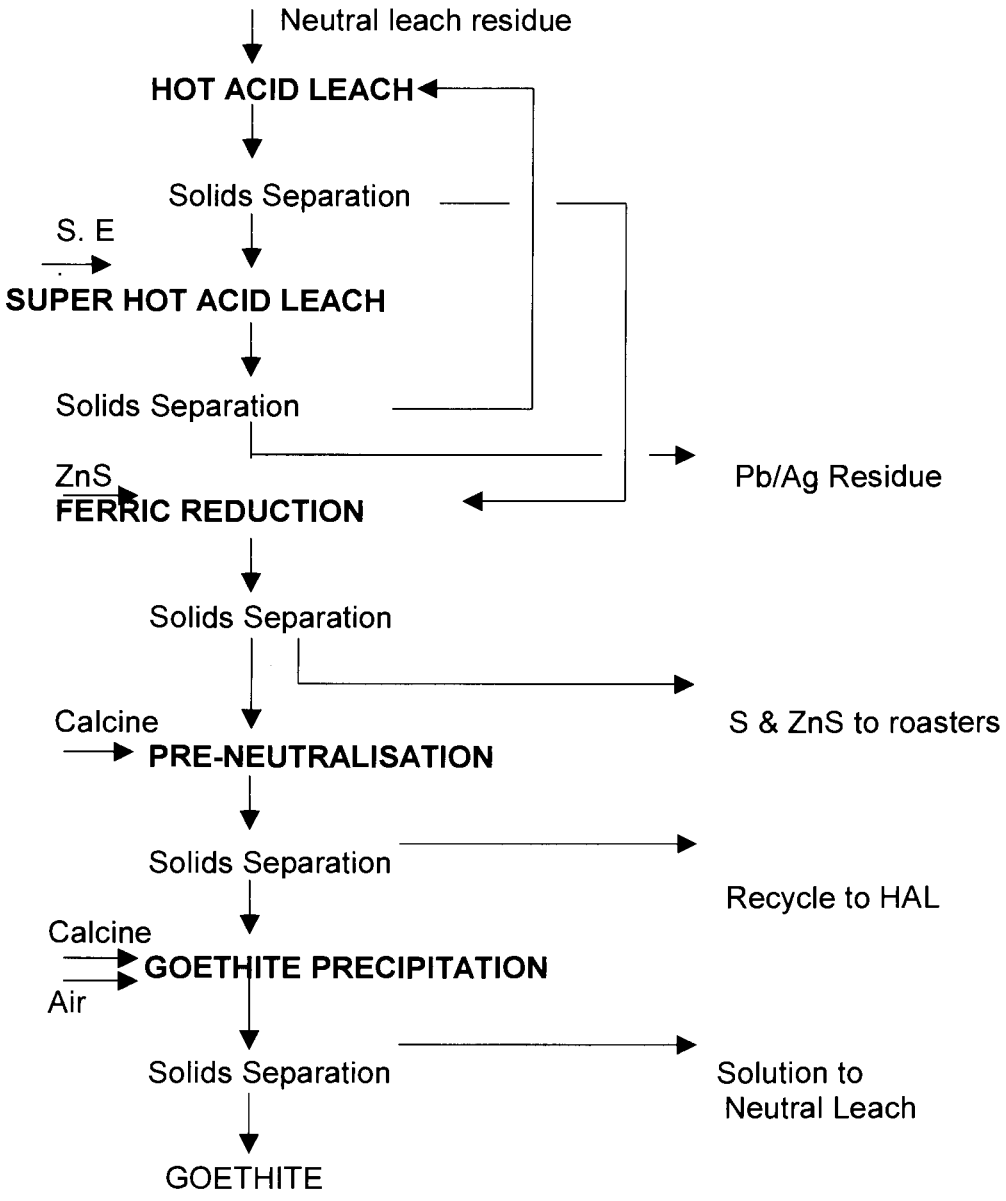

Figure 11: The Vieille Montagne goethite process (V.M. process) [Gordon and Pickering, 1975].

In this process, ferric iron in solution is reduced to the ferrous state by adding concentrate (ZnS) prior to the pre-neutralisation step. The solution that is then obtained from liquid-solid separation in the pre-neutralisation stage is transferred to the goethite precipitation step where calcine is added to control the pH at approximately 2.5 (pH can vary between 4.2 and 2.7 – Boxall and James, 1986). Air is injected to oxidise the ferrous iron in solution at 80°C to 90°C. Filterable goethite is precipitated and subsequently separated from solution.

Another patented goethite process [Patent, 1966] is the Union Miniere process (UM Process) described elsewhere [Torfs, 1996]. This process and the V.M. process is similar and are used today in several zinc smelters.

In the Electrolytic Zinc process (E.Z. process) [Patent, 1970], shown in Figure 12, calcine is added to a ferric iron solution to control the pH at 2.8 in a continuous heated precipitation stage where the ferric concentration is kept low (1-2 g/l Fe).

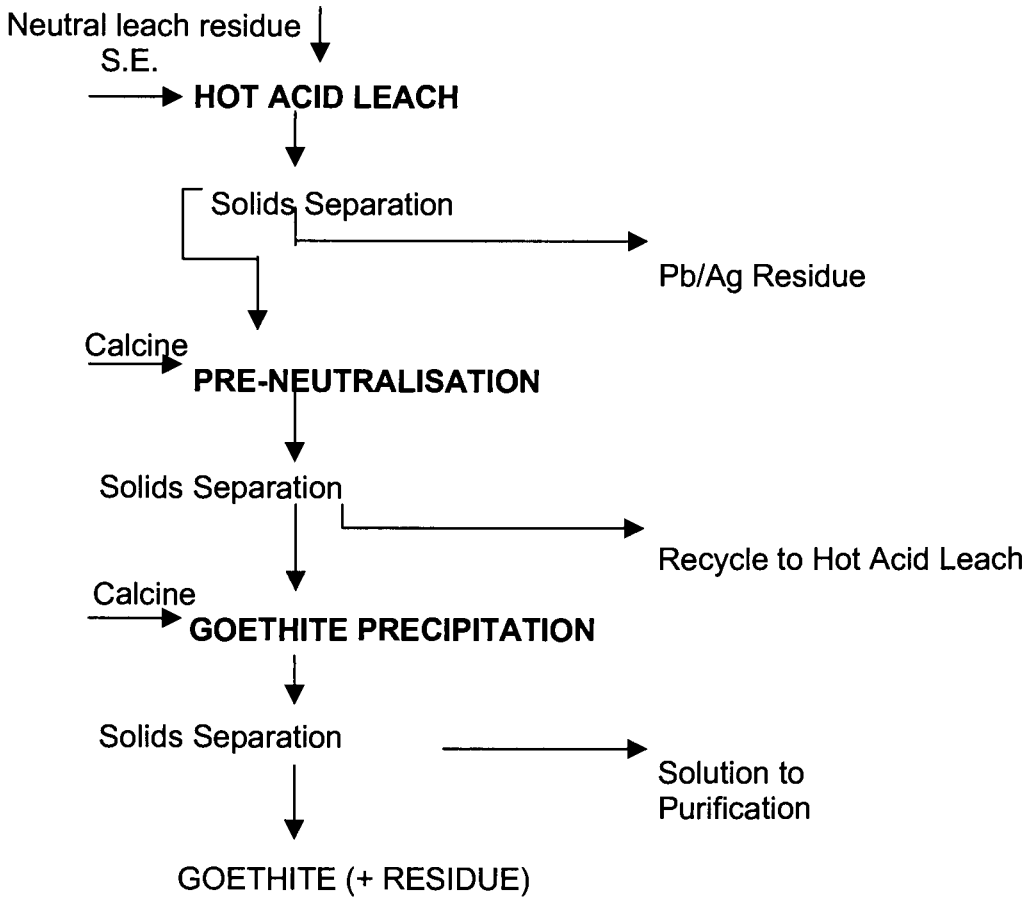

Figure 12: The E.Z. process. [Gordon and Pickering, 1975]

During this process, ferric iron is precipitated in a crystalline form [Fe_2O_3 .H_2O] that is readily separated from the solution. Earlier investigations of the residue, produced in this way, indicated that it is not goethite. Because the iron enters the process in the ferric state, 50% more calcine is used than in the V.M. process (stoichiometrically – no O_2 used). This usually results in an additional zinc loss because it is not possible to do an acid wash at pH values $\leq$ 2.0 (as is the case with jarosite) since it would dissolve the goethite residue.

1.5.3 Hematite Process

The hematite precipitated from iron bearing solutions in the zinc industry refers to the polymorph α-Fe_2O_3 also found in nature. The other polymorph found in nature is the iron-deficient spinel maghemite (γ-Fe_2O_3) that is important because of its use in magnetic tapes. The only operational zinc plant in the world that currently uses the hematite process for iron removal is the Iijima Electrolytic Zinc Plant near Akita in Japan [Tsunoda *et al.*, 1973]. Figure 13 shows a schematic presentation of this process.

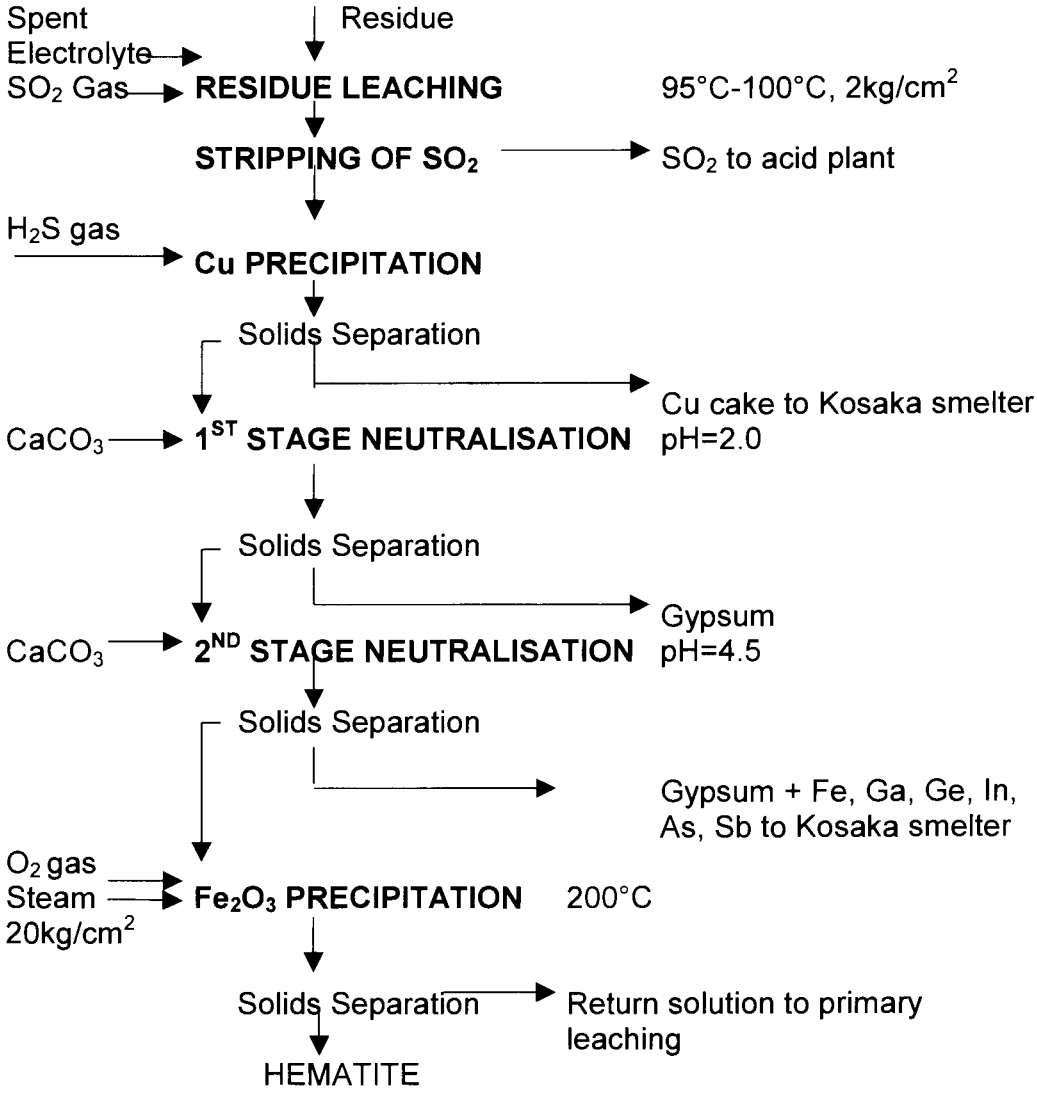

Figure 13: The hematite process of Iijima Zinc Plant [Onozaki *et al.*, 1986].

In the primary leaching stage of this process, ferric iron is reduced to the ferrous state through the addition of spent electrolyte and SO_2 gas at a solution temperature of 95°C to 100°C as follows:

$$2Fe^{3+} + SO_2 + 2H_2O = 2Fe^{2+} + SO_4^{2-} + 4H^+ \quad \ldots\ldots\ldots\ldots 3$$

Excess SO_2 is then removed from the solution and copper is precipitated by the addition of H_2S. The solution from this step is then neutralised in two stages using limestone. The limestone also removes sulphate, derived from SO_2, as gypsum.

The solution is then heated to 180°C to 200°C for 3 hours under 18 atm pressure in titanium-clad autoclaves to convert iron to the ferric state. Iron is precipitated as Fe_2O_3 with the iron in solution decreasing from 45 g/l to about 3.5 g/l. Figure 7 shows that although H_2SO_4 (*ca* 60g/l) is generated during hydrolysis, the precipitation of Fe_2O_3 at high temperatures will still proceed. The Fe_2O_3 precipitated, however contains up to 3% sulfur as sulphate and requires roasting before it can be accepted as steel plant feed.

Figure 7 also indicates that goethite will form at temperatures below 100°C probably due to kinetic reasons; this might explain the presence of this phase instead of the slightly more stable hematite phase in nature and low temperature processing environments. Above 130°C, however, Fe_2O_3 is both kinetically and thermodynamically the predominant phase.

1.5.4 Para-goethite process

The term para-goethite (PG) is confusing to say the least. In general, PG process describes the goethite precipitation route, which is probably why Gordon and Pickering [1975] classified the E.Z. process as a goethite process (see Section 1.5.2).

Another important fact to recognise is that such a mineral does not exist.

Gordon and Pickering [1975] mentioned that the exact nature of the residue has not been determined and it seems there is still some confusion as to what the residue comprises of. However, it has been recognised that the process does not produce goethite (see equation 4) although the thermodynamics indicate that it should be the case. It was proposed in the same paper that iron is removed through the following reaction:

$$Fe_2(SO_4)_3 + 2ZnO + 2H_2O = Fe_2O_3 .SO_3 .2H_2O + 2ZnSO_4 \quad \text{.....4}$$

The term para-goethite, therefore, probably refers to the fact that a similar process route than for goethite precipitation is followed. The PG iron removal processes in commercial use today [Cubeddu *et al.*, 1996; McCristal and Manning, 1998] basically follow the same route described by Gordon and Pickering [1975] as the E.Z. process (refer to Figure 12). The Enirisorse Porto Vesme Plant [Patrizi *et al.*, 1985] (process might have been changed in the meantime) and the Pasminco refinery in Hobart both use the para-goethite process patented by the Electrolytic Zinc Company of Australasia [Patent, 1970].

Zincor uses a similar process to remove iron from zinc bearing solutions [Meyer *et al.*, 1996]. A simplified flowsheet of the Zincor plant is shown in Figure 14. The reader is also referred to Figures 12 and 15 for a comparison between the existing Zincor- and E.Z./Para-goethite process.

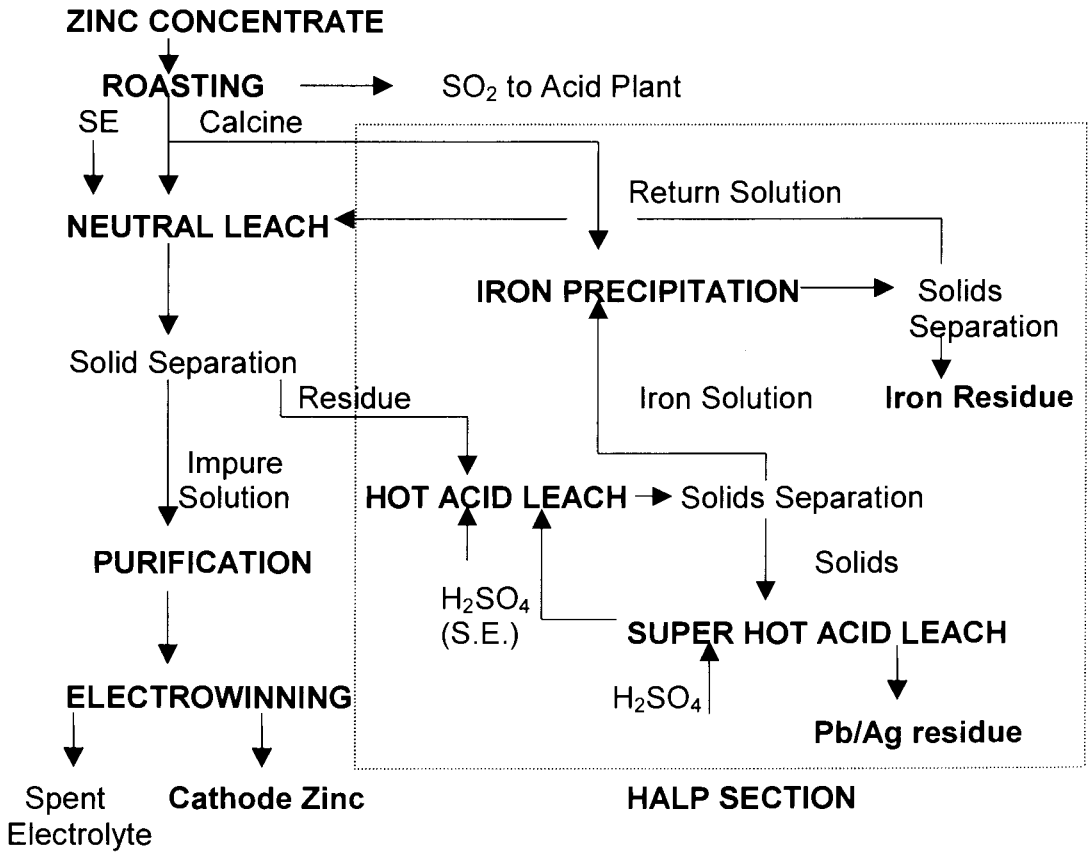

Figure 14: Simplified schematic presentation of the existing Zincor plant showing the residue treatment circuit (HALP section).

In the existing Zincor residue treatment plant (HALP section), re-pulped neutral leach filter cake is leached in two stages. In the hot acid leach stage, spent electrolyte is added and the residue is leached in four 83 m^3 stirred tanks at about 85°C for 4-5 hours. Acid levels drop from approximately 40 g/l H_2SO_4 in tank one to 25 g/l H_2SO_4 in tank four. The slurry is thickened and the overflow proceeds to iron precipitation. The thickener underflow is further treated with spent electrolyte and concentrated H_2SO_4 in four 65 m^3 stirred tanks in series at about 90°C - 95°C and a liquid/solid ratio of 3 for 6-7 hours. Acid levels currently vary between 150 g/l H_2SO_4

in tank one and 60-70 g/l H_2SO_4 in tank four. The slurry is settled and the overflow is returned to the hot acid leach stage. The underflow is filtered in two filter presses and the solids are re-pulped with dam return water and pumped to slimes dams.

As was previously mentioned, the hot acid leach thickener overflow proceeds to iron precipitation. This solution, the hot iron solution (HIS), is continuously fed to four $60m^3$ tanks in series at a temperature between 50°C and 60°C. Excess calcine slurry at a pH of 4.5 is also continuously added. HIS is fed at a rate such that the pH in this tank is controlled between 3.0 and 3.2. More HIS is added in tank 2 to control the pH level at approximately 2.7. The pH is then allowed to increase to about 3.0 in tank four. The slurry is then settled with the overflow going back to the neutral leach plant and the underflow going to filtration.

The Zincor Process and the composition of the iron residue currently being produced are discussed in more detail in Section 2.

1.6 Choice of an iron removal process

Factors that influence the choice of an iron removal process include among others cost of operation, zinc losses and environmental considerations. A comparison between the different iron removal processes discussed in the previous paragraphs is shown in Table 3.

Table 3: Comparison between the different iron removal processes. [Zincor internal reports, 1999-2000]

Variable	Item	Sub-item	PG & Zincor Process	Goethite Process	Jarosite Process	Hematite Process
Environment	Ponding	Management	Easier	Easier	Difficult	Easier
		Rehabilitation	Safer	Safer	Difficult	Safer
	Bleed	Fluorine	Yes	Yes	Partially	No
	Residue composition	% Fe	35 - 38	40 – 45	25 - 28	58 – 60
		% S	4 - 7	2.5 – 5	10 - 12	2 - 4
		% Zn	8 - 9	5 – 8	4 - 6	0.5 - 1
Economics	Reagents	Oxygen (kg/t Zn)	None	32	None	More than goethite
		NH_3 (kg/t Zn)	None	None	9	None
		Acid (kg/t Zn)	None	None	+120 vs. goethite	More than goethite
	Energy	Steam (t/t Zn)	None to 1.20	1.20	1.55	More than Goethite
	CAPEX		LOW	MED	MED	HIGH
	OPEX		LOW	MED	MED	HIGH
Zn recovery	Overall % Zn recovery		94 - 95	96 – 97	97 - 98	98 – 99
Flexibility towards the feed	High/low Fe & Si calcine usage		Yes	Yes	No	No

In terms of the environment, most residues are disposed of at pH values higher than 2. Under these conditions, jarosite might be converted to goethite [Dutrizac, 1983]:

$$KFe_3(SO_4)_2(OH)_6 = 3FeO.OH + K^+ + 2SO_4^{2-} + 3H^+ \quad \text{.....5}$$

The association of jarosite with goethite in nature probably confirms that reaction 5 occurs to some extent (also see Figure 7). Occurrences of jarosite, goethite and hematite in the same environments are suggested to be attributable to kinetic barriers in jarosite to goethite and goethite to hematite reactions [Chen and Cabri, 1986].

Liberation of ions as well as a drop in pH of the solution associated with the decomposition of jarosites to form goethite for example, probably makes iron removal through jarosite formation less attractive. Jarosites are also thixotropic, which makes it very difficult to dry and compact during the rehabilitation phase.

In terms of the economics of the different iron removal processes, the PG process compares very favorably with other processes. The simplicity, ease of operation and low OPEX of the Zincor process, for example contributed to the fact that the refinery has been one of the lowest cost producers of zinc in the world for the past three decades.

The total recovery figure quoted in Table 3 for the PG process is higher than what is currently achieved from the Zincor refinery. This is mainly due to poor washing efficiencies achieved on the existing drum filters as well as the absence of a pre-neutralisation step. A

comparison between different iron removal processes in this regard is shown in Figure 15.

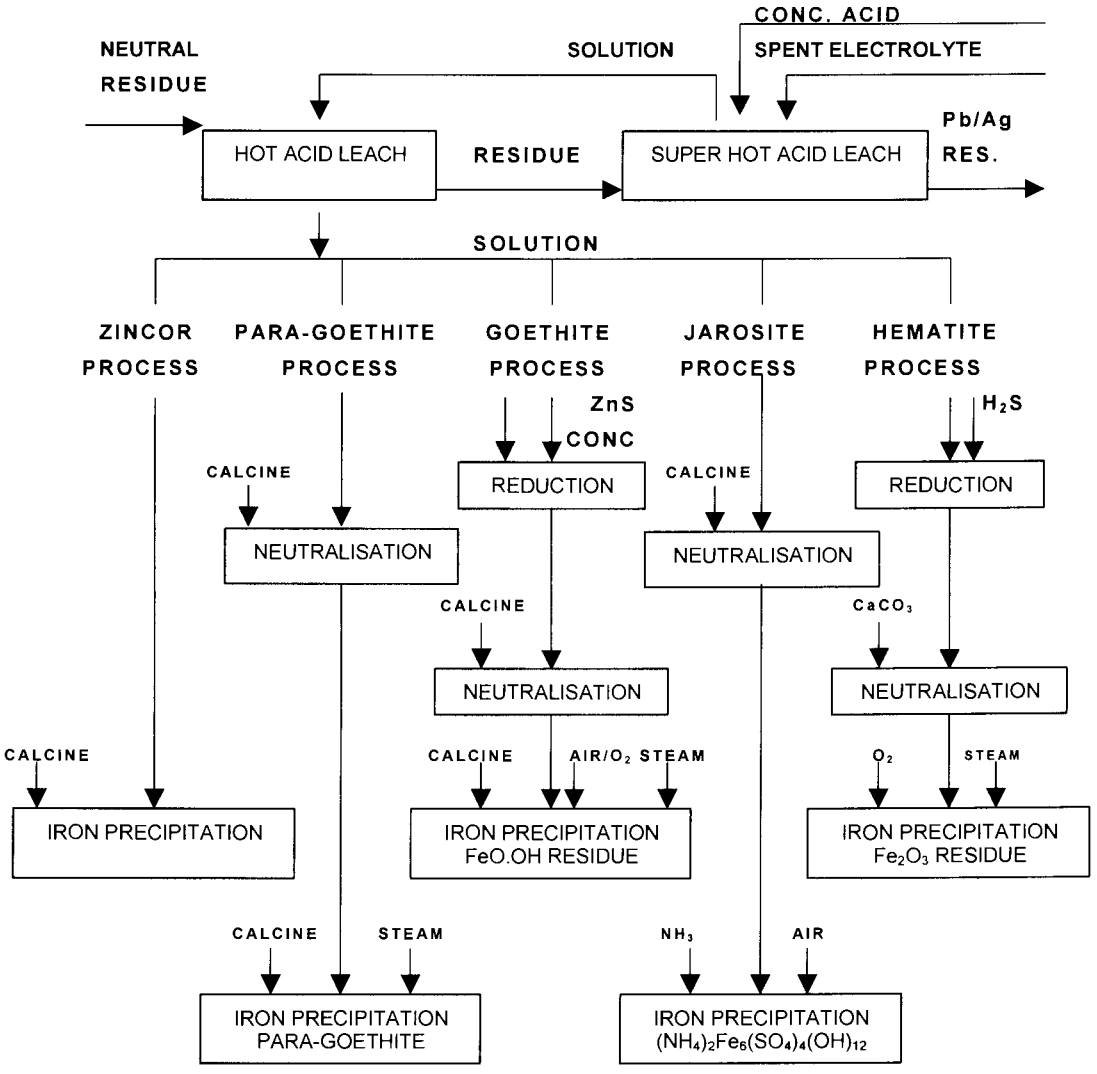

Figure 15: A comparison between different iron removal processes in terms of process steps and reagent additions.

The effect of the pre-neutralisation / weak acid leach step as well as the conditions of iron removal *i.e.* how much calcine is leached during iron removal, is shown in Figure 1.

Therefore, from an environmental and metal extraction perspective, the hematite process would probably be chosen. The CAPEX and OPEX involved in this process (see Table 3), however, make it less attractive. The lower costs involved with the goethite process, a more environmentally friendly residue as well as the relatively good zinc recoveries obtainable from the process, probably makes it the first choice for a greenfields operation. The possibility of utilising calcine with lower iron and silica contents for neutralisation purposes in the goethite (and PG process) process could further increase zinc recovery, which would make the process even more attractive.

Zincor considered the conversion of its iron removal process into a goethite process during the late 1990's. Due to, amongst other reasons, the high capital cost of almost US$ 20 million involved with the change over and the possibility to increase the zinc recovery at Zincor through other means to more or less the same level as that of the goethite process, it wasn't considered any further.

Therefore, relatively good zinc recovery expected from an optimised Zincor HALP circuit; simplicity and ease of operation of the Zincor iron removal process; relatively low operational costs involved with the process as well as the production of a residue that is believed to be more environmentally friendly than jarosite residues, should make the Zincor iron removal process a very attractive option for the Zinc Industry. Other strengths and weaknesses of the different iron removal processes have been summarised by Dutrizac [1980].

In the preceding paragraphs, the role iron plays in hydrometallurgical zinc circuits, parameters that influence iron removal in a filterable form as well as different iron removal processes in use today were addressed. In the following sections, attention is specifically given to the Zincor iron removal process. The inherent weakness of the process, *i.e.* high insoluble zinc loss associated with the use of calcine as a neutralising agent is also addressed in an attempt to make the "improved" Zincor Process an even more competitive process.

2 ZINCOR IRON REMOVAL PROCESS

2.1 History of the Zincor Process

The hydrometallurgical zinc smelter of the Zinc Corporation of South Africa (Zincor) is situated in Springs on the south-eastern border of the Gauteng Province. The need for a local zinc supplier was recognised by Gold Fields of South Africa Limited, who decided to convert their mothballed Vogelstruisbult G.M.C. uranium recovery plant, which had been closed some years previously, into an electrolytic zinc refinery. Prior to this event, all zinc used in South Africa had to be imported and the concentrate produced in the Southern African region was exported. This changed after the commissioning of Zincor's refinery during the late 1960's with the first sulphuric acid produced in December 1968 and the first zinc ingot casted almost four months later.

During the following three decades, Zincor has expanded to its present capacity of approximately 110 kt/a zinc and 210 kt/a sulphuric acid. During this time, Zincor was also one of the lowest cost producers of zinc in the world. In 1999, Gold Fields of South Africa Limited sold its majority share holding to Iscor Limited. The Zincor refinery is currently an integral part of growing Iscor's Base Metal Business. Zincor is still the only primary producer of zinc in Southern Africa and the zinc smelter maintains its role as one of South Africa's major producers of sulphuric acid.

Electrolytic smelting as a means of producing high purity zinc (higher than 99.995%) has been in commercial use since the early

part of the century and today approximately 80% of the world's zinc is produced in this way. At Zincor, a typical roast-leach-electrowinning circuit is used to process zinc sulphide concentrates to produce high purity zinc (refer to Figure 14). The original Zincor leaching circuit comprised of a neutral leach (with iron precipitation) and filter plant sections. During 1976, a hot acid leach- and an iron removal stage were commissioned. This was followed by the introduction of a super hot acid leach stage in 1984 into the same circuit. Prior to the commissioning of the first phase, an iron removal process was developed through a series of laboratory tests. The test work resulted in a patent, which was registered in 1976 [Patent, 1976].

The patent describes ferric iron removal from acidic iron bearing solutions in a form that is readily filterable. The iron-bearing solution is neutralised with the addition of zinc calcine slurry in a continuous process with the rate of addition of iron solution being so selected that the pH of the mixture does not drop below about 3.0 and is in the range of 3.0 to 5.5. The temperature, at which the neutralisation step is performed, is in the range of 50°C to the boiling point of the solution. Another important characteristic of the process is the acid leach performed, at a pH of approximately 2.7, on the iron precipitate to remove as much zinc as possible.

The application of the knowledge, gained from laboratory tests, on a commercial scale was found to be very challenging to say the least. Initially, the four iron precipitation tanks were used in parallel. It was filled with a calculated amount of calcine slurry before the hot iron solution was added. The pH in each tank was controlled at approximately 3.5 by the addition of extra calcine slurry. After 4 to 5 hours, the contents were pumped to the iron thickener and the

process was repeated. The high insoluble zinc loss obtained from this mode of operation led to the use of lime as a neutralising agent. This was changed again after settling and filtration problems were experienced, which at the time was thought to be attributable to the use of lime instead of calcine.

Since the problem of high zinc losses wasn't resolved, it was decided to change the process from a parallel process to four tanks in series and to install an automatic pH controller in the first iron precipitation tank. This change led to a reduction in insoluble zinc losses and it was generally easier to operate. In order to decrease the insoluble zinc losses even further, the use of an "acid" wash in the second iron precipitation tank was investigated. The investigation yielded good results and another automatic pH control system was installed to control the pH in the second tank at approximately 2.7 through the addition of hot iron solution.

Zincor is currently in the process of upgrading the residue treatment plant facility (HALP) by replacing the existing rotary drum filters with two horizontal vacuum belt filters to reduce soluble zinc losses as well as the addition of an extra leaching step (weak acid leach). The upgraded HALP circuit is schematically shown in Figure 16.

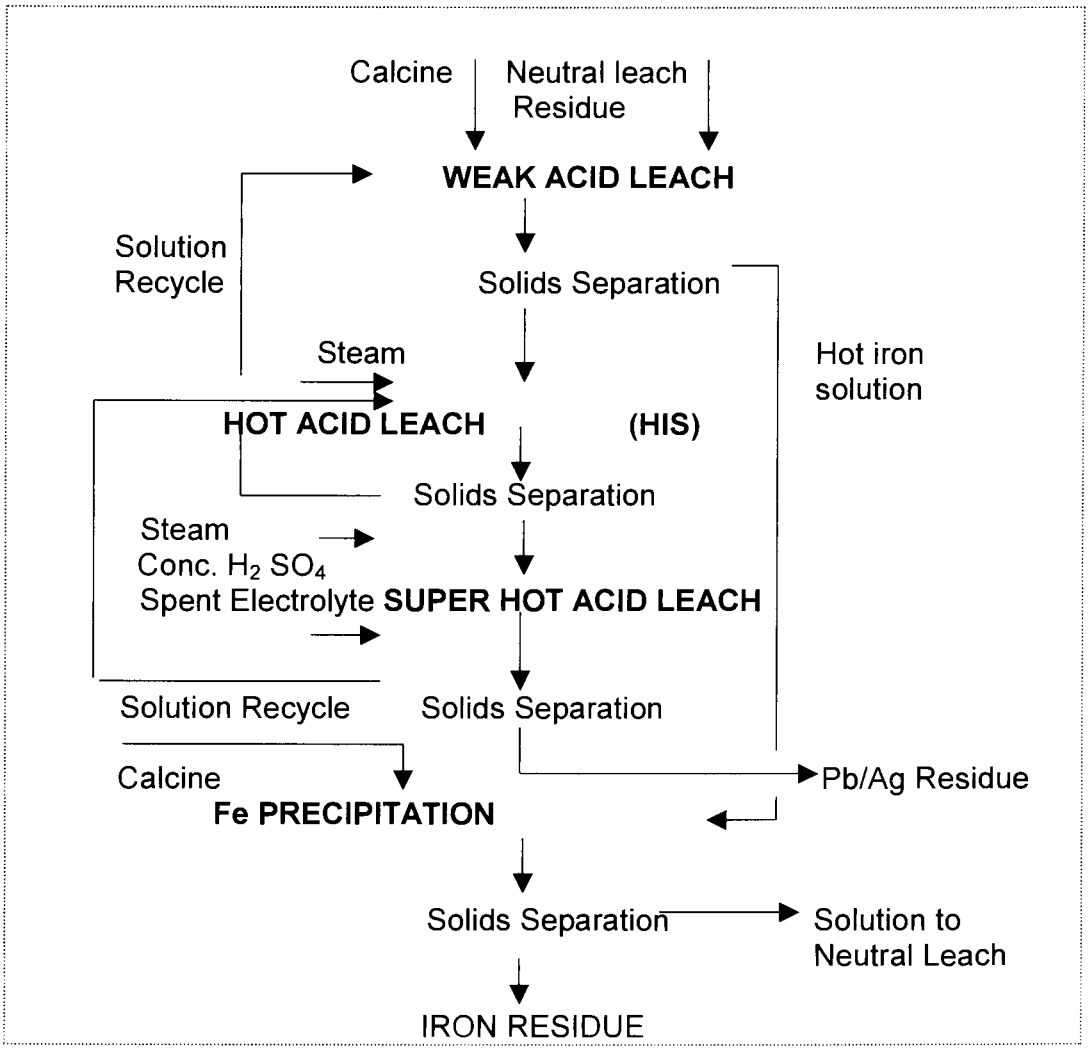

Figure 16: The future Zincor residue treatment circuit (HALP section; refer Figure 14).

The function of the weak acid leach step is mainly to neutralise excess acidity in the HIS before it is fed to the iron precipitation stage. Residual acidity over the weak acid leach stage will be decreased to approximately 10 g/l H_2SO_4, which would allow for operating the hot- and super hot acid leach stages at higher acidities. The higher expected acidities over the hot- and super hot acid stages are expected to dissolve more silica (and iron), which would probably also be removed during iron precipitation.

Despite all the improvements made to the Zincor iron removal process over more than three decades, process upsets still occur and insoluble zinc losses are still high compared to other iron removal processes (refer to Sections 1.5 and 1.6).

Various ideas were put on the table but it was soon realised that a lack of knowledge of Zincor's iron removal process was to blame for some of the difficulties experienced. The fact that this iron removal process is not used as widely, as for example the jarosite and goethite processes, as well as the difficulties associated with the characterisation of hydrometallurgical plant residues, probably contribute to the fact that certain aspects of the process are not well understood. Currently, the main areas of interest to Zincor include the nature of the amorphous iron phase(s) and whether it is possible to further improve the process after over three decades of operating the Zincor iron removal process.

The ensuing sections aim to address these issues as part of an exercise to optimise zinc recovery over the residue treatment circuit. First of all, the characterisation of the phases present in the iron residue will be discussed and then the optimum operating window will be defined in terms of controllable operating parameters. This part of the study will also deal with the use of alternative neutralising reagents as a means to reduce insoluble zinc loss associated with the iron residue.

2.2 Optimisation of the iron removal process

The optimisation of the Zincor process involves amongst other things the minimisation of both soluble- and insoluble zinc losses. However, before trying to improve zinc recovery in the iron removal process, it is essential that a proper understanding of the Zincor process be developed. In the next section the characterisation of the Zincor Process and the residues formed are discussed in detail.

2.3 Residue characterisation

2.3.1 Background

The characterisation of para-goethite (PG) residues has not received the same amount of attention in the past than for example jarosite residues. This is not strange when considering the fact that by 1995 approximately 67% of zinc produced in hydro-metallurgical zinc circuits went through a jarosite residue treatment process.

The information available today on the PG process is therefore mainly from work done at Pasminco's Hobart refinery, the Enirisorse Porto Vesme plant and the Zincor plant. Since not much information is available on the composition of the Hobart para-goethite residue, attention is given to the work previously done at Porto Vesme and Zincor as well as to some earlier work.

One of the earliest indications of the composition of PG residues (from the E.Z. process) is to be found in a paper from Gordon and Pickering [1975]. It was suggested that the precipitate formed, when hot iron solution containing ferric iron is neutralised, might not be goethite. However, when a chemical reaction for the removal of iron

by the E.Z. process was proposed, it showed the phase $Fe_2O_3.H_2O$ as the iron bearing product, which in its chemical form can be written as FeO.OH (goethite).

Cubeddu *et al.* [1996] also proposed that goethite is present along with other hydroxides and an amorphous phase in the Porto Vesme para-goethite residue. To illustrate this fact, a XRD spectrum of a laboratory-produced para-goethite product was included in the paper, which showed the presence of goethite and akaganeite. It was also recognised that the para-goethite residue contains varying amounts of sulphate (5% to 12%).

Van Niekerk and Begley [1991] also recognised that the Zincor iron residue contains a certain amount of sulphate. The iron phase that forms in the Zincor process was suggested to have the general formula $Fe_2O_3.SO_3.H_20$. In its chemical form, this however can be written in many different ways (as hydroxy salts). The exact nature of the Zincor iron residues was, however, not determined.

In order to solve this issue, an attempt was made to characterise Zincor's iron residue by Meyer *et al.* [1996]. However, the exact nature of the amorphous iron phases present was not determined and part of it was assumed to be goethite. It was also indicated in this study that a significant amount of iron (approximately 43%) is associated with one or more amorphous iron phases. These phases therefore appear to play a very important role in iron removal at Zincor and probably in other para-goethite processes as well. This fact makes the characterisation of Zincor's iron residue essential if a proper understanding of the operating parameters that influence iron removal is to be developed.

It is clear that a lot of uncertainty still exists concerning the nature of the so-called para-goethite residue. This probably alludes to the fact that the characterisation of fine-grained heterogeneous iron residues is not a straightforward task. Several analytical techniques are required to characterise these types of residues [Chen and Dutrizac, 1990 and Dutrizac, 1980].

The following paragraphs summarise the steps followed and give a brief discussion of some of the analytical techniques used to characterise Zincor's iron residue.

2.3.2 Experimental

The method used to characterise a heterogeneous residue is probably just as important as the results obtained. A well-planned sampling campaign, careful sample preparation and an understanding of the limitations of the various analytical techniques contribute towards the correct interpretation of the material.

The residue characterisation process involved more or less the following steps: sampling and sample preparation, chemical analysis, X-ray diffraction (XRD), compilation of a mass balance, scanning electron microscopy (SEM), X-ray photoelectron spectroscopy (XPS), Fourier-transform infrared spectroscopy (FT-IR), Fourier-transform Raman spectroscopy (FT-Raman), Mössbauer-effect spectroscopy (MES) and the synthesis of "para-goethite" residue.

Other techniques that can be used to characterise iron residues include ultraviolet-visible spectroscopy (UV-Vis), secondary ion imaging mass spectroscopy (SIMS), Auger electron spectroscopy, electron spin resonance (ESR) spectroscopy, nuclear magnetic resonance (NMR) spectroscopy, X-ray absorption spectroscopy (XAS), electron diffraction (ED), differential thermal analysis (DTA), differential scanning calorimetry (DSC), thermal gravimetric analysis (TGA), optical spectroscopy, transmission electron microscopy (TEM), scanning tunnelling microscopy (STM) and atomic force microscopy (AFM). The basic information on these techniques as well as data for some iron oxides were presented by Cornell and Schwertmann [1996].

The simultaneous use of these techniques to characterise one specific sample would probably not be worthwhile, as it can be very time consuming, expensive and a duplication of work in some instances. Generally, the techniques, which can complement each other, are selected. In this way, enough information can be gathered to describe the sought after phase(s) to the extent required. The techniques selected to characterise Zincor's iron residue as well as the experimental details are discussed in the following paragraphs.

2.3.2.1 Sampling and sample preparation

The iron precipitation stage was sampled in three campaigns over a six-month period. Samples were taken from the HIS stream, calcine slurry stream, iron precipitation tanks one, two and four and iron thickener underflow. The samples were taken from the overflow launders of the respective tanks.

The slurry samples were immediately filtered and taken to the laboratory. The filter cakes were washed with hot distilled water and dried at 100°C for 2 to 3 hours. Dried samples were subsequently divided into several portions for the following series of analyses.

Factors that need to be considered during sample preparation include:

- The composition of samples can be altered due to ageing effects. Therefore, depending on what analyses are required, the samples should be thoroughly washed before storing it.
- Drying of samples can also alter the composition of highly hydrated and adsorbed phases for example.

2.3.2.2 Chemical analysis

The first stage filtrate and the washed filter cakes were analysed in Zincor's plant laboratory.

2.3.2.3 XRD analysis

XRD is probably one of the best known and most widely used analytical techniques available. Where-as qualitative chemical tests do not distinguish between different compounds of the same elements, quantitative chemical analysis do not distinguish between polymorphs and refractory index measurements are not applicable to opaque minerals, X-ray methods can be used to identify all crystalline materials. However, most hydro-metallurgical plant residues contain some amorphous material. These amorphous phases and/or very fine particles are usually not easily detected in the presence of crystalline phases. Poorly crystalline phases are suppressed in the background noise or give very broad peaks, which are difficult to use for characterisation purposes. Nonetheless, at least part of a heterogeneous sample can be analysed by using XRD.

XRD involves the interaction of electromagnetic radiation with a wavelength comparable to the distances between atoms (nm scale), with atoms in a solid. At certain angles of incidence (Θ-Bragg angle) the scattered rays interfere constructively, giving higher intensities. An X-ray spectrum of a single crystal or powdered sample is therefore a plot of intensity versus the Bragg angle.

Minerals are identified by using these peak intensities as well as the characteristic set of d-values. The d_{hkl}-values or atomic interlayer-spacings are calculated from the Bragg equation (eq. 6) when a series of n reflections are produced.

$$n\lambda = 2d_{hkl} \sin\Theta \quad \text{.....6}$$

In this study, powdered samples (dried residue filter cake was slightly grinded using a mortar and pestle) were analysed using Cu-Kα radiation, which has a typical wavelength of approximately 0.154 nm.

2.3.2.4 Distribution of iron in the residue

The information gathered from the chemical- and XRD analyses was used to compile a preliminary residue composition. The preliminary residue composition highlights the deportment of iron in one or more amorphous phases.

The techniques that follow were selected to specifically supply information on the amorphous iron phase(s) present as well as the abundances of both crystalline- and amorphous phases in the residue.

2.3.2.5 SEM

This high magnification, high resolution electron microscopy technique can be used to great effect when combined with XRD. It can supply semi-quantitative information on the composition of the phases present, it can illustrate the morphology of the sample and the backscattered mode can be used to indicate phases with higher atomic numbers such as lead. As an observation technique, it is also useful in obtaining an idea of the genesis of hydrometallurgical residues notably when particles have a layered appearance.

Since the powdered samples were statically charged during data acquisition, samples were set in an epoxy resin. Specimens were subsequently covered with a very thin conductive layer (gold in this case) and electrically connected to the sample holder with a piece of carbon tape to improve the visual quality.

A JOEL JSM 6300 instrument was used to acquire all the data. The accelerating voltage was kept at 15 kV at all times.

2.3.2.6 XPS

X-ray Photoelectron Spectroscopy involves irradiating a sample under vacuum with mono-energetic soft X-rays and analysing emitted electrons by energy level. Mg Kα X-rays were used and because the photons have limited penetrating power in a solid (only 1 to 10 μm) the technique is usually used to investigate surface phenomena.

Photons interact with atoms causing electrons to be emitted by the photoelectric effect. Emitted electrons have specific kinetic energies and the spectrum obtained is a plot of the number of detected electrons per energy interval against its kinetic energy. Each element has a unique spectrum and the spectrum from a mixture of elements is approximately the sum of the peaks of the individual elements.

The technique is very useful to obtain quantitative data. Peak heights or peak areas are usually measured to give an indication of the abundance of an element.

In this study, a PHI 5400 X-Ray Photoelectron Spectrometer was used. Samples were manually ground with a mortar and pestle to obtain a uniform fine powder. The powder was subsequently pressed into indium pellets to hold the material into place under high vacuum. The vacuum inside the chamber was always better than 2×10^{-8} torr during acquisition of the data. The instrument was operated at 15 kV and 300 W.

Because the samples were not good electrical conductors, even as mounted in indium, a static charge accumulated on the surface when exposed to X-rays. The effect of this charge was corrected by noting the shift of the carbon 1s peak at high resolution relative to the reference value of 284.6 eV.

2.3.2.7 FT-IR spectroscopy

Fourier – transform infrared spectroscopy is a variation of the better known IR spectroscopy. FT-IR gives better resolution and an improved signal to noise ratio (increased sensitivity). It also allows more rapid data collection compared to the conventional IR spectroscopy method.

An infrared spectrum is a plot of the percent radiation absorbed against the frequency of the incident radiation given in cm^{-1}. The plot is a result of the interaction between sample material and electromagnetic radiation in the wavelength range 1 to 300 μm or 10 000 to 33 cm^{-1}. Every compound has its characteristic IR bands, which results from the excitation of vibrations or rotation of molecules in the ground state and are associated with stretching deformations of the interatomic bonds and bending deformations of the interbond angles.

Mid-infrared absorbance spectra obtained were recorded with a Bruker® 113V FT-IR spectrometer. The instrument was evacuated during recordings to remove CO_2 and water vapour. The resolution was always better than 2 cm^{-1} and the spectra were baseline corrected to make comparisons between spectra easier.

The sample preparation involved mixing powder with KBr (1 mg sample and 100 mg KBr), grounding the mixture to a fine uniform powder and pressing it into pellets. In some cases, the pellets were also heated for 3 hours at approximately 150°C to remove as much water as possible.

2.3.2.8 Raman spectroscopy

The technique provides complementary information to IR data. Samples are usually measured in the ultraviolet or visible regions and not the infrared region as in IR spectroscopy. Raman bands shown on spectra are a result of a change in the polarisation of the system when molecules are electromagnetically radiated.

Due to relatively high noise levels and heating effects, Raman bands generated in this study were not very distinct even at liquid nitrogen temperature and the results obtained are therefore not discussed in the next section.

2.3.2.9 MES

The ^{57}Fe Mössbauer technique only detects Fe-bearing phases within a sample, *i.e.* it is "blind" to most other isotopes. This characteristic feature makes it the ideal technique to characterise both the crystalline- and the amorphous phases present in an iron residue.

The sensitivity (MES can detect changes in nuclear levels as small as 1 part in 10^{12}) to the local surroundings of ^{57}Fe atoms is a result of recoilless γ-ray emission and adsorption by the source and the ^{57}Fe nuclei, respectively. The local surroundings of the iron nuclei are primarily constituted by the electronic structure of the Fe atom, the compositional make-up of neighbouring atoms and neighbouring defect structures. Therefore, in the case of iron-bearing compounds, the local-probe nature of the technique makes it a powerful non-destructive analytical tool for establishing oxidation state of iron,

quantifying the abundance's of different iron compounds within the same sample (*i.e.*, phase analysis) and establishing the overall crystal chemistry when used in conjunction with complementary techniques such as XRD and SEM.

Typically, iron-phase abundances as low as 5% may be detected with high accuracy. As an atomic-scale local probe, it is therefore equally effective in the analysis of poorly crystalline or amorphous materials where conventional macroscopic-type probes such as XRD have considerable limitations.

Spectral parameters (the so-called hyperfine interactions), that are used in conventional transmission MES to characterise the chemical state of Fe in the solid phase, are the isomer shift δ (provides information about coordination number, valency and spin state), quadrupole splitting ΔE_q (provides information about site distortion) and internal magnetic field B_{hf} (provides information about valence and magnetic properties of the compound).

In terms of sample preparation, each sample was mounted in a specially designed powder-clamp holder (ϕ=1.5 cm). Sample quantities of 30-40 mg at densities of approximately 15 mg/cm^3 and 30 mg/cm^3 were used for room- and low temperature (7K) measurements, respectively. The samples were grounded under acetone using an agate pestle and mortar, thoroughly mixed with an inorganic buffer material to obtain the above mentioned densities and the mixture of sample and buffer distributed in the sample holder to form a disk of uniform thickness for transmission Mössbauer measurements.

^{57}Fe Mössbauer measurements were performed in conventional transmission geometry. A K3 Austin Associates linear motor, driven by a triangular reference waveform, was used to scan the resonance profile. A Kr-CO_2 proportional counter was used to detect the transmitted 14.4 keV resonance radiation from a ~25 mCi ^{57}Co(Rh) radioactive source. The spectra obtained are therefore plots of the transmission of γ-rays against the velocity of its source.

Typical count-rates in the discriminator window set to select the 14.4 keV resonance radiation were in the range of 2000-4000 counts per second. Data acquisition of each spectrum and its mirror image was for a period of 12-24 hours to obtain ~100000 counts in each of 1024 channels of a PCA-based multi-channel analyser. Prior to analysis, each spectrum was folded with its mirror image and adjacent channels subsequently added. This serves to remove geometrical base-line distortions and reduces the ($\sqrt{N}$) statistical scatter in the final data set used for analysis.

The fitting program, NORMOS, (distributed by WISSEL-Germany) was used for theoretical fits of the data with Lorentzian lineshapes to deconvolute various sub-components (phases) in the spectrum. A minimum number of sub-spectra (doublets and sextets) were used to obtain the best fit to the total spectrum. In the case of strongly overlapping components or for components with abundance's near the detection limit of ~5%, linewidths were normally constrained to be equal to that obtained for the most intense well-resolved component or that obtained for an Fe reference foil (typically 0.30 – 0.35 mm/s). This reduces the number of fitting parameters.

Distinct Fe-bearing phases or oxidation states were identified in theoretical fits to the spectrum at room temperature through the hyperfine interaction parameters of each spectral component: isomer (centroid) shift IS, quadrupole (doublet) splitting QS, and magnetic hyperfine field B_{hf}. Phase abundances were obtained from the area under each of the spectral components.

2.3.2.10 Synthesis of Zincor's amorphous iron phase(s):

The experimental setup used to precipitate synthetic iron containing phases is shown in Figure 17.

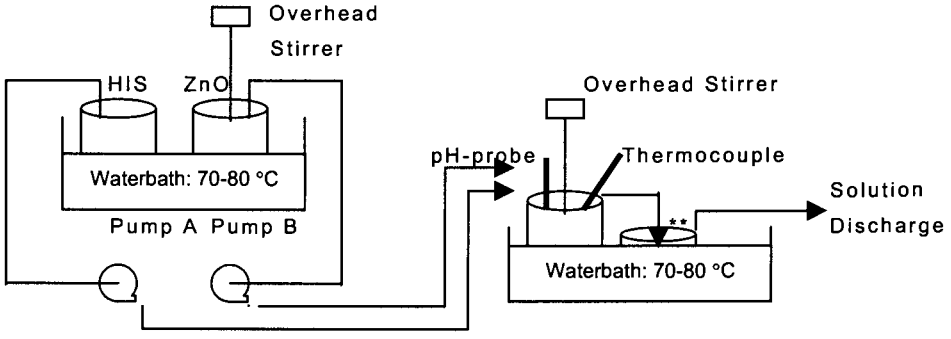

(**Second tank used for sample collection purposes only)

Variable	HIS	ZnO Slurry	Fe – precipitate
Acidity (g/l)*/pH	20.0*	6.0	3.2
Flow rate (ml/min)	15.5	4.5-5.5	---
Temperature (°C)	60	60	60
% Solids	---	12.5	---
Zn (g/l)	90	0	---
Ferric iron (g/l)	25	0	---
Ferrous iron (g/l)	5	0	---

Agitator speed was approximately 120 rpm.

Figure 17: Experimental setup, solution/slurry compositions and conditions used to precipitate synthetic iron containing phases.

The experimental setup reflects the modus operandi of the Zincor process. The HIS and ZnO-slurry were simultaneously fed to the precipitation reactor. HIS was fed at a fixed flow rate whereas the ZnO-slurry flow rate was manually controlled (Pump B) to maintain the precipitation pH at 3.2 $\pm$ 0.05 (the pH-probe was calibrated hourly) for a period of 5 hours.

Temperature in the precipitation vessel was automatically controlled within 1°C of the setpoint. Chemically pure reagents (ferrous sulphate, ferric sulphate, zinc oxide, zinc sulphate and sulphuric acid) from Associated Chemicals Pty. Ltd. and distilled water were used to make up the HIS and the oxide slurry.

After 5 hours, the collected precipitate was filtered and thoroughly washed with hot water. The filter cake was then dried at 70°C for approximately 2 hours.

The synthetic iron precipitate was prepared for XRD-, SEM- and MES analysis.

2.3.3 Results and discussions

2.3.3.1 Chemical Analysis

The assays obtained for the actual Zincor process plant iron precipitate are presented in Tables 4 and 5. The samples were taken from the overflow launders of the respective tanks during normal operations (refer to Section 1.5.4).

Table 4: Compositions of washed filter cakes from Zincor Plant.

Set	1				2				3			
Position	CS	Fe T1	Fe T2	Fe T4	CS	Fe T1	Fe T2	Fe T4	CS	Fe T1	Fe T2	Fe T4
%Fe	13.0	36.7	36.8	34.9	12.5	36.4	36.3	35.8	13.7	35.1	35.6	36.2
%Zn	39.3	9.2	8.7	8.8	41.7	9.4	7.2	6.8	41.2	9.03	6.79	6.83
%Pb	2.1	2.3	2.2	2.0	2.1	2.5	2.4	2.4	2.4	3.0	3.0	3.1
%SO4	8.5	11.4	13.1	13.5	12.1	12.6	13.4	13.6	10.4	10.4	11.0	11.7
%S*	3.7	4.8	5.3	5.4	3.8	4.0	4.4	4.2	3.8	4.1	4.4	4.5
%SiO2**	2.43	4.78	4.23	4.26	3.5	9.3	9.7	9.9	1.89	2.95	2.89	2.85
%Na	0.01	0.01	0.01	0.01	6E-3	9E-3	1E-3	1E-3	0.02	0.02	0.02	0.02
%K	0.02	0.03	0.03	0.03	0.02	0.05	0.07	0.07	0.03	0.05	0.06	0.06
%Ag	0.01	0.01	0.01	0.01	0.01	0.01	0.01	0.01	0.01	0.01	0.01	0.01
%Al	---	---	---	---	---	---	---	---	0.2	0.6	0.6	0.7
%Cu	---	---	---	---	---	---	---	---	0.78	0.95	0.67	0.79
%Ca	0.82	0.17	0.18	0.2	0.76	0.21	0.14	0.19	---	---	---	---
%Ge	7E-3	6E-3	7E-3	9E-3	3E-3	5E-3	6E-3	6E-3	---	---	---	---

CS=calcine slurry taken from feed launder; Tx = number of tank of 4 in series

* Elemental sulphur: water insoluble

** Silica: solubilised with HF (from gangue material and precipitated silica)

Table 5: Composition of collected filtrate (Plant samples)

Set	Position	Fe^{2+} g/l	Fe^{3+} g/l	Zn g/l	SO4 g/l	H2SO4 g/l	SiO2 ppm	Na ppm	K ppm	F ppm	Cl ppm	Mn g/l
1	CS	0.34	0.45	80	208	1.6	---	139	111	0.04	276	4.9
	HIS	2.46	30.24	113	286	28.0	---	148	72	0.93	296	6.1
	Fe T1	1.68	2.13	124	243	1.6	---	145	89	0.05	276	5.5
	Fe T2	2.02	2.13	124	236	2.8	---	145	71	0.08	284	5.4
	Fe T4	1.90	2.08	124	254	2.0	---	142	64	0.47	274	5.7
2	CS	2.61	0.62	85	155	1.0	21	84	101	0.4	225	3.5
	HIS	4.2	26.33	93.8	256	15.2	1050	116	14	1.6	<1	5.7
	Fe T1	6.05	0.39	111	207	1.8	57	96	21	0.2	303	4.7
	Fe T2	5.85	0.82	109	208	1.4	98	98	4	0.6	301	4.7
	Fe T4	5.85	0.53	108	207	2.0	79	95	2	0.4	295	4.7
3	CS	0.39	0.17	79.5	153	0.5	12	67	96	0.1	216	4.6
	HIS	3.3	16.13	84	291	19.4	623	187	14	1.6	<1	8.3
	Fe T1	2.46	0.31	112	223	0.3	86	130	8	0.2	223	6.3
	Fe T2	2.58	0.22	114	226	0.8	131	132	2	0.2	285	6.4
	Fe T4	2.24	0.27	113	218	0.3	102	123	1	0.1	225	6.4

CS = calcine slurry taken from feed launder; Tx = number of tank of 4 in series

No assays were obtained for elements such as nickel, chromium, titanium, cobalt, etc. Typical values for these and other elements are listed in Meyer *et al.* [1996].

2.3.3.2 XRD Analysis

The results from the XRD analysis are summarised in Table 6.

Table 6: Mineralogical composition of the neutralising agent (calcine) and Zincor's iron residue (refer Section 5 for list of relevant minerals and XRD spectra).

Set	Sample identification	Main	Minor	Accessory	Trace
1	**CS 035 calcine slurry**	Zincite	Franklinite	Quartz, Silica oxide & Silicates (other)*	Willemite. Anglesite, Sphalerite
	Fe 435 Iron ppt.	Franklinite	Quartz	Plumbo-& Argento jarosite	Willemite, Sphalerite
2	**CS 719 calcine slurry**	Zincite	Franklinite, Silica oxide	---	Willemite. Anglesite, Sphalerite, Quartz, Silicates (other)*
	Fe 719 Iron ppt.	Franklinite, Plumbo-& Argento jarosite	---	---	Willemite, Quartz
3	**CS 927 calcine slurry**	Zincite	Franklinite	Quartz, Silica oxide & Silicates (other)*	Willemite. Anglesite, Sphalerite
	Fe 927 Iron ppt.	Franklinite	Plumbo-& Argento jarosite, Quartz	Willemite	Plagioclase

Silicates (other)*: include Fe-silicates, Pb-silicates, larsenite and alamosite

These results are more or less in agreement with the work done by Meyer *et al.* [1996]. The presence of the highly crystalline zinc spinel, *i.e.* franklinite, was easy to recognize and is an indication of the stability of this species under the iron removal process conditions. Most of the insoluble zinc losses are also associated with franklinite as discussed in previous sections.

In terms of other iron-bearing phases present in the iron residue, it was found that plumbo- and argento-jarosites gave the best fit to the data. The alkali jarosites, *i.e.* sodium- and potassium-jarosite, however, cannot be discarded and small amounts are probably present.

No hydronium-jarosite was found, which is in agreement with the findings of Wang *et al.* [1985] who indicated that hydronium-jarosite is more stable at temperatures above 100°C. The presence of solid solution phases such as K-hydronium- and Na-hydronium jarosite are therefore also to be doubted.

Another crystalline iron-bearing phase that was expected to be present in the residue, is beaverite ($PbCuFe_2(SO_4)(OH)_6$). However, no trace of this mineral was found; it is also not clear in what form the relatively large amount of copper in the residue (refer Table 4) is.

Both the chemical analysis of the iron precipitate as well as the XRD analysis indicated the presence of unexpectedly high levels of silica. Apart from the presence of willemite and gangue material, which include plagioclase ($CaAl_2Si_2O_8$) and quartz, silica might also be present in the form of other silicates that include lead silicate ($Pb_3Si_2O_7$), alamosite ($PbSiO_3$), larsenite ($PbZnSiO_4$) and iron

silicate (Fe_7SiO_{10}). Another source of silica is probably silica in solution. Table 5 shows levels of silica in the HIS as high as 1 g/l from which, what appears to be a crystalline form of silica (silica oxide-synthetic SiO_2, quartz), is precipitated.

2.3.3.3 Distribution of iron in the precipitate

An effort was made to determine how much of the iron present in the actual Zincor plant iron precipitate is unaccounted for by the XRD-analyses. By combining the information obtained from the chemical – and XRD analyses, an idea of the amount of iron that is unaccounted for by the XRD analyses could be obtained (refer to Table 7).

Table 7: Approximation of the distribution of iron in Zincor's iron residue.

Sample: Set 3, Fe T4		
Element/Compound:	**Symbol/Formula**	**Analysis***
		(g/kg)
Iron	Fe	362
Zinc	Zn	68.3
Lead	Pb	31
Sodium	Na	0.2
Potassium	K	0.6
Silver	Ag	0.1
Sulphate	SO4	117
Sulphur	S	45
Total sulphur	S + SO4	84.1
Jarosites:		
Plumbo jarosite	PbFe6(SO4)4(OH)12	160.68
Argento jarosite	AgFe3(SO4)2(OH)6	0.53
Sodium jarosite	NaFe3(SO4)2(OH)6	4.22
Potassium jarosite	KFe3(SO4)2(OH)6	7.69
Sub-total Fe (g/kg): [Fe in jarosites]	**50.3**	
Other phase(s):		
Franklinite	ZnO.Fe2O3	239.3
Sub-total Fe (g/kg): [Fe in franklinite]	**110.9**	
Unaccounted Fe:		
Amorphous phases		
Sub-total Fe (g/kg):	**200.8**	
Total (g/kg Fe):	**362**	
% Fe in amorphous phase(s)	**55**	

*Chemical analyses of the actual Zincor plant iron residue.

The calculations were based on the assumptions that 95% of the zinc present is associated with franklinite and that 95% of the lead available is contained in plumbo jarosite. These assumptions resulted in an insoluble zinc loss of almost 7%, which is a very realistic figure.

The table proves that the bulk of the iron removed (approximately 80% of the precipitated species) in the actual Zincor process is in a poorly crystalline form or as very fine particles. A definite effort should therefore be made to study the amorphous iron phase(s) present in the iron residue as it appears to play an important role in the removal of iron from Zincor's circuit.

2.3.3.4 SEM Analysis

The SEM used in backscattered mode showed the presence of basically three iron species in the Zincor iron residue. Figure 18 shows a particle, which contains only Fe and O. The high surface area (open structure) is a characteristic feature [McCristal and Manning, 1998] of the so-called para-goethite precipitate.

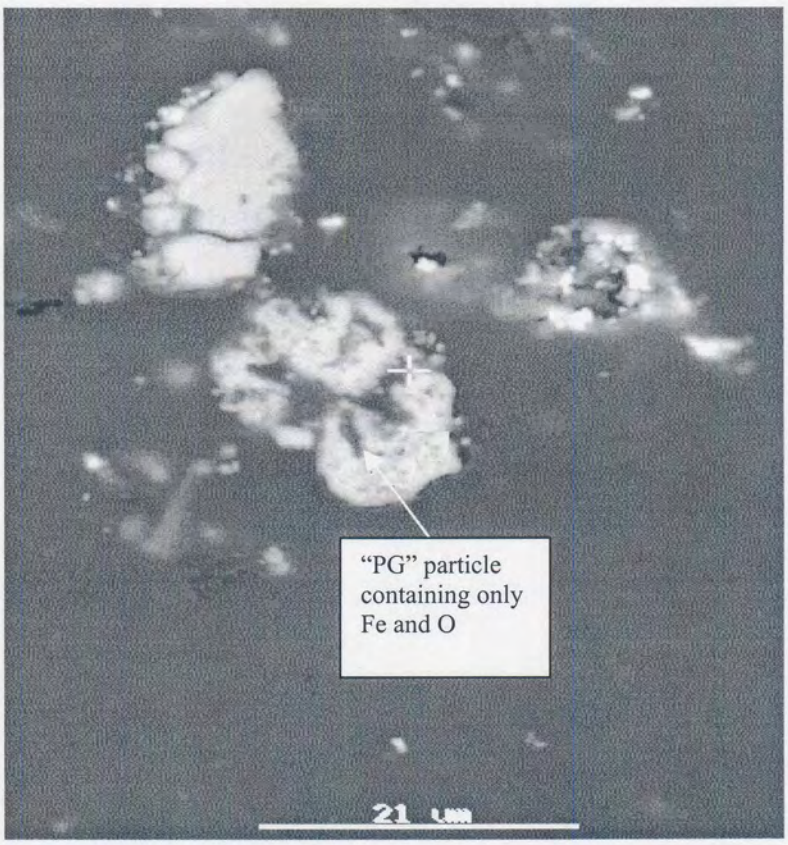

Figure 18: SEM image of a so-called para-goethite particle. Sample taken from the overflow launder of the first precipitation tank (Backscattered mode).

Figure 19 shows an iron phase that contains mainly Fe, S and O.

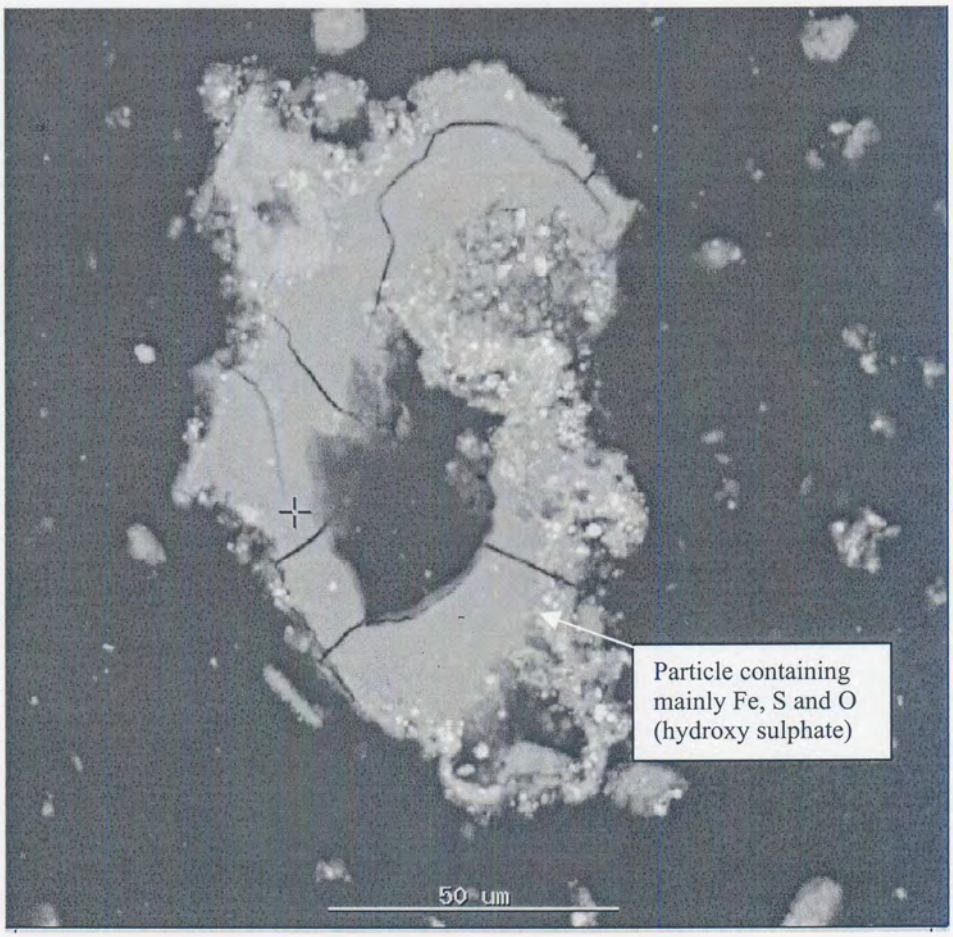

Figure 19: SEM image of an iron-bearing particle containing sulphur. Sample taken from the overflow launder of the fourth precipitation tank. (Backscattered mode)

The last distinct iron-bearing phase that was identified is shown in Figure 20. Here the iron precipitate contains a significant amount of lead and is associated in most cases with distinct $PbSO_4$ inclusions.

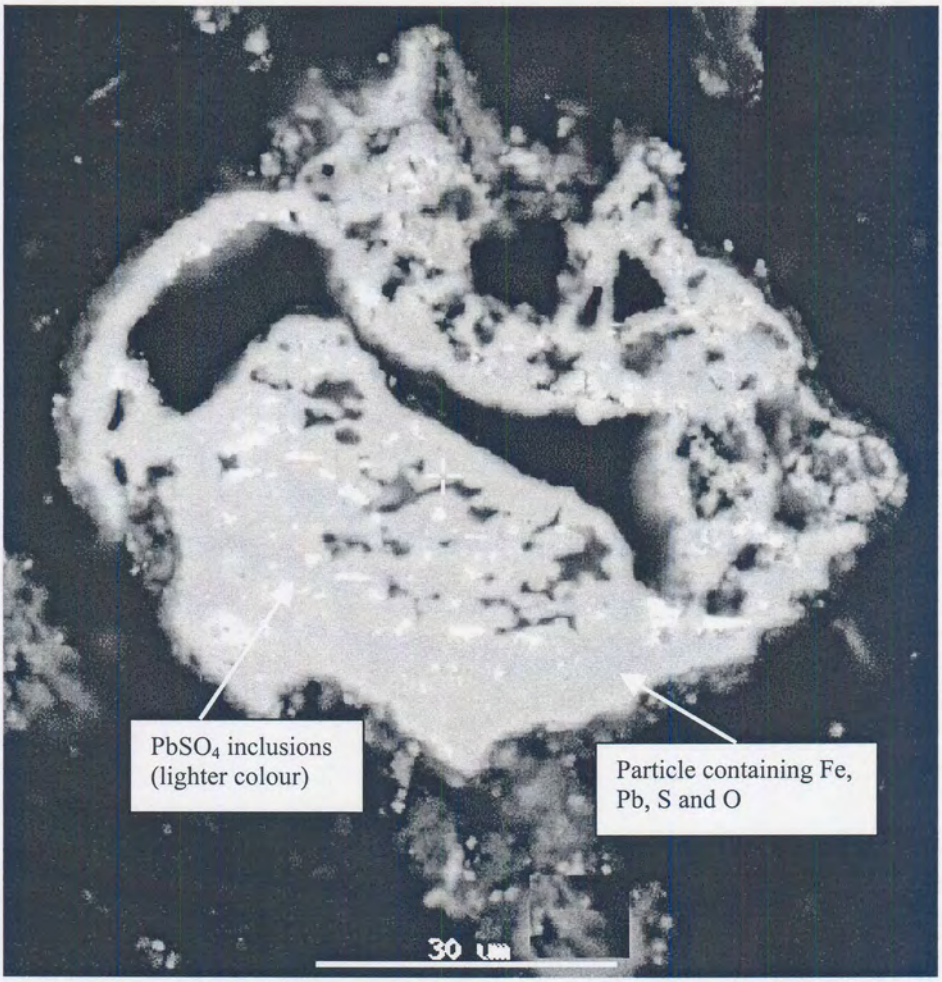

Figure 20: SEM image of an iron-bearing particle containing lead. Sample taken from the overflow launder of the second precipitation tank. (Backscattered mode)

Figure 20 probably depicts a particle that contains plumbo-jarosite. It is well known that Pb-jarosite forms when anglesite reacts with ferric sulphate, which explains the presence of $PbSO_4$ inclusions in many of the iron-bearing particles. The SEM study also showed that the precipitate formed in the first tank contained a much larger portion of the so-called "PG"-particles (Figure 18: phase that

contains only Fe and O) than the final residue (material from tank 4). In the few cases where "PG"-particles were found in the final residue, it was covered with the iron-bearing phase that also contains sulphur (sulphate). This is shown in Figure 21.

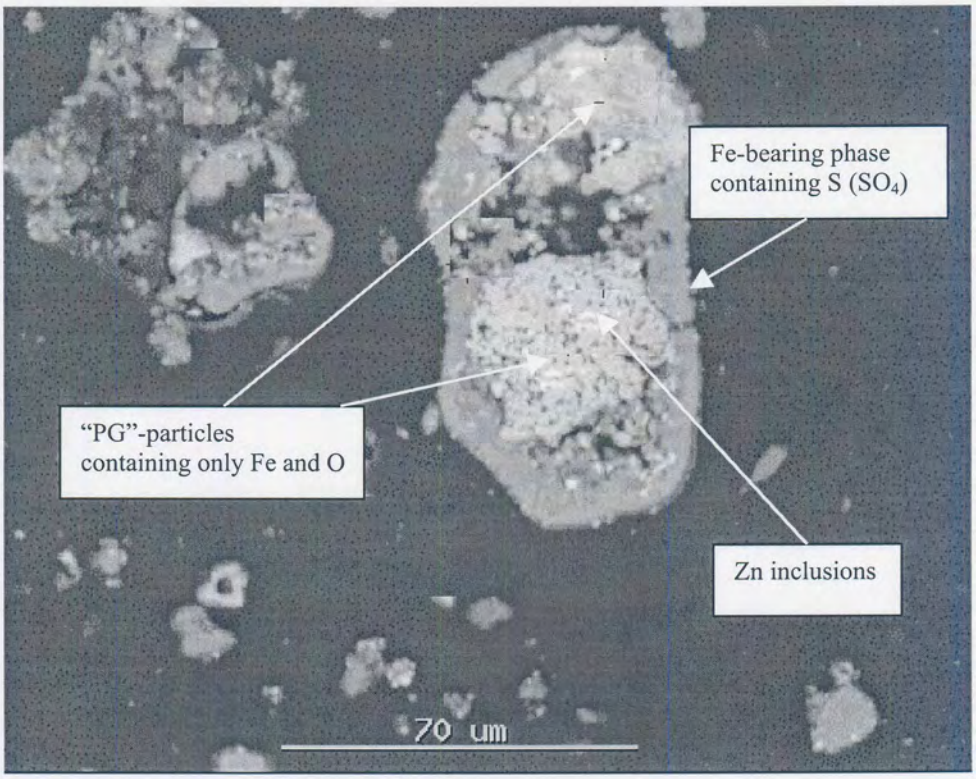

Figure 21: SEM image of an iron-bearing particle with two types of precipitates. Sample taken from the overflow launder of the fourth precipitation tank. (Backscattered mode)

It was found that the final residue contains more of the sulphate-containing phase than the precipitate from the first tank. Table 4 confirms the increase in the amount of sulphate in the precipitate from tank 1 to tank 4. This change in the residue composition is probably a result of the "acid wash" that was incorporated into the iron removal step, which aims to reduce zinc losses. The

effectiveness of the "acid wash" in the second iron removal tank was confirmed with data obtained from XPS. The oxygen and sulphur contents of the precipitates from tank 1 are compared with those from the second tank in Table 8.

Table 8: Atomic % of total O and S calculated for two residue samples (Set 1: Fe T1 and Fe T2) obtained from XPS analyses.

Oxygen species	Precipitation tank #1	Precipitation tank #2
Oxide	23.3	5.6
Hydroxide	16.4	35.0
Sulphate*	60.3	59.4
Sulphur species		
Sulphate	72.6	89.7
Sulphide	9.5	10.2
Thiosulphate	17.9	0.0

* This sulphate includes sulphates of zinc, iron sulphate, thiosulphates and sulfoxy species such as hydroxy salts (jarosites). The distribution of the species in tank 2 is more or less the same than in the last tank.

The reduction in the oxide content from the first to the second tank is accompanied by a reduction of almost 16% in the zinc content of the residue. However, it appears as though iron oxide(s) are also redissolved in tank 2 and reprecipitated as hydroxy sulphate(s). The increases of 113% and 23.5% of respectively the hydroxide and sulphate contents of the precipitate might be as a result of this. This phenomenon would also explain why most of the "PG"-particles in the final residue are covered with a sulphate containing iron phase.

It appears therefore that at least two additional iron phases, which are probably amorphous to X-rays, were identified from the SEM study. The presence of plumbo-jarosite in the iron residue was also confirmed. The exact compositions of the additional phases could however not be determined.

With the aid of XPS it was also shown that the composition of the iron residue is significantly altered by the "acid wash" applied in the second iron precipitation tank. It could therefore be deduced that the final residue composition is not only a function of the operating conditions prevailing in the first precipitation tank where most of the iron is removed but also of the conditions applied in the second tank.

2.3.3.5 MES Analysis

XRD analysis indicated the presence of various crystalline phases in the iron residue and by combining this information with the chemical analysis it was found that most of the iron is actually present as poorly crystalline phase(s). SEM studies showed that the amorphous phases are probably in the form of one or more iron hydroxide or oxide hydroxide (the so-called para-goethite particles) and one or more hydroxy sulphate (excluding jarosites). The exact nature of these amorphous iron phases however has not been determined and will subsequently be investigated.

To start off with, a list of all the candidate phases, which comprised of goethite and its polymorphs, bernalite ($Fe(OH)_3$), ferrihydrite, different jarosite species, franklinite and schwertmannite, with its characteristic hyperfine interaction parameters, was compiled. Two samples were selected (Fe 4719-set 2, Fe T4 and Fe 4927-set 3, Fe T4) for Mössbauer analysis at room- (≈300K), liquid nitrogen- (≈77K) and liquid helium temperature (≈5K). A calcine sample was also analysed at room temperature. The results obtained from the Mössbauer analysis were compared with the tabled values. Since the various minerals are magnetically ordered at different temperatures, goethite and akaganeite (the two most probable oxide hydroxide phases) were both discarded after no sextets were found at respectively room- and liquid nitrogen temperature. Lepidocrocite was discarded on the basis of a different precipitation mechanism and precipitation conditions that prevails during its formation (refer Figure 10). Bernalite was also discarded after the liquid nitrogen temperature analysis as no sextet was found. A shortened list of the candidate phases was subsequently compiled. Table 9 gives a summary of these phases along with its parameters.

Table 9: MES candidate phases with its nuclear hyperfine interaction parameters.

	RT, 300K			LHe, 5K		
	IS/Fe mm/s	QS mm/s	B_{hf} T	IS/Fe mm/s	QS mm/s	B_{hf} T
Jarosite - Na	0.43 (0.40)	1.20 (1.05)	---	---	---	47.0
Jarosite – K	0.43 (0.40)	1.24 (1.15)	---	---	---	47.0
Jarosite -Pb	0.43 (0.40)	(1.15)	---	---	---	---
$Zn_{0.2}Fe_{2.8}O_4$	0.42 0.75	0.14 0.08	48 (5) 44(5)			
$Zn_{0.4}Fe_{2.6}O_4$	0.40 0.71	0.21 0.15	46.4(5) 41.4(4)			
$Zn_{0.6}Fe_{2.4}O_4$	0.49 0.62	0.08 0.09	42(5) 35(5)			
$ZnFe_2O_4$	0.35(1)	0.33	---	?	-0.1 0.17	50.2 50.3
Ferrihydrite $5Fe_2O_3.9H2O$	0.35	0.71		0.32	0.02	49.2
	0.34	0.71		0.34	0.02	48.4
	0.33 0.34	0.87 0.54		0.33	≈0 ≈0 ≈0	50.8 48.4 44.4
	0.34	0.62		0.47	≈0	49.8
Schwertmannite $Fe_{16}O_{16}(OH)_{12}(SO_4)_2$	0.36	0.64		0.49	-0.41	45.6
	0.33 0.39	0.68 0.68			-0.03 -0.03	44.9 45.0

IS=isomer (chemical) shift, QS=quadrupole (doublet) splitting, B_{hf}=internal magnetic field (sextet splitting)

The parameters for these phases were taken mainly from Stevens *et al.* [1998]. Data was also obtained from Varret *et al.* [1971], Murad [1988], Madsen *et al.* [1986], Bigham *et al.* [1994], Schwertmann *et al.* [1995] and Bishop and Murad [1996]. The results obtained from the MES study are depicted in Figures 22 to 24 and summarised in Table 10.

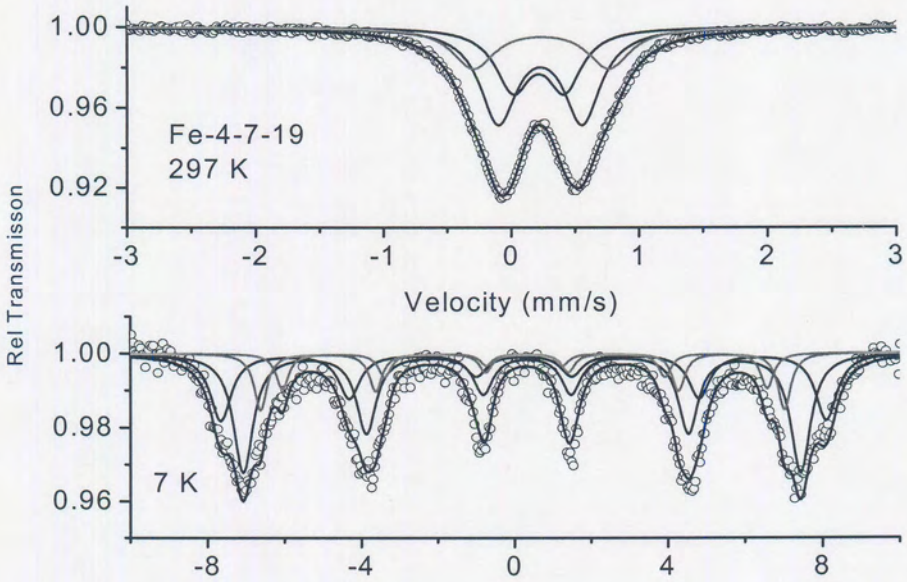

Figure 22: Mössbauer spectra for sample Fe 4719 at room- and liquid helium temperature. The solid lines are theoretical fits to the data (circles).

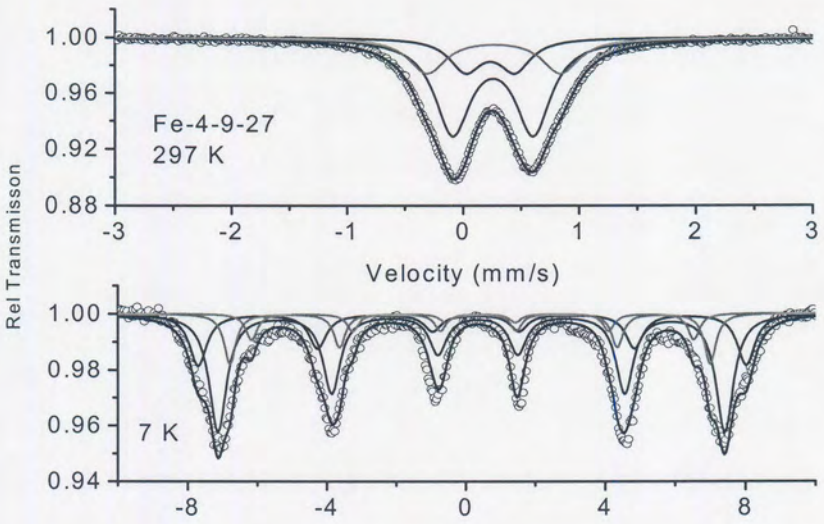

Figure 23: Mössbauer spectra for sample Fe 4927 at room- and liquid helium temperature. The solid lines are theoretical fits to the data (circles).

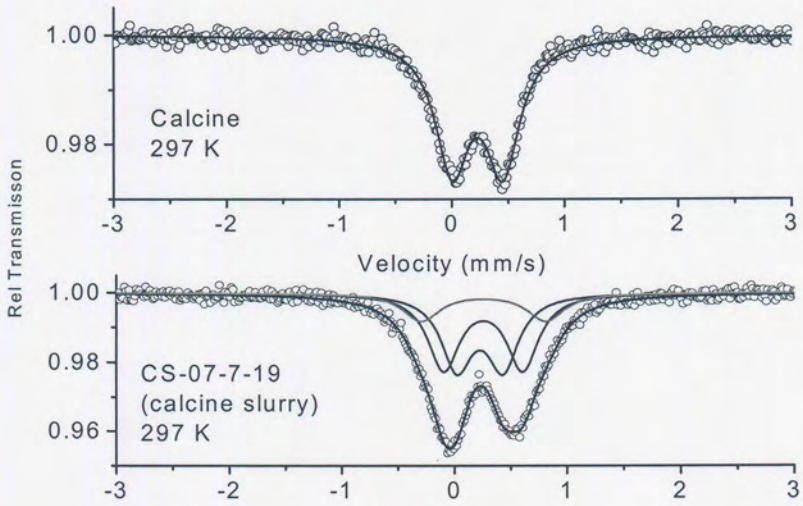

Figure 24: Mössbauer spectra for the calcine samples at room temperature. The solid lines are theoretical fits to the data (circles).

Each spectrum at room temperature was found to be a broadened doublet (non-magnetic or paramagnetic), which is indicative of a super-position of highly overlapping sub-component doublets, *i.e.* there is more than one iron-bearing phase present in the sample. Due to the strong overlap of the spectral components, a minimum number of components have been used to obtain the best fit to the spectra. In most cases, three components were required to obtain a satisfactory fit. In terms of the liquid helium temperature measurements, spectra were found to be a super-position of sextets (super-paramagnetic phases) due to the fact that each phase is below the magnetic ordering temperature and the ^{57}Fe nucleus thus experiences an internal magnetic field as determined by its local electronic and atomic environment. Here again a minimum number of overlapping sextets (four) were used to best fit each spectrum recorded. A very important issue is to judge whether the correct combination of components were used to fit the recorded spectra. The measure used here was to find optimum consistency between the phase abundances at room- and liquid helium temperatures since the phase abundances are not expected to change as the sample is cycled down to cryogenic temperatures. Typical errors obtained when this mode of operation was used varied between 5% and 15%. The parameters and abundances obtained for the fitted spectral lines, which define the different iron phases present are given in Table 10.

Table 10: Phase identification from nuclear hyperfine interaction parameters obtained from fits to the data of various samples.

	297K (room temperature-RT)					
Sample	IS mm/s	QS mm/s	LW mm/s	B_{hf} Tesla	Abundance %	Phase(s)
Calcine	0.23	0.45	0.37	--	100	Fr.
Calcine slurry	0.22	0.42	0.35	--	40	Fr.
	0.25	0.69	0.37	--	42	Sch.
	0.25	1.10	0.40	--	18	Unk.
Fe 4719	0.21	0.41	0.33	--	29	Fr.
	0.23	0.66	0.34	--	48	Sch.
	0.23	1.07	0.39	--	23	Jar.+ Unk.
Fe 4927	0.22	0.42	0.33	--	18	Fr.
	0.26	0.69	0.37	--	59	Sch.
	0.20	1.05	0.39	--	23	Jar + Unk.
	7K (liquid helium temperature-LT)					
Sample	IS mm/s	QS mm/s	LW mm/s	B_{hf} Tesla	Abundance %	Phase(s)
Calcine	--	--	--	--	--	--
Calcine slurry	--	--	--	--	--	--
	--	--	--	--	--	--
	--	--	--	--	--	--
Fe 4719	0.23	-0.03	0.67	49	29	Fr.
	0.26	-0.15	0.62	45	47	Sch.
	0.26	-0.12	0.40*	42	15	Jar +
	0.26	0	0.40*	39	9	Unk.
Fe 4927	0.22	-0.13	0.6	49	24	Fr.
	0.24	-0.21	0.60	45	53	Sch.
	0.23	-0.25	0.40*	43	15	Jar +
	0.30	-0.24	0.40*	39	8	Unk.

Fr. = franklinite ($Zn_xFe_{3-x}O_4$),

Sch. = schwertmannite $Fe_8O_8(OH)_6SO_4$),

Jar. = jarosites ($RFe_3(SO_4)_2(OH)_6$)

At room temperature add 0.114mm/s and at liquid helium temperature add 0.20mm/s to quote the value with respect to Fe-metal at room temperature (for comparison with the literature values in table 9). In ideal samples (crystalline and homogeneous), linewidth values of appr. 0.28mm/s are expected.

* Fixed parameter value to obtain consistency between RT and LT. The two sextets with fixed relatively narrow linewidths of appr. 0.4mm/s may be replaced by a single sextet with a much broader linewidth.

The calcine sample exhibits a symmetric doublet and narrow lines at room temperature. The spectrum was well fitted with one component. The higher QS value (0.45 mm/s) and the line broadening observed (> 0.28 mm/s) might have been a result of the fact that an inhomogeneous $Zn_xFe_{3-x}O_4$ sample was analysed where x probably has a value close to 1. These parameters were successfully imposed in the precipitated samples, which confirmed that zinc ferrite occurred as an unreacted phase in the iron residue.

The calcine slurry sample was distinctly different with an asymmetric doublet (unequal intensities) and broad linewidths. The sample had appreciably more franklinite than the precipitates (40%), a component that is compatible with schwertmannite and an additional unknown component with a large QS value of approximately 1.1mm/s, which is similar to that for jarosite. If jarosite is discounted then this is an unknown, possibly an amorphous phase.

The combination of the unknown component and that ascribed to schwertmannite are similar to the two doublets normally ascribed to ferrihydrite. This possibility therefore cannot be discounted since a detail study was not performed on the calcine slurry. This finding indicates that even the calcine slurrying system might have an effect on the iron removal process. This is an area that needs to be investigated further.

The iron precipitate samples were well characterised by three doublet sub-components at room temperature. The components had small QS values of ≈0.4 mm/s (zinc-ferrite), intermediate value of 0.6-0.7 mm/s (schwertmannite and ferrihydrite) and large QS values of 1.1 mm/s (jarosites and unknown poorly crystalline phase). Because both schwertmannite and ferrihydrite are poorly crystalline

phases [Bigham *et al.*, 1990; Jambor and Dutrizac, 1998], broadened doublets are obtained at room temperature, which make it very difficult to distinguish the phases from each other.

At liquid helium temperature, both phases exhibit sextets and instead of having a well defined internal magnetic field as in typical crystalline samples, a "smeared-out" distribution of magnetic fields are observed, which again make it nearly impossible to distinguish these phases from each other. However, when the frequencies of the magnetic fields obtained are plotted as a function of the magnetic field values, a distribution is obtained with a peak at approximately 49-50T for ferrihydrite and approximately 45T for schwertmannite. These B_{hf} distributions for each phase were modelled in the theoretical fittings using a single sextet with broad linewidths.

Even though it was difficult to distinguish ferrihydrite from schwertmannite in the Mössbauer patterns at both room- and liquid helium temperature, visual inspection of the spectra at liquid helium temperature suggested that there was appreciably more intensity at $B_{hf} \approx 45T$ than at $B_{hf} \approx 50T$. This suggested that schwertmannite is significantly more abundant than any ferrihydrite present in Zincor's final iron residue. This is in agreement with the SEM study findings, which showed that the final residue contains a larger proportion of (a) hydroxy sulphate(s) than hydroxide and/or oxide hydroxide(s).

From the discussions above, it is proposed that the amorphous material in Zincor's final iron residue is comprised of mainly schwertmannite, a small amount of ferrihydrite and a small amount of an unknown phase. MES data obtained for the jarosite species could not be used to distinguish between the different phases present in the residue. The identification obtained from XRD analyses should be used.

2.3.3.6 Synthetic iron analysis

In order to put the presence of schwertmannite and ferrihydrite in Zincor's iron residue beyond any doubt, the Zincor process was simulated using the experimental setup depicted in Figure 17. The conditions in the first iron precipitation tank were simulated.

The chemical analyses of the washed filter cake and the filtrate are presented in Table 11.

Table 11: Chemical compositions of filter cake and filtrate of a synthetic iron residue sample.

Filter cake	**%Fe**	**%SO_4**	**%Zn**
	50.2	14.01	1.28

Filtrate	**g/l Zn**	**g/l Fe^{3+}**	**g/l Fe^{2+}**	**g/lSO_4**
	65	0.04	1.98	107

The values for iron and sulphate obtained for the filter cake are comparable with values quoted in the literature [Bigham *et al.*, 1990]. The synthetic sample prepared here, however, was expected to contain a certain amount of ferrihydrite that needs to be taken into account when interpreting the above-mentioned results.

Two samples (Fe 104 and Fe 123) were prepared for XRD analysis. The spectra obtained for these samples are shown in Figures 25 and 26.

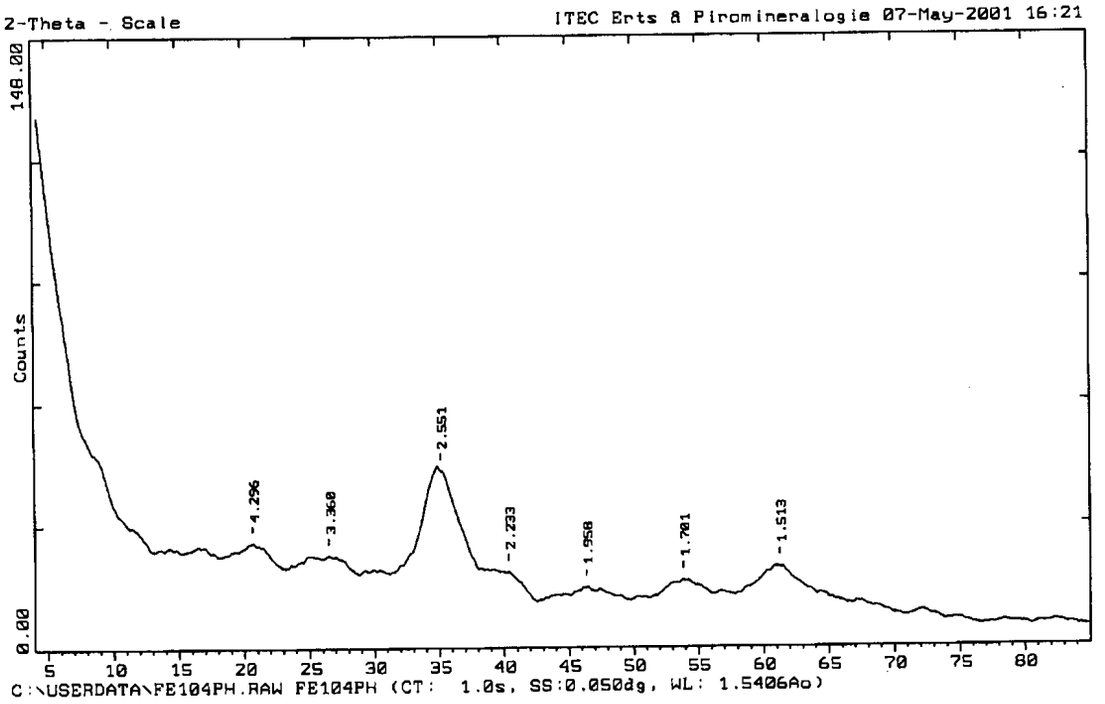

Figure 25: X-ray diffractogram of sample Fe 104.

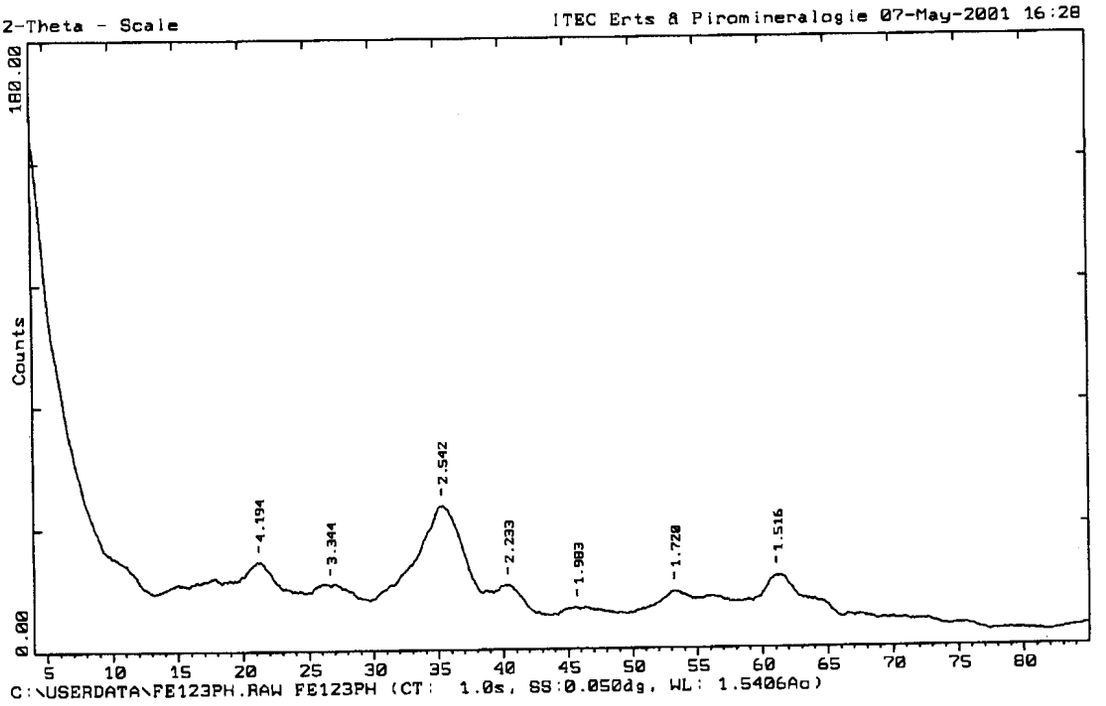

Figure 26: X-ray diffractogram of sample Fe 123.

In order to assist the comparison of the data obtained with that in the literature, Table 12 was compiled. It summarises the d-values of the synthetic samples and values taken from the literature.

Table 12: X-ray results from natural and synthetic iron residue samples.

d-values (nm)				
Zincor synthetic samples		**Schwertmannite**		**Ferrihydrite**
Sample 104	Sample 123	Natural*	Synthetic*	Synthetic**
0.4296	0.4193	0.483	0.502	Uncertain
0.3360	0.3344	0.338	0.334	Uncertain
0.2551	0.2542	0.254	0.255	0.254
0.2233	0.2233	0.233	0.227	0.221
0.1958	0.1983	0.195	0.195	0.198
0.1701	0.1720	0.165	0.166	0.1725
0.1513	0.1516	0.151	0.1561	0.1515
Very weak	Very weak	0.143	0.145	0.147

* **Bigham *et al.*, 1990**

** **Jambor and Dutrizac, 1998**

The XRD spectra depicted in Figures 25 and 26 show two peaks at approximately 21 2θ and 26 2θ, respectively. These two peaks are an indication that schwertmannite is present in the synthetic samples and the d-values summarised in Table 12 indicate that ferrihydrite cannot be discarded. In fact, the RT MES spectrum of sample Fe 123 showed a symmetric doublet with broad lines, which was successfully fitted with two components typically of poorly crystalline ferrihydrite. This might be a confirmation of what was observed with the SEM, *i.e.* the residue formed in the first precipitation tank probably contains more ferrihydrite ("PG' particles) than the final residue. A SEM image of synthetic iron-bearing particles is shown in Figure 27.

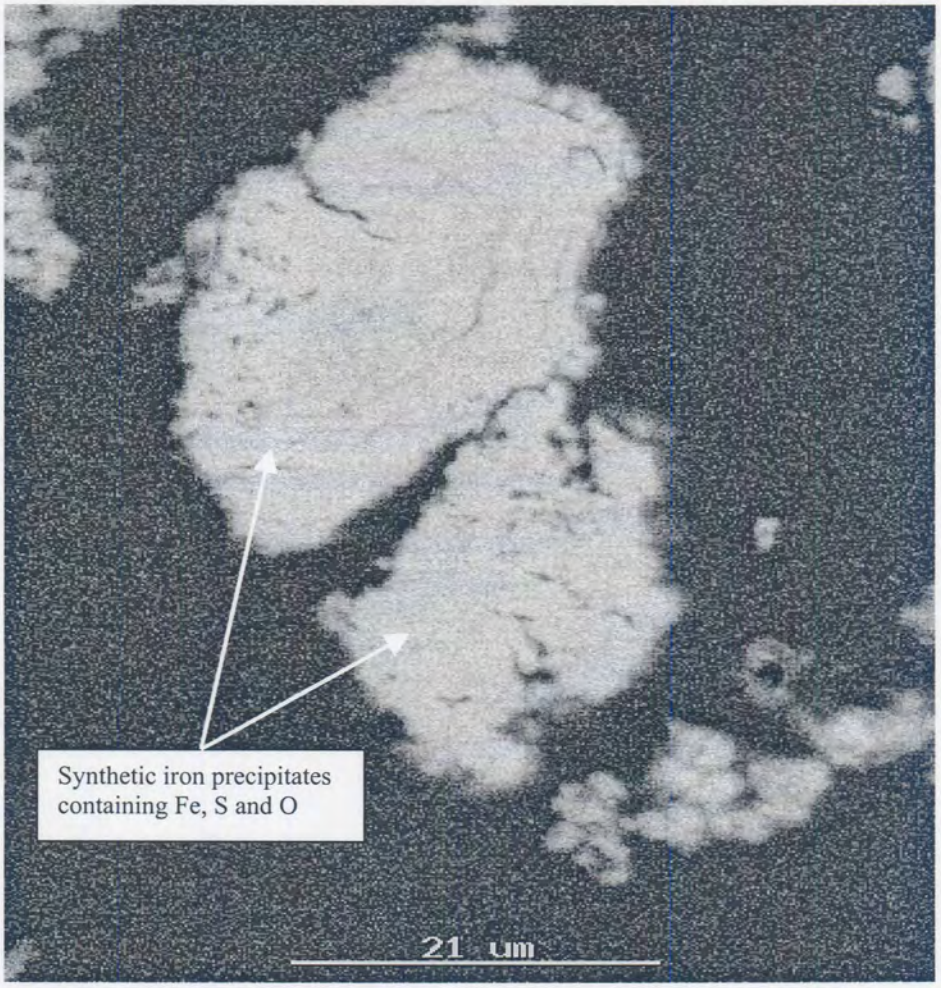

Figure 27: SEM image of synthetic iron-bearing particles.

In summary, the production and analysis of synthetic iron precipitate confirmed the presence of at least schwertmannite in the sample. However, it is possible that some ferrihydrite might have been present in the samples.

2.3.3.7 FT-IR Spectroscopic Analysis

The infrared patterns obtained for samples Fe 135, Fe 235 and Fe 435 (Set 1, T1, T2 & T4) are shown in Figure 28.

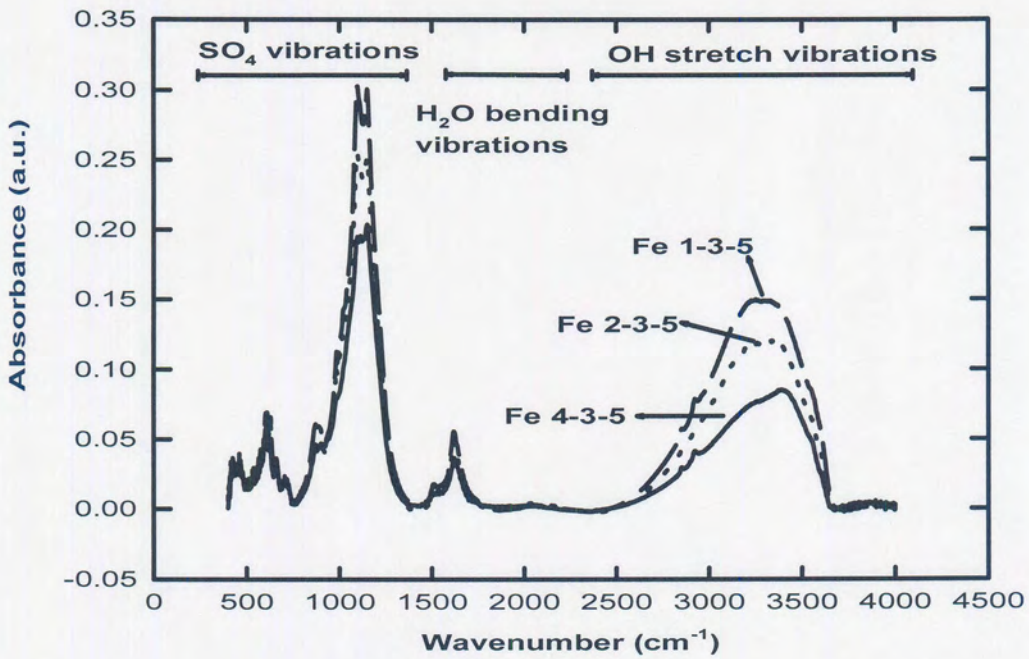

Figure 28: Mid-infrared spectra of samples Fe 135, Fe 235 and Fe 435.

The wavenumbers of the adsorption bands depicted in Figure 28 are compared with values for schwertmannite and ferrihydrite in Table 13.

Table 13: Identification of infrared absorption bands for Zincor iron residue samples, a sample (Py-4) discussed by Bigham *et al.* [1994] and ferrihydrite [Cornell and Schwertmann, 1996].

Wavenumbers (cm^{-1})		
Zincor	**Schwertmannite (Bigham *et al.*,1994)**	**Ferrihydrite (Cornell and Schwertmann, 1996)**
470	483	450*
614	608	---
660	704	650*
1008	976	---
1109	1038	---
1152	1124	---
1184	1186	---
1609	1634	---
3331	3299	3430**

*** Bulk OH deformations**

**** Bulk OH stretch**

Even though there seem to be a fair amount of agreement between the experimental values obtained and the data from the literature, there are too many species contributing to the bands shown in Figure 28, making it extremely difficult to identify one or more of the species present.

2.3.4 Summary

The study of Zincor's iron residue indicated that amorphous iron phases play a very important role in the removal of iron from the zinc rich process solution. Approximately 50% of the iron is associated with at least two amorphous phases and probably a third unknown phase. Even though the thermodynamics predicts that goethite should be present in the Zincor residue, no trace of it or any of its polymorphs were found. Instead, the majority of the iron is removed in the form of a combination of schwertmannite and ferrihydrite, which are both metastable towards goethite, *i.e.* iron is removed as intermediate phases. The transformation of these phases to goethite is probably hindered by the presence of impurities such as silica, which will be discussed in more detail in the next section.

The distribution of iron in the iron residue was found to be more or less the following:

- 45% in schwertmannite - $Fe_8O_8(OH)_6SO_4$
- ≈ 5% in ferrihydrite - $Fe_5O_7(OH).\ 4H_2O$
- ≈ 20% in jarosites - $Pb[Fe_3\ (SO_4)_2\ (OH)_6\ ]_2$
- ≈ 25% in franklinite - $ZnFe_2O_4$
- 5% in a poorly crystalline, unknown phase.

It is proposed that iron is removed according to the following reactions (in order of importance):

$$4Fe_2(SO_4)_3 + ZnO(s) + 13H_2O = Fe_8O_8(OH)_6SO_4(s) + ZnSO_4 + 10H_2SO_4 \quad \ldots\ldots\ldots 7$$

$$3Fe_2(SO_4)_3 + PbSO_4(s) + ZnO(s) + 11H_2O = 2Pb_{0.5}Fe_3(SO_4)_2(OH)_6(s) + ZnSO_4 + 5H_2SO_4 \quad \ldots\ldots\ldots 8$$

$$5Fe_2(SO_4)_3 + ZnO(s) + 23H_2O = 2[Fe_5O_7(OH).\ 4H_2O](s) + ZnSO_4 + 14H_2SO_4 \quad \ldots\ldots\ldots 9$$

It can also be concluded that the specific residue composition is not only a function of the operating conditions in precipitation tank 1, where most of the iron is removed, but also of the conditions prevailing in tank 2 where the "acid wash" is applied. These conditions appear to be beneficial to the formation of schwertmannite rather than ferrihydrite. This is in contrast to the para-goethite process used by Pasminco's Hobart smelter, which operates at much higher pH-values and probably produces more ferrihydrite. The para-goethite-particles with high surface area, often referred to in literature, are therefore probably nothing else but ferrihydrite. If this is the case, then Zincor doesn't produce a para-goethite residue as such, but rather a residue containing mainly hydroxy sulphates (jarosites and schwertmannite) that is unique to the Zincor process.

2.4 Defining the optimum operating conditions

2.4.1 Introduction

In the previous section, it was shown with a fair amount of certainty that the bulk of the iron in Zincor's iron residue is associated with amorphous iron phases and specifically schwertmannite. Since the stability of this phase have only been described in terms of the natural environment (refer section on the thermodynamics of iron removal), this section will focus on the behaviour of schwertmannite (it is actually a mixture of schwertmannite and a small amount of ferrihydrite) under typical plant conditions. The need to perform an investigation of this nature also arises from pressures to continuously improve zinc recovery of the Zincor plant.

Zinc lost as a result of iron removal, is mainly a function of optimum utilisation of neutralising medium (zinc calcine in this case) and filterability of the residue slurry. The first of these factors accounts for the so-called insoluble zinc losses whereas the filterability of the residue gives an indication of the soluble zinc losses. The aim from a production perspective is therefore to produce a filterable iron residue and secondly to improve the efficiency of the process in terms of minimising the insoluble zinc losses.

The soluble- and insoluble zinc losses are determined by many factors, which include pH, temperature, seeding, flow rate, slurry potential, initial HIS acidity and the presence of impurities such as silica. In order to evaluate the relative impact these factors have on iron removal, the filterability expressed in terms of the rate of filtration ($kg/m^2.h$) of a synthetic iron residue was used.

The filtration rate for fairly rigid and incompressible cakes as derived from Poiseuille's equation can be expressed as follows:

$$\text{Rate} = \frac{A \times P}{\mu\alpha'(W/A)} \qquad \text{.....10}$$

Where:

- A = filtration area
- P = total pressure drop
- W = mass of cake
- μ = viscosity of the filtrate
- α' = function mainly of particle size

Equation 10 shows that if the experimental conditions (see Section 2.4.2) are kept constant, the filtration rate is mainly influenced by the size and size distribution of the precipitated particles. Measuring the average size (d_{50}) of the precipitated particles over time therefore might in most cases not only explain changes in the filtration rate but also give an indication of the relative growth rate of particles.

In this way an understanding of both the stability (relative stability) of the iron precipitate and the kinetics (relative rates) of iron removal under different conditions can be formed.

2.4.2 Experimental

The experimental setup (Figure 17) used to produce a synthetic iron residue that reflects the composition of the amorphous iron phases in the Zincor iron residue in the previous section, was also utilised to investigate the relative influence the mentioned variables might have on iron removal.

Since the experimental setup mainly reflects only the basic reactions of iron removal in the Zincor process and not the physical layout and flow conditions, which has a significant impact on particle size [Bryson, 1986], the trends rather than the actual filtration rates were considered. However, since the size of the precipitated particles was a very important variable in this study, an effort was made to operate the reaction vessel as a perfect mixer. Because the speed of the agitator might inhibit particle growth [Bryson, 1986] if it is too high, it was decided to decrease the speed slightly (120 rpm for this experimental setup). The effect of a lower agitator speed was a slight accumulation of coarse particles in the reaction vessel. The average particle size (d_{50}-value) of the material at the end of the experiments was found to be between 4% and 7% more than the material captured in the second vessel. No correction for this phenomenon was made however, since variations of less than 10% were obtained in most cases when the experiments were repeated.

A Malvern particle analyser was used to determine the size distribution of samples taken at regular intervals. In order to get good repeatability of data, it was found that the samples should be analysed after cooling down first. The use of ultrasonic sound to dispearse the particles was stopped, as it was found that it fractured them.

In terms of determining the relative filtration rates (on a dried solids basis) of the synthetic residue slurry produced, an effort was made to keep the variables mentioned in equation 10 constant throughout the study. This included:

- maintaining the vacuum at 60±2 kPa;
- the thickness of the filter cake was always between 4mm and 4.5 mm (this was done by varying the amount of slurry fed to the filter);
- a specially designed Buchner funnel was used, which prevented any short-circuiting from occurring and had a fixed filtration area of 50cm^2;
- the temperature of the slurry was maintained at 60°C before the flocculant (5 ml of 0.1% Montan 7022H) was added;
- the density of the filtrate was nearly always 1.144 g/cm^3 (the synthetic HIS contained 90 g/l zinc in the form of zinc sulphate and nearly always at least 15 g/l iron as iron sulphate).

Before the initiation of an experiment, 50 g/l seed (produced beforehand using the same setup) was added in the reaction vessel except where the effect of seeding was investigated.

2.4.3 Results and discussions

2.4.3.1 Effect of pH

The effect of pH on filtration rate and variation of average particle size with time are shown in Figures 29 and 30.

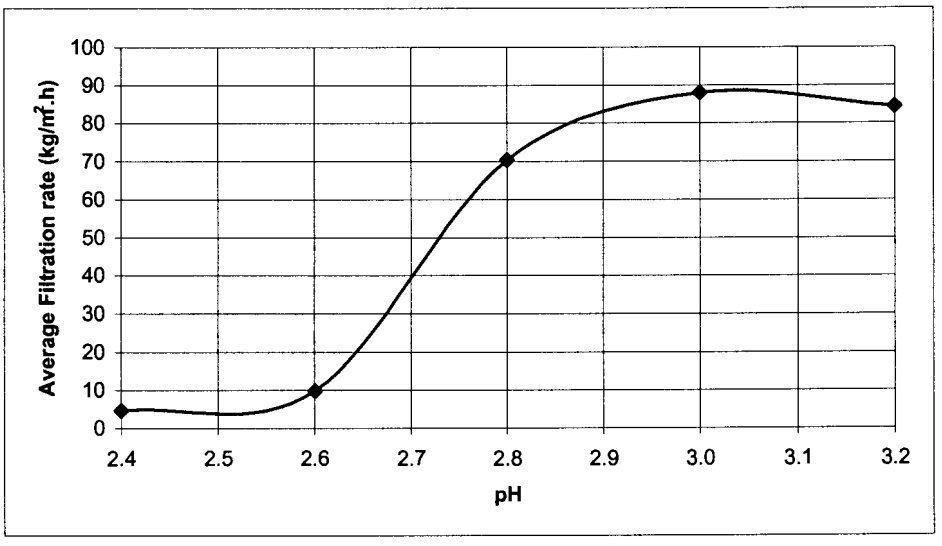

Figure 29: Filtration rate as a function of pH for synthetic iron residue slurry. (Experiments performed at 60°C for 5 hours. Composition of initial HIS: 20 g/l acid, 90 g/l zinc, 25 g/l ferric iron and 5 g/l ferrous iron. Zinc oxide slurry at 12.5% solids was used to control pH. 50 g/l initial seeding was used in all cases.)

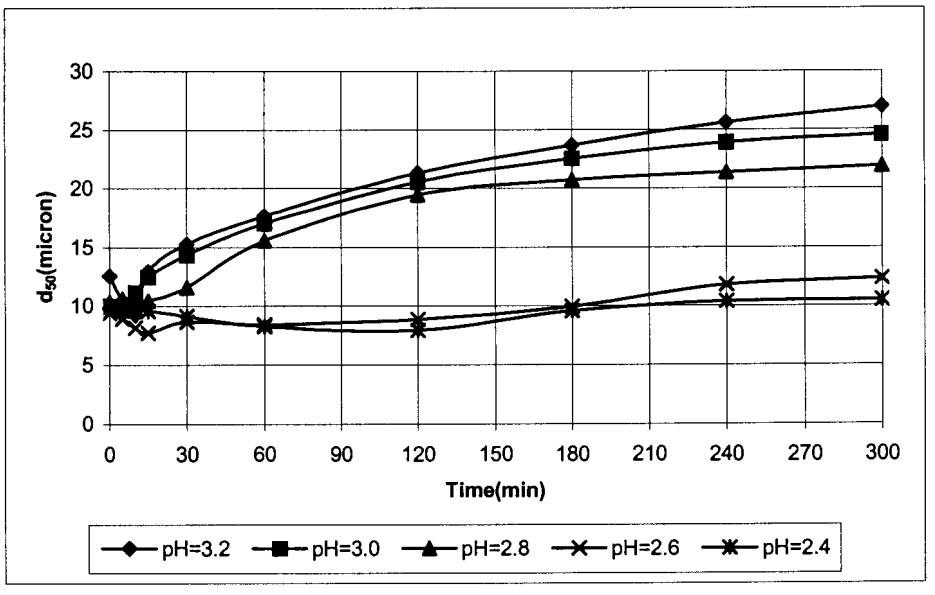

Figure 30: d_{50} as a function of time for synthetic iron residue slurry at different pH-values.

From Figures 29 and 30, it appears as though the sudden drop in filtration rate below a pH level of 2.8 might be a result of the fact that nearly no particle growth occurred at the relatively low [OH^-]. The darker colour of the filtrate at the lower pH-values also suggested that not all the iron was removed from the feed solution (5 g/l ferric iron at a pH of 2.4 versus 40 ppm ferric iron at a pH of 3.0 remained in the filtrate).

For optimum performance of the iron removal step in terms of soluble- and insoluble zinc losses, it appears as though a final pH of 3.0 and a retention time of approximately 4 hours at this pH are required.

Control of pH during iron removal is not as straightforward as it might seem. In order to optimise an iron removal step, it became clear that an effort should be made to control pH more accurately (within less than 0.1 of a pH unit), specifically at pH values below

approximately 2.8 for the following reasons. The first reason is because pH control at lower values is more difficult (probe to be cleaned more often, typically hourly) and if the probe is not calibrated often enough or poorly calibrated as a result of contaminated buffer solutions, the error is bigger.

Another reason is because pH determines up to a certain point the amount of zinc lost in the residue as insoluble zinc. In this regard, it would be beneficial to monitor the final pH – value more accurately. If the pH is above 3, unnecessary zinc is probably lost. The third reason is because silica in solution gels at a pH below approximately 2.5 (discussed in more detail in Section 2.4.3.7). When pH is controlled at a value close to 2.5 and the pH probe doesn't give an accurate reading for whatever reason, then silica might have a detrimental effect on the settling and filtration of the iron residue. The last reason is because calcine is very often only added once (usually at the start/ first tank if tanks are in series) to the system, which makes it difficult to quickly rectify settling and filtration problems caused by running the process at a too low pH level.

Another important issue related to a change in pH is the role that sulphate plays (between a pH of 2.6 and 3.2 the free sulphate concentration varies from 0.05% to 0.01%) during the formation of schwertmannite. It has been suggested [Bigham *et al.*, 1990] that schwertmannite might have a structure similar (similar infrared spectra) to that of akaganeite even though poor crystallinity and small particle size hindered the direct structural analysis of the specific samples. The essential role that chloride plays in akaganeite formation is therefore probably taken by sulphate in the schwertmannite structure. However, since it has never been directly proven that sulphate forms an essential rather than an accidental part in the sulphate structure it might only be adsorbed

and it might be argued that schwertmannite is a very poorly crystalline form of goethite.

If, however, it appears that sulphate is required to stabilise the schwertmannite structure, then variations in the free sulphate concentration during precipitation might have an impact on iron stability, *i.e.* at higher pH-values schwertmannite might be destabilised. This appeared to have been the case if it is assumed that variations in free sulphate concentration will affect the schwertmannite structure. In all the experiments performed at a pH of 3.2, lower filtration rates were obtained than at a pH of 3.0.

Total sulphate concentration in the HIS in the zinc industry usually varies between 10% and 30%. If it is the case that adsorbed sulphate plays an integral part in stabilising the schwertmannite structure, then the lower filtration rates obtained at a pH of 3.2 are probably due to an experimental error. The role sulphate plays in the schwertmannite structure is an area that definitely needs more research.

2.4.3.2 Effect of temperature

The effect of operational temperature on the filterability of residue is depicted in Figure 31.

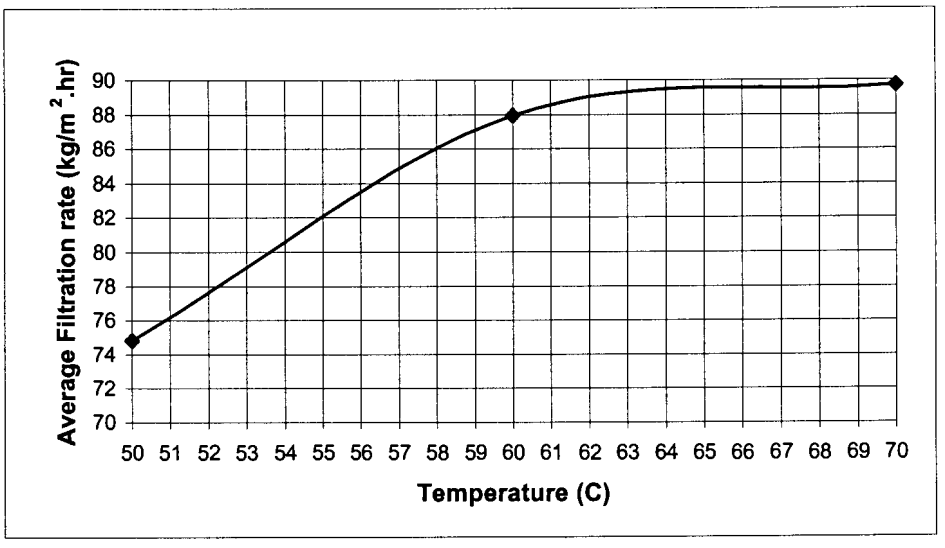

Figure 31: Filtration rate as a function of the temperature prevailing during iron removal for synthetic iron residue slurry. (Experiments preformed at a pH of 3.0 for 5 hours. Composition of initial HIS: 20 g/l acid, 90 g/l zinc, 25 g/l ferric iron and 5 g/l ferrous iron. Zinc oxide slurry at 12.5% solids was used to control pH. 50 g/l initial seeding was used in all cases. Filtration performed at 60°C).

The beneficial effect of higher temperatures on filtration rate is well known (see Equation 10) and it was not the objective of this study to investigate this phenomenon. Instead, the temperature during filtration was always kept as close as possible to 60°C (this was done by either heating or cooling the residue slurry before filtration) and an effort was made to evaluate the effect of temperature on precipitation and growth. This is shown in Figure 32.

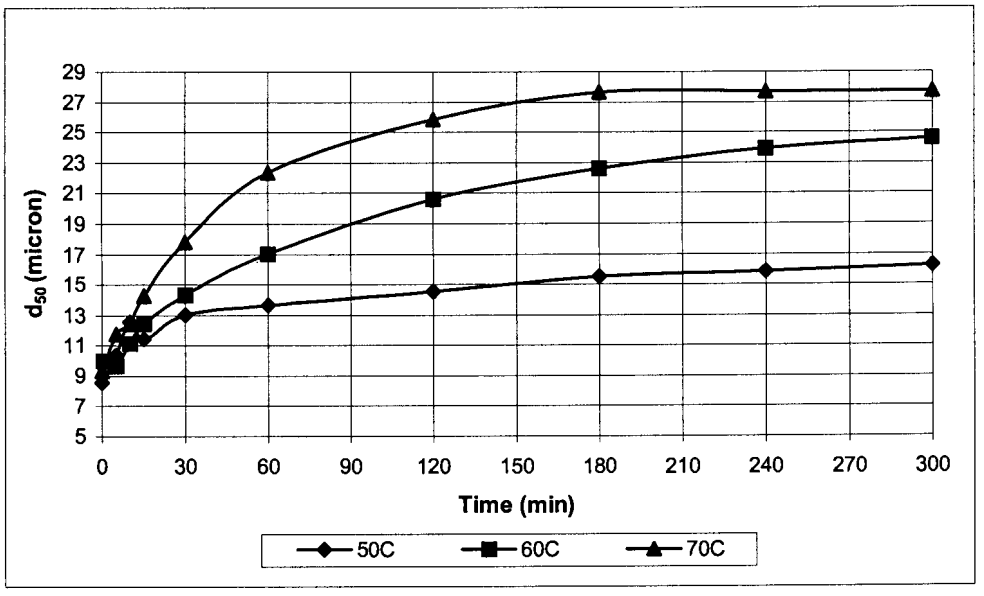

Figure 32: d_{50} as a function of time at various temperatures.

Figure 32 shows that higher initial growth rates were obtained at the higher temperatures and that the maximum particle size was obtained at 70°C after 3 hours. The figure also indicates that, if it can be assumed that particle size is an indication of the expected filtration rate, a similar filtration rate is obtainable after 90 minutes at a temperature of 70°C than was achieved after 5 hours at 60°C. It appears therefore that the retention time over an iron removal stage can be shortened by over 50% if the temperature is increased from 60°C to 70°C.

Figure 33 might explain why the filtration rate levelled off at higher temperatures in Figure 32 (similar trend with lower filtration rates obtained at smaller average particle sizes).

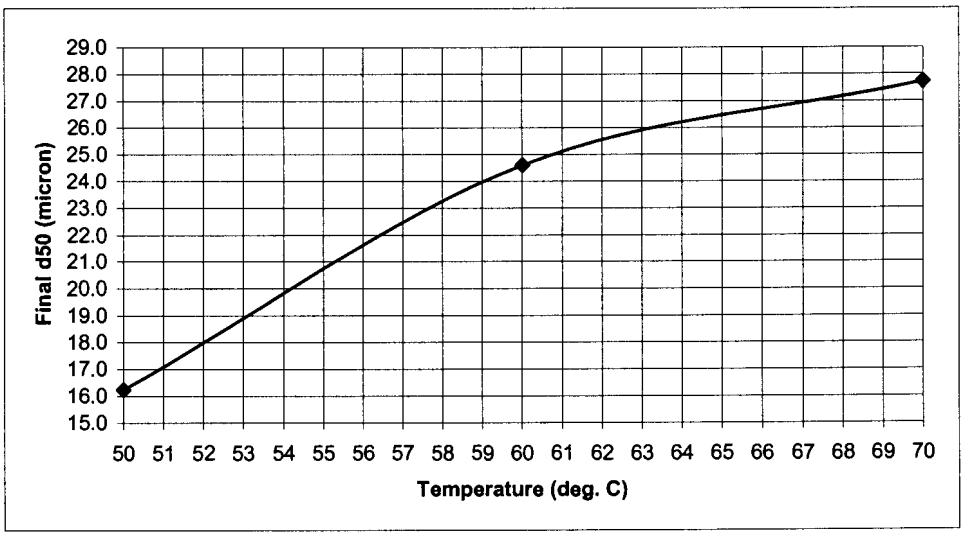

Figure 33: Final d_{50}-values as a function of temperature.

The benefits of running the iron removal process at Zincor at higher temperatures are therefore not only limited to the known effect it has on solution viscosity, but also extends to the formation of larger particles, which also assist filtration.

2.4.3.3 Effect of seeding

Seed was only added to the initial volume in the reaction vessel and not continuously as would be the case under normal operating conditions. The benefit of seeding is nonetheless evident from Figure 34 and probably would have been even greater if seed was added continuously.

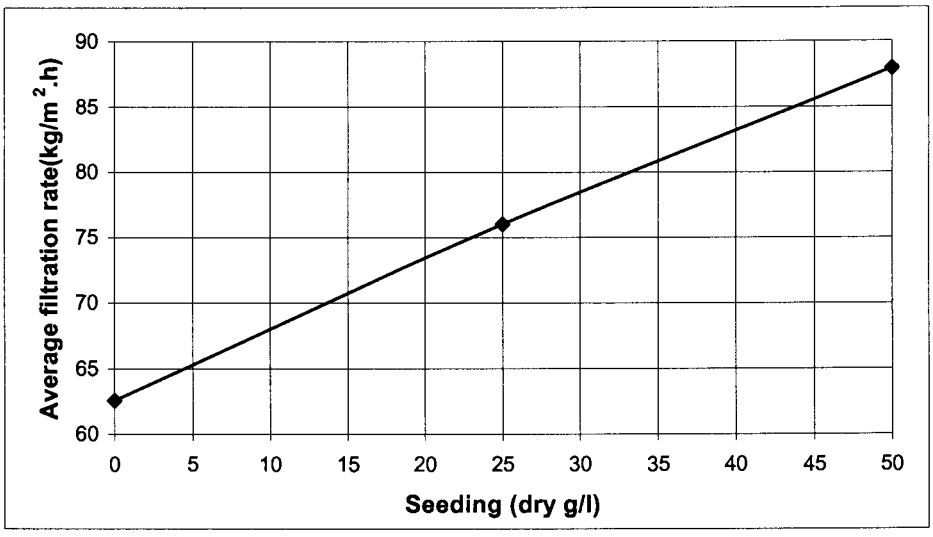

Figure 34: Influence of seeding on filtration rate. (Experiments performed at 60° and a pH of 3.0 for 5 hours. The composition of the HIS was as follows: 20 g/l acid, 90 g/l zinc, 25 g/l ferric iron and 5 g/l ferrous iron. Zinc oxide slurry at 12.5% solids was used to control pH. Seed addition refers to initial seed addition and not a continuous addition. Seed was made up from recycled synthetic iron precipitate with an average particle size of 10μm.)

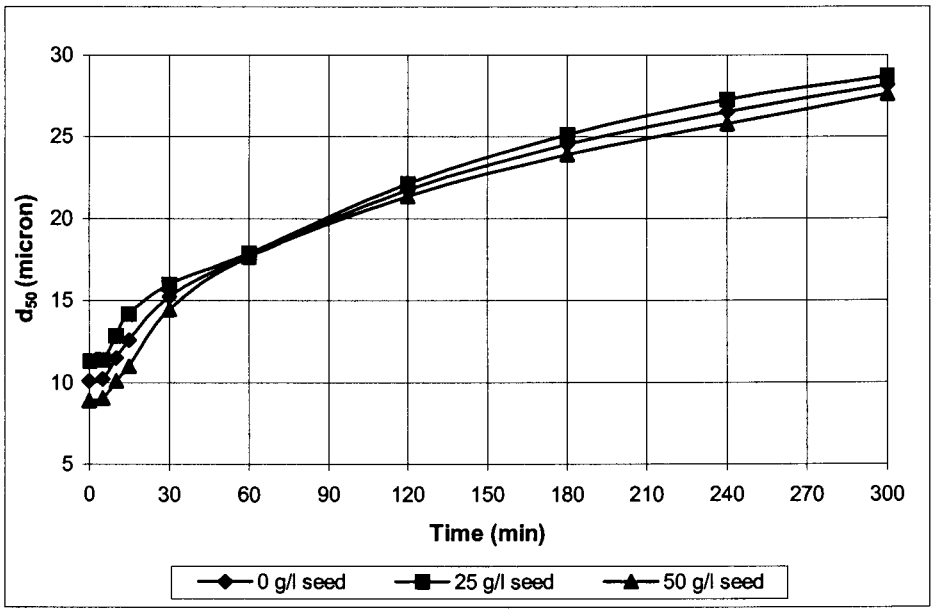

Figure 35: d_{50} as a function of time for different amounts of seed added.

This is one example where particle size could not be used to explain changes in filtration rate (refer Figure 35). A visual inspection of the filter cakes, however, revealed a number of important facts. The first was that the filter cakes where no or little seed was used, appeared more voluminous (retained more moisture -11% on average), which might explain why it took longer to filter.

The other observation was that these filter cakes also appeared to contain more insoluble zinc (6% more zinc oxide was used to control pH at 3.0). The filter cakes were therefore thoroughly washed with hot water, filtered, dried and analysed. It was found that the filter cakes where 50 g/l initial seeding was used, contained approximately 18% less zinc than the filter cakes produced where no seed was added.

Both these observations probably indicate that iron was preferentially precipitated on surfaces of seed crystals and that, in the absence of seeds, it was precipitated on surfaces of zinc oxide particles. The higher zinc losses therefore were probably a result of the fact that the oxide particles were coated.

The existence of hollow precipitates, very often found (refer to Figures 18 to 21) in the so-called para-goethite residues, might be related to this phenomenon, *i.e.* when the oxide particle is only partially coated it can still dissolve to leave what looks like a hollow particle. The insoluble zinc losses associated with the use of zinc calcine during iron precipitation therefore appears to be not only a function of the amount of franklinite present in the calcine but also of the physical encapsulation of zinc containing material. This implies that as long as a zinc containing neutralisation agent (zinc calcine, secondary zinc oxides, basic zinc sulphate, etc.) is used, insoluble zinc losses might be higher than expected.

2.4.3.4 Effect of slurry potential

Ferrous iron was added to the HIS as ferrous sulphate to control slurry potential. The influence it had on filtration rate is shown in Figure 36.

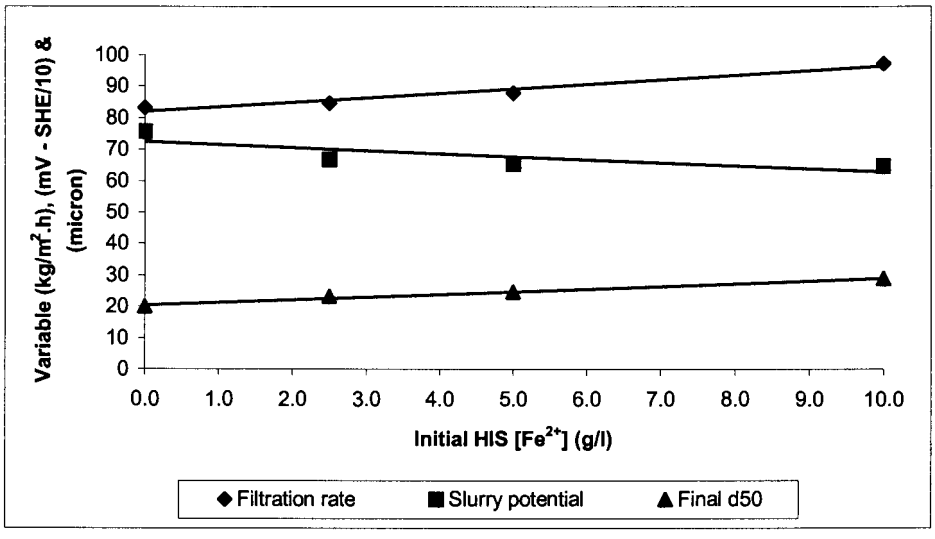

Figure 36: Filtration rate, slurry potential and final average particle size as a function of ferrous iron concentration in solution. (Experiments performed at 60°C and a pH of 3.0 for 5 hours. Composition of the HIS was as follows: 20 g/l acid, 90 g/l zinc, 25 g/l ferric iron and various amounts of ferrous iron. Zinc oxide slurry at 12.5% solids was used to control pH. 50 g/l initial seed was added.)

Ferrous iron of 1 g/l in the HIS was equivalent to approximately 0.78 g/l ferrous in solution at the time of precipitation during each experiment. Figure 36 shows that there is a gradual increase in final average particle size and filtration rate with a decrease in slurry potential. The ferrous iron concentration in hot iron solutions in the zinc industry is typically less than 5 g/l. These concentrations are probably not contributing much in terms of

improved filterability under normal plant conditions. However, the presence of other elements in solution such as copper, cobalt, cadmium and manganese might result in even lower potentials (less than 600 mV –SHE) than was simulated here with the resulting effect on filtration rate.

The higher filtration rates achieved at lower potentials imply that it had a beneficial effect on particle growth. This was indeed the case as can also be seen in Figure 37.

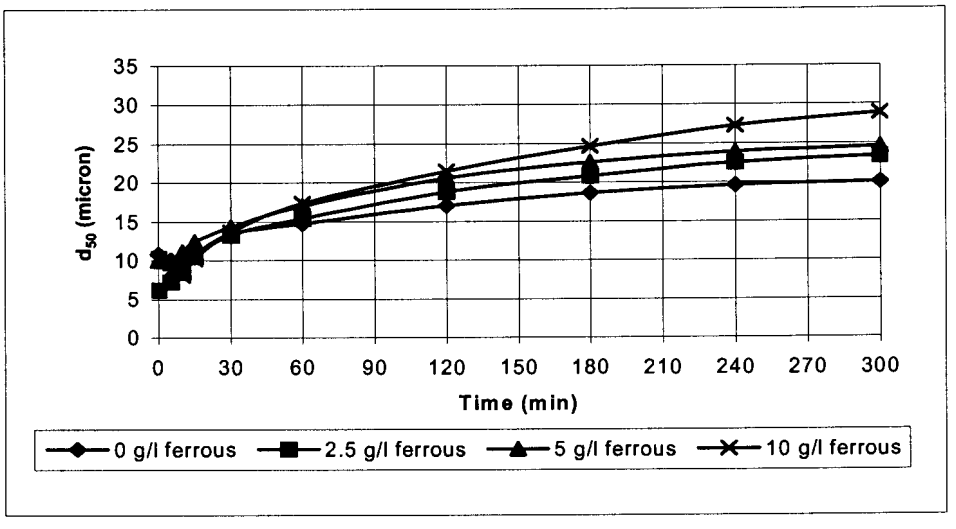

Figure 37: d_{50} as a function of time at different ferrous iron concentrations.

The exact role slurry potential play in the formation of the precipitate is not clear. However, the importance of surface potential (zeta-potential) in precipitation processes have been recognised [Cornell and Schwertmann, 1996]. As it was beyond the scope of this study to investigate this area in more detail, it is proposed that this area be studied further.

2.4.3.5 Effect of $[Fe]^{3+}$

In this part of the study, ferric iron concentration was varied between 15 g/l and 35 g/l in the initial HIS while pump speed was maintained at 15.5 ml/min. An increase/decrease in the iron concentration was therefore equivalent to an increase/decrease in the mass flow rate to the reaction vessel. A change of 10 g/l in the concentration of iron was equivalent to a 155 mg/min change in flow rate. The results obtained are shown in Figure 38.

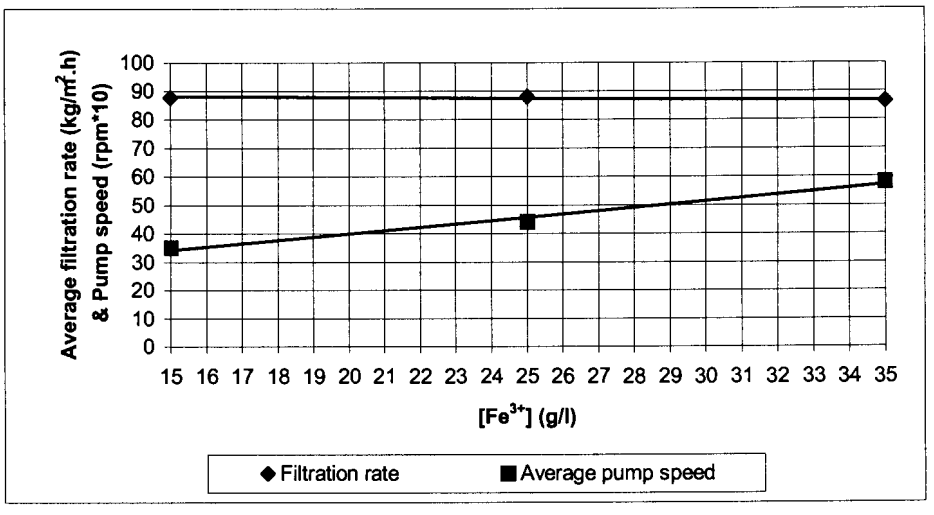

Figure 38: Filtration rate and zinc oxide pump speed as a function of ferric iron concentration. (Experiments performed at 60°C and a pH of 3.0 for 5 hours. The composition of the HIS was as follows: 20 g/l acid, 90 g/l zinc, 5 g/l ferrous iron and various amounts of ferric iron. Zinc oxide slurry at 12.5% solids was used to control pH. 50 g/l initial seed was added.)

The change in flow rate had very little effect on the filtration rate of the residue slurry. It was expected that bigger particles will result from an increase in the mass flow rate of iron, but it wasn't the case. An investigation into the size distribution data showed that more than one mechanism might actually determine the final size of the precipitate.

Apart from the expected mechanism of precipitation, it appeared as though bigger particles were formed through agglomeration and even bigger particles through flocculation [Burkhart and Voight, 1986]. If this was the case, then it might explain why very little difference in the final particle sizes and filtration rates were obtained.

Figure 39 was included to show the three distinct groups of precipitate sizes obtained in each experiment. The first peak, which almost disappeared towards the end of the experiment, was at approximately 5 μm (precipitated virgin particles), the second peak was at approximately 20 μm (agglomerated particles) where the bulk of the material lay and the last peak lay around 200 μm (flocculated particles).

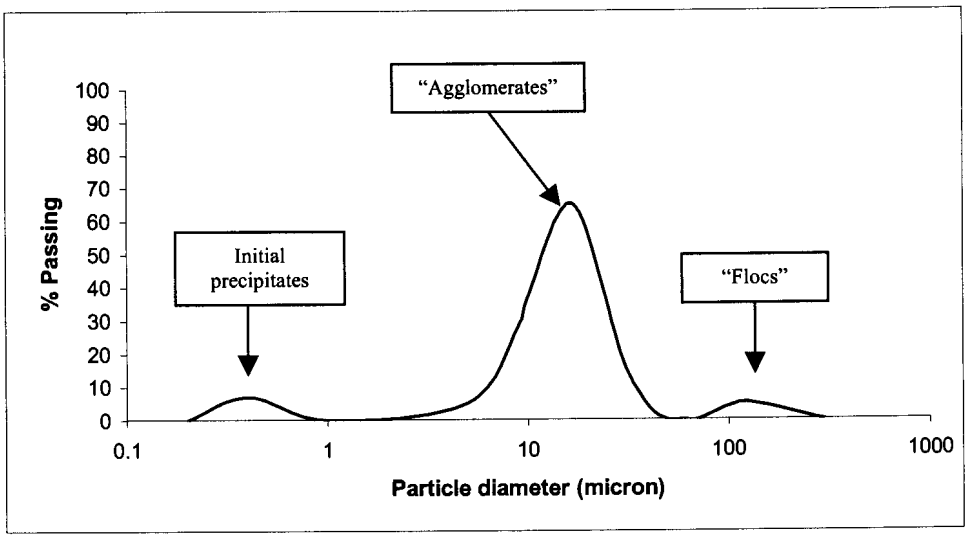

Figure 39: A typical size distribution graph of synthetic iron precipitate produced from solutions containing 15 g/l, 25 g/l and 35 g/l ferric iron.

Another important fact to realise is that the neutralising capacity of the oxide is mainly used to neutralise the acid that is generated during iron precipitation (see Figure 38-increase in pump speed) and not to neutralise the free acid in the HIS. To really improve recovery, from an insoluble zinc loss perspective, it is therefore advisable to keep the iron concentration at the lowest levels possible by acquiring concentrates with a low iron content. This, however, is not always possible due to the higher cost of this material as well as blending and roasting constraints. One permanent solution to this problem would be to use alternative neutralising agents such as lime and limestone ($CaCO_3$) to remove the iron. These options and results obtained from trial runs are discussed in more detail later.

2.4.3.6 Effect of initial HIS acidity

These experiments were conducted to confirm whether the change in initial acidity as a result of the inclusion of a weak acid leach step in the future Zincor residue treatment circuit is going to affect the filterability of the iron residue. The results obtained are shown in Figure 40.

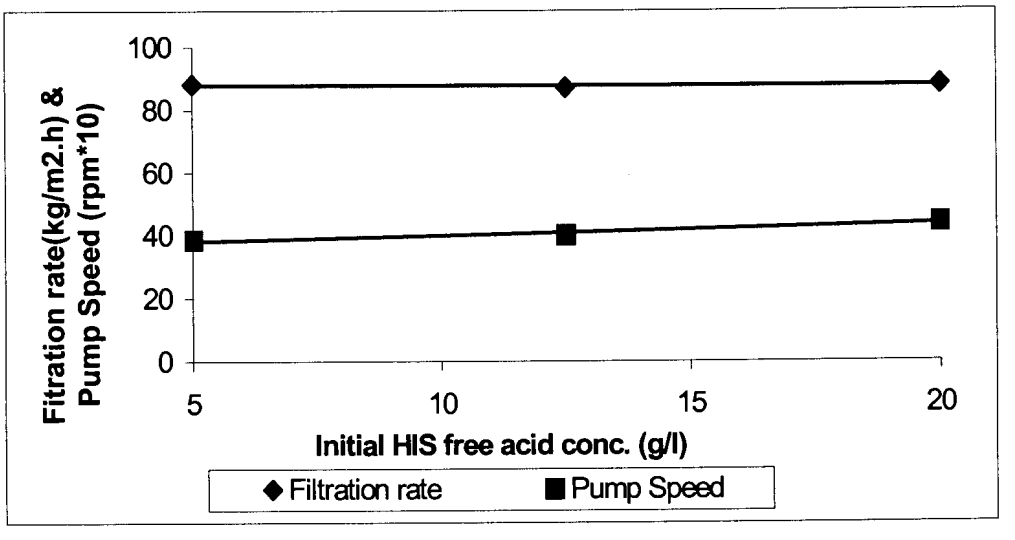

Figure 40: Filtration rate as a function of initial HIS acidity. (Experiments were performed at 60°C and a pH of 3.0 for 5 hours. Initial HIS composition was as follows: various acid concentrations investigated, 90 g/l zinc, 25 g/l ferric iron and 5 g/l ferrous iron. Zinc oxide slurry was used to control pH. 50 g/l initial seed was used.)

As expected, very little change was observed in the filtration rate and only a slight decrease in the consumption of zinc oxide was detected. This is probably due to the fact that the stability of the precipitate is mainly governed by the conditions during precipitation, which were not influenced by the change in initial HIS acidity.

2.4.3.7 Effect of silica

The role of silica in zinc hydrometallurgy is a complex subject [Queneau and Berthold, 1986] and it was therefore decided to only highlight a few very important points related to the role silica plays in iron removal at Zincor.

Even though the silica content in the concentrates treated at Zincor contains relatively low levels of silica, typically 2% to 3%, (refer to Table 2), significant amounts of silica were detected in the HIS and the iron precipitate (refer to Tables 4 to 6). This might suggest that silica is concentrated in the residue treatment circuit and that it cannot be ignored specifically in the light of the impact it might have on Zincor's iron removal process.

Cornell and Schwertmann [1996] reported that silica is one of the impurities responsible for delaying the transformation of intermediate phases such as schwertmannite and ferrihydrite to goethite. It is not clear what the exact mechanism of this phenomenon is. One possibility is that the precipitate surface is covered with silica, which will then form a physical barrier that might prevent the necessary mass transfer to occur. This implies that silica is precipitated along with the iron during the iron removal step but at a slightly lower rate. Figure 41 might support this argument.

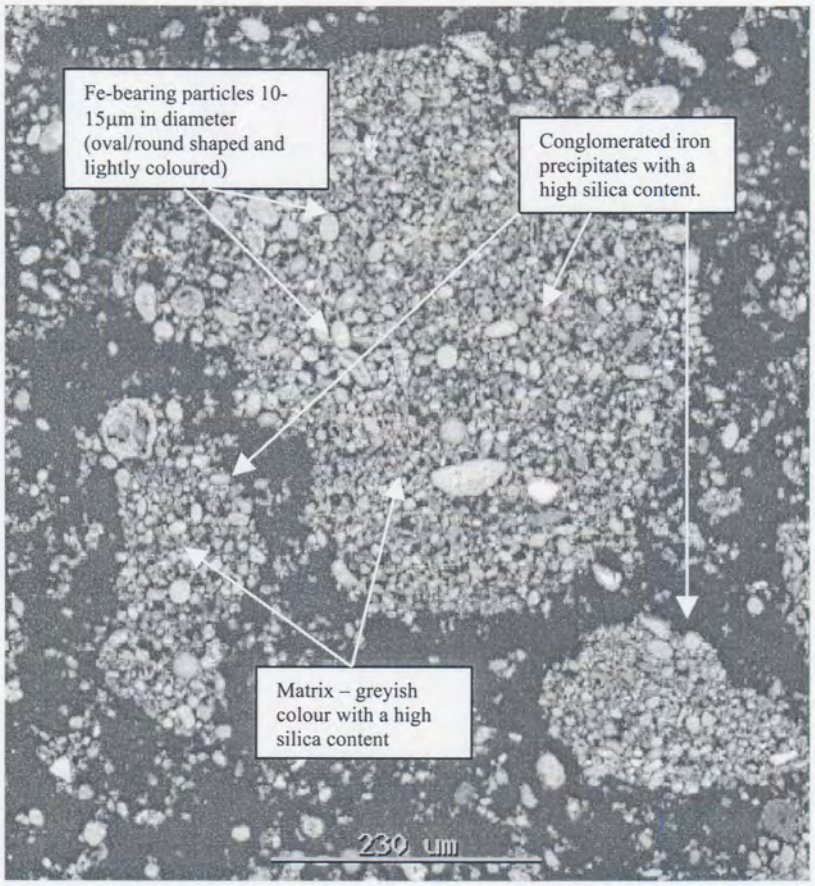

Figure 41: SEM picture of a Zincor iron precipitate showing the presence of precipitated silica. (Sample taken from the overflow launder of the second iron removal tank) Backscattered mode.

From Figure 41 it appears as though silica not only covered most of the precipitated iron particles, but it also might have acted as a flocculant. It is known [Fuerstenau, 1987] that silica is negatively charged over a wide pH range (pzc between a pH of 1.0 and 2.0 for silica gel and between 2.0 and 3.0 for α-quartz), whereas iron oxides are mostly positively charged at these low pH levels. This difference in charge, therefore, might explain the tendency of silica to act as a flocculant during iron removal. Some of these iron conglomerates were found to have diameters close to 1 mm.

This finding implied that silica was successfully removed during iron precipitation and that it actually might have contributed towards improving the settling and filtration properties of the iron residue. In order to ensure that silica is treated successfully at Zincor in future and to exploit the flocculation effect it had shown, the conditions that promote silica removal need to be considered further.

Various patents [US Patents, 1972, 1976 & 1979] were filed describing the conditions that contribute towards silica removal. A paper by Ikenobu [2000] also discusses the treatment of high zinc-silicate concentrates and the precipitation of solubilised silica from the zinc-rich process solution in a filterable form. From the literature it appears as though the basic principles of iron removal (from the ferric state as is the case at Zincor) could be applied to the removal of silica, *i.e.* that the silica concentration in the initial solution must be at a relatively low level (in silica's case preferably around 1 g/l) and kept at these levels by utilising the right combination of pH, temperature and seed addition. It was shown that silica could be removed from solution in a filterable form when the pH was higher than 2.5, the temperature as high as possible and the ratio of recycled seed addition to acid soluble silica around 0.3. These results probably confirm why the "acid wash" in the second iron removal tank at Zincor is never operated at a pH below 2.5. When operating the "acid wash" close to a pH of 2.5, accurate pH control is therefore of utmost importance to avoid settling and filtration problems as explained earlier.

a) Introduction

In the previous sections, conditions that influence soluble zinc losses were investigated. However, it also became clear that the insoluble zinc loss generally experienced during iron removal are not only a function of the amount of iron in the zinc calcine used to control pH, but are also probably a result of the encapsulation of zinc-rich material. Since the highest driving force for iron removal probably exists at the solution – oxide interface, it is possible that zinc oxide particles found in the zinc calcine are coated with iron precipitate contributing towards the insoluble zinc loss experienced during iron removal.

The hollow precipitated particles that are typical of the "para-goethite process", and other similar processes, and the fact that the total insoluble zinc losses are much higher than what may be expected when only the zinc in franklinite is considered, are probably indicative that the above-mentioned mechanism also contributes towards zinc losses during iron removal. As long as zinc containing neutralising agents are therefore used to aid iron removal, additional zinc losses will be suffered. These insoluble zinc losses make the Zincor- and similar iron removal processes less attractive even though they are relatively simple and cheap to operate.

One possible solution to this problem might be to use alternative neutralising agents, which contain no zinc or have a low zinc content. The possibilities that first come to mind include slaked lime ($Ca(OH)_2$) and lime rock (mined $CaCO_3$). Shortly after the commissioning of the Zincor iron removal stage at Zincor, slaked

lime was tested as an alternative to zinc calcine to remove iron from the zinc-rich solution. All efforts were however terminated when poor settling and filtration of the residue slurry was experienced. After this trial run, the use of lime and/or other neutralising agents to control pH over the iron removal stage was never reinvestigated up until now.

The utilisation of mined $CaCO_3$ for neutralisation purposes in the hydrometallurgical zinc environment is fairly common today. Lime rock is utilised (see Figure 13) in the hematite process to neutralise excess acidity in the process solution before iron removal as well as to aid iron and silica removal before the solvent extraction of zinc [Garcia *et al.*, 2000].

Another variety of $CaCO_3$ is the so-called chemically precipitated limestone produced as waste product in the paper and pulp industry. It is a very attractive alternative to mined limestone and slaked lime as it is far less expensive.

A comparison between various alternative neutralising agents that highlights the difference in cost as well as some other important facts is given in Table 14.

Table 14: A comparison between lime and limestone used for the neutralisation of acidic solutions. [Internal Zincor Report, 2000]

Parameter	Alkali				
	Calcine	Slaked lime (slurry)	Unslaked lime	Natural Mined limestone	Chemically precipitated limestone
Formula	ZnO	$Ca(OH)_2$	CaO	$CaCO_3$	$CaCO_3$
Purity (%)	75-80	90	90	90	75
Particle size (µm)	< 250	< 5000	<5000	<5000	<150
Price * (R/t)	0	490	450	170	100
Utilisation efficiency (%)	74	88	85	90	90
Cost ratio**	0	3.09	2.22	1.42	1.00

* The figure is influenced by transport cost relative to Zincor.

** Calculation based on consumption over a period of a year for a similar application.

A very important characteristic of chemically precipitated limestone is the much smaller average particle size distribution of the material, which probably contributes towards its utilisation efficiency and ease of handling (less grit). However, the impact of certain other impurities contained in the reagent needs to be considered as it might have a detrimental effect on the purity of the zinc-rich process solution.

Some of the impurities of interest in chemically precipitated limestone include sodium (approximately 1%, which can aid iron removal as sodium jarosite), silicon (1.2%, which will probably not be dissolved and can act as seed for silica removal), manganese (0.6%), magnesium (0.7%, which can be bled from the system along with manganese) and fluoride (0.13%, which will probably be removed as an adsorbed phase along with the iron).

Another neutralising agent that can be used to remove iron is basic zinc sulphate ($ZnSO_4.xH_2O$). This material can typically be produced during the magnesium bleed process. Utilisation of this material has the advantage that no foreign elements are introduced into the processing circuit whilst gypsum present will aid settling and filtration of the residue slurry. Additional insoluble zinc losses, however might be incurred due to the use of a zinc containing neutralising agent as explained earlier in this section.

b) Experimental

The experimental setup to evaluate the use of slaked lime, powder limestone and a zinc oxide and basic zinc sulphate mixture as alternative neutralising agents to zinc calcine is the same as depicted in Figure 17. The composition of the HIS for the various experiments as well as the conditions during iron removal are summarised in Table 15.

Table 15: Conditions prevailing during iron removal with various neutralising agents.

Variable	HIS	Oxide slurry	Fe - precipitate
Acidity*/pH (g/l)*	15*	5.0-6.0	3.0
Flow rate** (ml/min)	55.6	App. 20-40	---
Temperature (°C)	60	60	60
% Solids	---	12.5	---
Zn (g/l)	80	0	---
Ferric iron (g/l)	25	0	---
Ferrous iron (g/l)	3	0	---

** The flow rate of the calcine slurry determined the HIS flow rate as settling of solids in the pipes occurred at lower flow rates. The total flow rate equates to a residence time of about 30 minutes in the reaction vessel.

The performance of the alternative neutralising agents was compared with that of zinc calcine, as the experimental setup was not calibrated to reflect the flow environment in the actual Zincor iron removal stage. Each experiment was terminated after 200 minutes after which the contents of the reaction vessel were used in filtration tests. The filter cakes were prepared for chemical analysis by washing it thoroughly with hot water and drying it at 100°C for 1 hour. The results obtained are shown and discussed in the next section.

c) Results and Discussions

The results obtained by running the experimental setup with different neutralising agents are shown in Table 16.

Table 16: Comparison between different neutralising agents used to remove iron from a synthetic hot iron solution.

Variable	Neutralising Agent				
	Calcine ZnO PLANT*	Calcine ZnO EXP.**	"Slaked lime" $Ca(OH)_2$	Basic zinc sulphate + ZnO $ZnO/ZnSO_4.H_20$	Chemically precipitated limestone $CaCO_3$
Filtration rate ($kg/m^2.h$)	130	60.4	2584	79.8	1033
Consumption (ml/min)	---	38.9	22.2	30.0	32.0
Dry solids mass ratio	---	1.0	2.9	1.1	2.2
Filter cake:					
%Zn	8.04	7.48	2.22	2.26	0.44
Zn mass ratio	1.1	1.0	0.9	0.3	0.1
%Fe	35.6	42.7	15.3	41.9	15.1
%Ca	0.58	0.05	19.87	2.15	21.14
$\%SO_4$	12.9	8.27	26.75	10.28	28.04
%Na	0.01	0.004	0.004	0.005	0.008
Filtrate:					
ppm Fe (III)	960	40	<1	<1	40
ppm Ca	300-400	413	676	682	665
ppm Na	120	9.5	5.3	6.2	363
ppm Cl	265	66.4	<1.0	73.3	75.5
ppm F	0.32	<0.1	<0.1	<0.1	<0.1

* Average actual Zincor plant values. ** Experimental synthetic values.
Slaked lime: used chemically pure grade material to prevent blockages.
Basic zinc sulphate mixture contained approximately 65% ZnO (CP).
Precipitated limestone: material was dried, screened and ground to prevent blockages. It normally contains approximately 20% moisture. Consumption figure adjusted for moisture.
Seed continuously added at 25 g/l except when calcine was used. Mass ratio figure adjusted for continuous seed addition where applicable.

From Table 16, it is clear that insoluble zinc losses can in some cases be significantly reduced in the iron precipitate if a neutralising agent that contains no or very little zinc is used. The relatively low insoluble zinc losses obtained for the basic zinc sulphate/zinc oxide mixture compared to the value for slaked lime might be a result of the higher reactivity of the zinc oxide fraction. In the previous section insoluble zinc loss of about 1.3% were obtained at lower feed rates when zinc oxide was used. The insoluble zinc loss obtained for slaked lime and the basic zinc sulphate/zinc oxide mixture also probably proves that zinc-rich solution is entrapped in the precipitate.

However, the higher reactivity of chemically precipitated limestone probably inhibits the coating of particles and the encapsulation of zinc containing material, which might explain the very low insoluble zinc loss incurred when it was used to aid iron removal.

Other benefits of using calcium based neutralising agents such as lime or slaked lime ($Ca(OH)_2$) and $CaCO_3$ that needs to be considered, include higher filtration rates, which would probably result in lower soluble zinc loss, due to gypsum formation (gypsum acts as a filter aid) as well as the possibility to bleed more sulphate from the system. The fact that more than double the amount of residue (on a dry solids basis) was produced, however, needs to be taken into account when applying this mode of operation in practice.

In terms of the filtrate, the relatively high level of sodium detected is an issue that probably should be considered where chemically precipitated limestone was used to aid iron removal. A build up of sodium in the processing circuit will probably only

result in the precipitation of a slightly higher portion of iron as sodium jarosite in the residue. This needs confirmation, as does the effect of the higher fluoride content of this reagent.

2.4.4 Summary

In this part of the study, it was shown that the stability of the precipitated amorphous iron phases (mixture of ferrihydrite and schwertmannite) is mainly influenced by pH. It was also indicated that the filterability of this residue slurry was influenced by pH, temperature, slurry potential and seeding. As such, it was indicated that the optimum operating conditions in terms of filterability (washability and soluble zinc losses) were as follows:

- pH around 3.0;
- temperature as high as possible (70°C);
- at least 25 kg/m^3 initial seeding; and
- as low slurry potential as possible (< 650 mV, SHE)

The important role silica might play in iron removal was also discussed as well as a possible mechanism which might explain the higher than expected insoluble zinc losses in the iron residue. The test work also showed that insoluble zinc losses could be significantly reduced if chemically precipitated limestone is used.

3 CONCLUSIONS

3.1 Residue Characterisation

Several changes to the initial "Zincor iron removal process" were made shortly after it was commissioned. This and the fact that there are today probably only two other similar iron removal processes in operation, the uncertainty surrounding the presence and character of amorphous iron phases in the Zincor iron residue, and the need to improve the process in terms of soluble and insoluble zinc losses, were the main reasons why a study of this nature was initiated.

Prior to this study, it has always been assumed locally that Zincor operates an iron removal process similar to the so-called para-goethite process employed by Pasminco's Hobart Plant and the Enirisorse Porto Vesme Plant. Published literature, however, confirmed that the exact nature of the "para-goethite" iron residues have not been determined yet. The conflicting reports found on this topic are probably a result of the state of uncertainty that surrounds these processes. The outcome of thermodynamic studies and the difficulties associated with the characterisation of amorphous iron phases probably contributed towards this state of uncertainty.

The thermodynamics predicts that goethite should be present when hot iron solutions containing ferric iron are neutralised under conditions prevailing in the "para-goethite" iron removal processes. It was further recognised, from work done mainly in natural environments during the past decade, that two distinct phases (schwertmannite and ferrihydrite) exist, which are both metastable towards goethite. It was also recognised that what was very often described as amorphous ferric hydroxide, is actually nothing else but ferrihydrite.

Many of the iron phases found in hydrometallurgical zinc circuits are very often fine grained and amorphous to X-rays. Various analytical techniques have therefore to be employed to identify these phases. A combination of chemical-, XRD-, SEM-, XPS- and Mössbauer-effect-spectroscopic (MES) analyses were found to be adequate to characterise Zincor's iron residue. The combination of the data obtained from chemical- and XRD analyses indicated that the majority (almost 50%) of the iron present was associated with phases that are amorphous to X-rays and these phases therefore play a very important role in the removal of iron at Zincor. XRD analysis showed that the main crystalline iron phases present in the iron residue were franklinite and plumbo jarosite. Information obtained from SEM and XPS supported the findings from MES, which indicated that the amorphous part of the residue comprised of schwertmannite, ferrihydrite and a small amount of an unknown phase.

The production of synthetic iron residue slurry confirmed the presence of schwertmannite and ferrihydrite in the Zincor iron residue.

From the results obtained it can be concluded that:

- Iron is removed mainly as intermediate iron phases in the form of schwertmannite and ferrihydrite.

- The transformation of these phases to goethite is probably hindered by the presence of impurities such as silica.

- The specific pH profile employed by Zincor to remove iron from its process solution is mainly responsible for the specific residue composition found.

- The fact that the iron residue mainly comprised of schwertmannite distinguishes the Zincor Process from other similar processes (para-goethite processes), which probably primarily produce ferrihydrite.

- It might be argued that the Zincor Process has a unique character based on the composition of the residue that is being produced.

3.2 Optimum operating conditions for iron removal

The inherent weakness of the Zincor iron removal process and similar processes is specifically the insoluble zinc loss associated with iron removal, even though it is relatively simple and cheap to operate. It is mainly due to these significant zinc losses encountered that these processes cannot compete with the other better known iron removal processes. However, if the insoluble zinc losses could be minimised, then the Zincor process would probably be a very attractive alternative for iron removal. Apart from the insoluble zinc loss present, it is also important to ensure that soluble losses are minimised. In the definition of an optimum operating window the focus was thus primarily on the conditions that influence both soluble and insoluble zinc losses during iron removal.

Whereas soluble zinc loss are mainly a function of the filterability of the residue slurry, insoluble zinc loss are determined primarily by the type of neutralising agent used to control pH. In the first part of this section it was shown that the filterability of the amorphous iron phases produced was influenced by pH (ideally equal to 3.0), temperature (as high as possible), seeding (at least 25 kg/m^3) and slurry potential (more negative than 650 mV-SHE). In the second part, alternative neutralising agents such as slaked lime, chemically precipitated $CaCO_3$ and a mixture of basic zinc sulphate and zinc oxide were used to remove iron from zinc-rich solutions. It was specifically chemically precipitated $CaCO_3$ that gave very low insoluble zinc loss values compared to zinc calcine normally used in operational zinc plants.

Based on these findings it was concluded that:

- Close pH control is essential to ensure optimum filterability of the residue slurry specifically at lower pH-values.

- An increase in temperature not only assisted filterability but it was also shown that the retention time required could be reduced.

- The addition of seed crystals seemed to have had a positive influence on insoluble zinc losses as it appeared as though a portion of the iron was precipitated on the existing seed surfaces.

- The simultaneous precipitation of silica not only appeared to have inhibited the transformation of schwertmannite and ferrihydrite to goethite but it also appeared to have acted as a flocculant, which assisted settling and filtration.

- Insoluble zinc loss was reduced to less than 1% in the case where chemically precipitated $CaCO_3$was used to remove the iron.

- If chemically precipitated $CaCO_3$ could be used on a larger scale to remove iron at Zincor, up to an additional 1.5% zinc (110 kt/a zinc slab basis) should be recovered on an annual basis.

4 LIST OF ABBREVIATIONS

- E.Z.: Electrolytic Zinc
- B_{hf}: Internal Magnetic Field
- FT-IR: Fourier Transform Infrared (Spectroscopy)
- HAL: Hot Acid Leach
- HALP: Hot Acid Leach Plant
- HIS: Hot Iron Solution
- IS: Isomeric Shift
- LT: Liquid Helium Temperature
- MES: Mössbauer Effect Spectroscopy
- PG: Para-Goethite
- RT: Room Temperature
- QS: Quadrupole Splitting
- S.E.: Spent Electrolyte
- SEM: Scanning Electron Microscopy
- V.M.: Vieille Montagne
- XPS: X-ray Photoelectron Spectroscopy
- XRD: X-ray Diffraction

5 LIST OF RELEVANT MINERALS

- Akaganeite: β-FeO.OH
- Alamosite: $PbSiO_3$
- Anglesite: $PbSO_4$
- Argento-jarosite: $AgFe_3(SO_4)_2(OH)_6$
- Beaverite: $PbCuFe_2(SO_4)(OH)_6$
- Bernalite: $Fe(OH)_3$
- Chalcopyrite: $CuFeS_2$
- Ferrihydrite: $Fe_5O_7.OH.4H_2O$
- Feroxyhite: δ-FeO.OH
- Franklinite: $ZnO.Fe_2O_3$
- Goethite: α-FeO.OH
- Gypsum: $CaSO_4.2H_2O$
- Hematite: α-Fe_2O_3
- Hydronium-jarosite: $H_3OFe_3(SO_4)_2(OH)_6$
- Larsenite: $PbZnSiO_4$
- Lepidocrocite: γ-FeO.OH
- Schwertmannite: $Fe_8O_8\ (SO_4)(OH)_6$
- Sodium-jarosite: $NaFe_3(SO_4)_2(OH)_6$
- Sphalerite: ZnS
- Plagioclase: $CaAl_2Si_2O_8$
- Plumbo-jarosite: $Pb[Fe_3\ (SO_4)_2(OH)_6]_2$
- Potassium-jarosite: $KFe_3(SO_4)_2(OH)_6$
- Pyrrhotite: FeS
- Pyrite: FeS_2
- Willemite: Zn_2SiO_4
- Zincite: ZnO

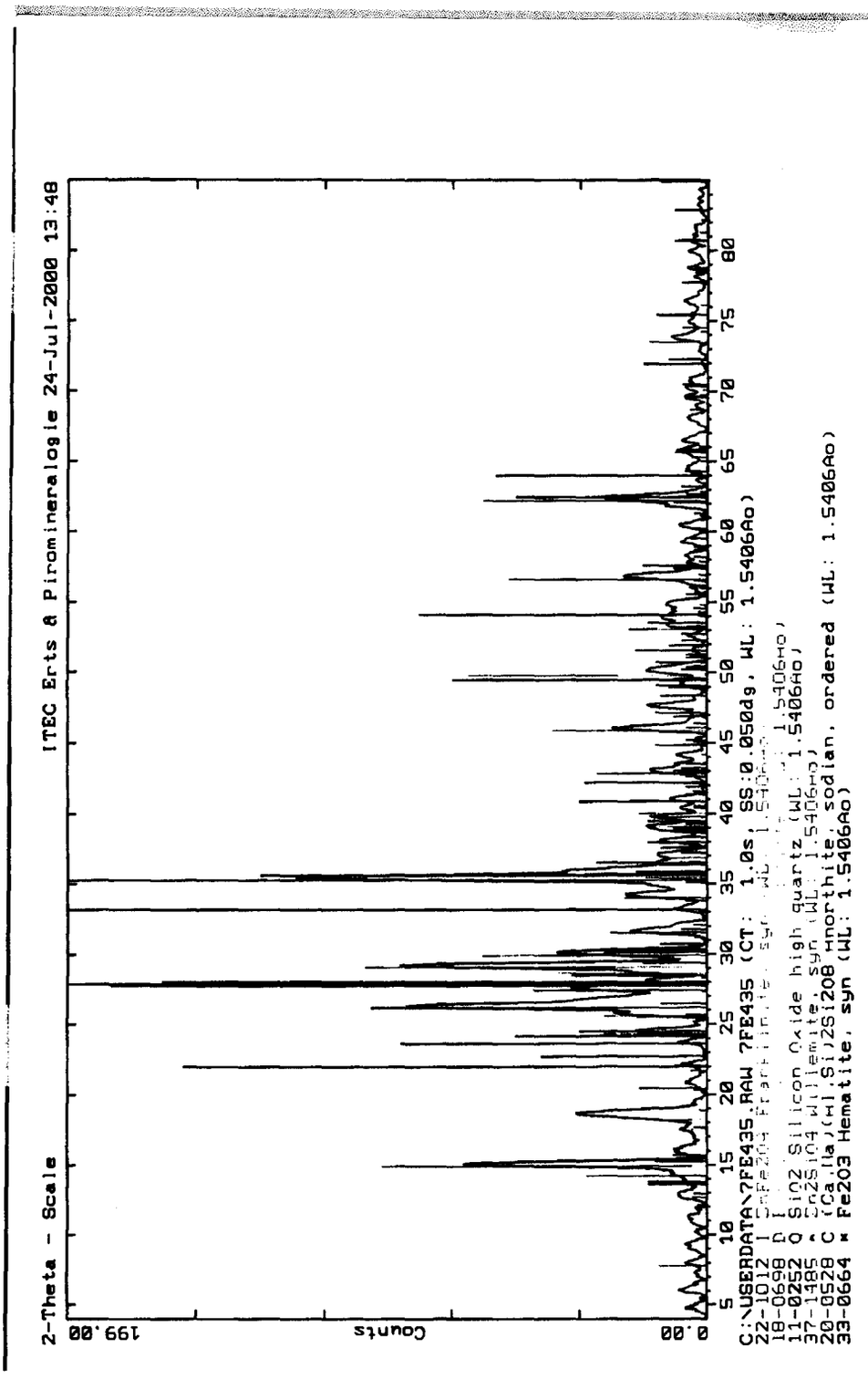

Figure 42: XRD spectrum of Zincor's final iron residue.

6 LIST OF FIGURES

7 LIST OF TABLES

8 REFERENCE LIST:

Arregui, V., Gordon, A.R., and Steinveit, G., "The Jarosite Process – Past, Present and Future", *Lead-Zinc-Tin '80, Proceedings of the 109th Annual Meeting, Las Vegas, Nevada, February 24-28*, 1980, 97-123.

Ashurst, K.G. and Hancock, R.D., "The thermodynamics of the Formation of Sulphate Complexes of Iron(III), Cobalt(II), Iron(II), Manganese(II) and Copper(II) in Perchlorate Medium", *NIM Report No. 1914*, Randburg, South Africa, 1977.

Babcan, J., "Synthesis of Jarosite - $KFe_3(SO_4)_2(OH)_6$", *Geol. Zb., 22, 2*, 1971, 299-304.

Bigham, J. M., Carlson, L. and Murad, E., "Schwertmannite, a new iron oxyhydroxy-sulphate from Pyhasalmi, Finland, and other localities", *Min. Mag., 58*, 1994, 641-648.

Bigham, J.M., Schwertmann, U., Carlson, L. and Murad, E, "A poorly crystallized oxyhydroxysulfate of iron formed by bacterial oxidation of Fe(II) in acid mine waters", *Geochim. Cosmochim. Acta, 54*, 1990, 2743 – 2758.

Bigham, J.M., Schwertmann, U., Traina, S.J., Winland, R.L. and Wolf, M., "Schwertmannite and the chemical modeling of iron in acid surface waters", *Geochim. Cosmochim. Acta, 60*, 1996, 2111 – 2121.

Bishop, J.L. and Murad, E.,"Schwertmannite on Mars? Spectroscopic analysis of Schwertmannite, its relationship to other ferric minerals and its possible presence in the surface material on Mars", *Min. Spectro: A tribute to Rog G Burns, 5*, 1996, 337-358.

Boxall, J.M. and James, S.E., "Experience with the goethite process at National Zinc", *Proceedings of the First International Symposium on Iron Control in Hydrometallurgy, England 1986, J.E. Dutrizac and A.J. Monhemius, Eds., Ellis Horwood, England*, 1986, 676 - 686.

Brady, K.S., Bigham, J.M., Jaynes, W.F. and Logan, T.F., "Influence of sulfate on Fe-oxide formation: comparisons with a stream receiving acid mine drainage", *Clays and Clay Minerals, 34*, 1986, 266-274.

Bryson, A. W., "Factors that effect the kinetics of nucleation and growth and the purity of goethite precipitates produced from sulphates solutions", *Proceedings of the First International Symposium on Iron Control in Hydrometallurgy, England 1986, J.E. Dutrizac and A.J. Monhemius, Eds., Ellis Horwood, England*, 1986, 377 - 390.

Burkhart, L. & Voight, J., "Aqueous Precipitation in Hydrometallurgy, Hydrometallurgical Reactor Design and Kinetics", *Baurista, R. G., Weseley, R.J. and Warren, G.W., Eds., 2-6 March 1986, New Orleans, AIME Metallurgical Society*, 1986, 441- 456.

Chen, T.T. and Cabri, L.J., "Mineralogical overview of iron control in hydrometallurgical processing", *Proceedings of the First International Symposium on Iron Control in Hydrometallurgy, England 1986, J.E. Dutrizac and A.J. Monhemius, Eds., Ellis Horwood, England*, 1986, 19 – 55.

Chen, T.T. & Dutrizac, J.E., "Practical Mineralogical Techniques for the Characterization of Hydrometallurgical Products", *Process Mineralogy IX, Ed. William Petruk, Richard Hagni, Susanne Pignolet-Brandom & Donald Hausen, The Minerals, Metals & Materials Society, TMS*, 1990, 289-309.

Ciriello, C. and Synnott, J. A., "The effect of process parameters on the precipitation of sodium jarosite at Kidd", *Proceedings of the Second International Symposium on Iron Control in Hydrometallurgy, Ottawa 1996, J.E. Dutrizac and G.B. Harris, Eds., The Canadian Institute of Mining, Metallurgy and Petroleum, Canada*, 1996, 117 – 134.

Cornell, R.M. and Schwertmann, U., "The Iron Oxides-Structure, Properties, Reactions, Occurrence and Uses", *Weinheim, New York*, 1996, 573p.

Cubeddu, F., Piasentin, M. and Reilly, F., "The para-goethite process at the Enirisorse-Porto Vesme plant", *Proceedings of the Second International Symposium on Iron Control in Hydrometallurgy, Ottawa 1996, J.E. Dutrizac and G.B. Harris, Eds., The Canadian Institute of Mining, Metallurgy and Petroleum, Canada*, 1996, 147 – 162.

Dutrizac, J.E., "Determination of Schwertmannite in Hydrometallurgical leach residues. Part 1 – The Nature of Schwertmannite. Part 2 – Examination of Hydrometallurgical Leach Residues", *Department of Public Works and Government Services Canada, Contract 028SQ.23440-7-1012, unpublished*, 1999.

Dutrizac, J.E., "Jarosite type compounds and their application in the metallurgical industry", *Hydrometallurgy, Research, Developments and Plant Practice, Proc. 112th AIME Ann. Mtg., Atlanta, Georgia. 6-10 March 1983, K. Osseo-Asare and J.D. Miller, TMS-AIME Ed.*, 1983, 531 – 551.

Dutrizac, J.E., "The Physical Chemistry of Iron Precipitation in the Zinc Industry", *Lead-Zinc-Tin '80, J.M. Cigan, T.S. Mackey and T.J. O'Keefe, Eds., The Metallurgical Society of AIMC, Warrendale, P.A.*, 1980, 532-564.

Filippou, D., and Demopoulus, G.P., "A kinetic model for the leaching of industrial zinc ferrite particulates in sulphuric acid media", *Canadian Metallurgical Quarterly, 31, 1*, 1992, 41 – 54.

Franz, E.D., "Synthetic solid solutions between goethite and diaspore", *Mineral. Mag., 42*, 1978, 159.

Fuerstenau, D.W., "Mineral/water interfaces and the electrical double layer", *SAIMM, Principles of flotation, Vacation School, Johannesburg*, 1987, 389 – 417.

Garcia, M.A., Mejias, A., Martin, D. and Diaz, G., "Upcoming Zinc Mine Projects: The key for success is ZINCEX Solvent Extraction", *Lead-Zinc 2000, Dutrizac, J.E., Gonzalez, G.A., Henke, D.M., James, S.E. and Siegmund, A.H.J., Eds., TMS*, 2000, 751-761.

Gordon, A.R. and Pickering, R.W., "Improved Leaching Technologies in the Electrolytic Zinc Industry", *Metal. Trans., 6B*, 1975, 43-53.

Graydon, J.W. and Kirk, D.W., "A Microscopic Study of the Transformation of Sphalerite Particles during the Roasting of Zinc Concentrates", *Metall. Trans.B, 19B*, 1988, 141-146.

Hearne, T.M. and Haegele, R. "Hydrometallurgical recovery of zinc from Sulphide ores and concentrates", *Zinc and Lead Processing 1998, J.E. Dutrizac, J.A. Gonzalez, G.L. Bolton and P. Hancock, Eds., The Metallurgical Society of CIM*, 1998, 765-780.

Ikenobu, S., "Method for processing siliceous zinc ores", *Lead-Zinc 2000, Dutrizac, J.E., Gonzales, J.A., Henke, D.M., James, S.E. & Siegmund, A.H.-J., Eds., TMS*, 2000, 427-435.

Jambor, J.L. & Dutrizac, J.E., "Beaverite-Plumbojarosite Solid Solutions", *Canadian Mineralogist, 21*, 1986, 101-113.

Jambor, J.L. and Dutrizac, J. E., "Occurrence and Constitution of Natural and Synthetic Ferrihydrite, a Widespread Iron Oxy-hydroxide", *Chemical Reviews, 98, 7*, 1998, 2549 – 2585.

Kershaw, M.G., and Pickering, R.W., "The Jarosite Process – Phase Equilibria", *Lead-Zinc-Tin '80, J.M. Cigan, T.S. Mackey and T.J. O'Keefe, Eds., The Metallurgical Society of AIMC, Warrendale, P.A.*, 1980, 565 – 580.

Lister, M.W. and Rivington, D.E., "Ferric Sulphate Complexes and Ternary Complexes with Thiocyanate Ions", *Can. J. Chem., 33*, 1955, 1591 – 1602.

Madsen, M.B., Mørup, S. and Koch, C.W.J., "Magnetic Properties of Ferrihydrite", *Hyperfine Int., 27*, 1986, 329.

Magini, M., "Solute Structuring in Aqueous Iron(III)-Sulphate Complexes", *J. Chem. Phys., 70, 1*, 1979, 317 – 324.

McAndrew, R.T., Wang, S.S. and Brown, W.R., "Precipitation of Iron Compounds from Sulphuric Acid Leach Solutions", *CIM Bull., 68, 753*, 1975, 101 – 110.

McCristal, T.G. and Manning, J., "Conversion of the Pasminco Hobart Smelter to para-goethite", *Zinc and Lead Processing, J. E. Dutrizac, J. A. Gonzales, G.L. Bolton and P. Hancock, Eds., The Metallurgical Society of CIM*, 1998, 439 – 453.

Meyer, E.H.O., Howard, G., Heagele, R. and Beck, R.D., "Iron Control and Removal at the Zinc Corporation of South Africa", *Proceedings of the Second International Symposium on Iron Control in Hydrometallurgy, Ottawa, 1996, J.E. Dutrizac and G.B. Harris, Eds., The Canadian Institute of Mining, Metallurgy and Petroleum, Canada*, 1996, 163 – 182.

Murad, E., "The Mössbauer spectrum of "well" crystallized ferrihydrite", *J. Magnetism Magnetic Mat., 74*, 1988, 53-157.

Onozaki, A., Sato, K. and Kuramochi, S., "Effect of some impurities on iron precipitation at the Iijima Zinc Refinery", *Proceedings of the First International Symposium on Iron Control in Hydrometallurgy, England 1986, J.E. Dutrizac and A.J. Monhemius, Eds., Ellis Horwood, England*, 1986, 742 - 752.

Pammenter, R.V., Kershaw, M.G. and Horsham, T.R., "The Low-contaminant Jarosite Process – Further developments and the implementation of the process", *Proceedings of the First International Symposium on Iron Control in Hydrometallurgy, England 1986, J.E. Dutrizac and A.J. Monhemius, Eds., Ellis Horwood, England*, 1986, 603 - 617.

Patent, 1964, Asturiana de Zinc S. A., *Spanish Patent No. 304,601*, Application lodged October 1964. Equivalent U.S. Patent No. 3,434,798 granted March 25, 1969.

Patent, 1965a, *Det Norske Zinkkompani A/S Norwegian Patent NO. 108,047*, Application lodged April 30, 1965. Equivalent U.S. Patent No. 3,434,947 granted March 25, 1969.

Patent, 1965b, *Electrolytic Zinc Company of Australasia Limited, Australian Patent No. 401,724*. Application lodged 31st March, 1965. Equivalent U.S. Patent No. 3,493,365 granted 3rd February, 1970.

Patent, 1966, "Procédé de préparation d'oxydes de fer hydraté", Belgian Patent, No. 676.970,24, February 1966.

Patent, 1970, Electrolytic Zinc Company of Australasia Limited, Australian Patent No. 424,095. Application lodged 15th May, 1970. Equivalent U.S. Patent No. 3,781,405 granted 25th December, 1973.

Patent, 1972, Societe de la Vieille Montagne, *Belgian Patent No. 724,214*. Application lodged November 20, 1968, Equivalent U.S. Patent No. 3,652,264, granted March 28, 1972.

Patent, 1976, Zinc Corporation of South Africa Limited, "Extraction of metals", *South African Patent Application No. 75/27/37*, April 1, 1976.

Patrizi, A., Persia, G. and Pescetelli, A., "The New Electrolytic Zinc Plant at Porto Vesme, Italy", *Zinc '85: International Symposium on Extractive Metallurgy of Zinc, Tokyo, 1985, K. Tozawa, Ed., The Mining and Metallurgical Institute of Japan, Tokyo*, 1985, 413 – 434.

Posnjak E., and Merwin, H.E., "The system Fe_2O_3 – SO_3 – H_2O", *Journal American Chemical Society, 44, 2*, 1922, 1965 – 1994.

Pourbaix, M., "Atlas of Electrochemical Equilibria in Aqueous Solutions", *2nd Edition, NACE International*, 1974, 644p

Queneau, P.B. and Berthold, C.E., "Silica in hydrometallurgy : an overview", *Canadian Metallurgical Quarterly, 25, 3*, 1986, 201-209.

Ramachandra Sarma, V.N., Deo, K. and Biswas, A.K., "Dissolution of zinc ferrite samples in acids", *Hydrometallurgy, 2*, 1976, 171 – 184.

Ritcey, G.M., "Iron-an overview of its control in the solvent extraction of metals", *Proceedings of the International Symposium on Iron Control in Hydrometallurgy, Toronto, October 19-22, 1986, J.E. Dutrizac and A.J.Monhemius, Eds., The Metallurgical Society of CIM/Ellis Horwood, 1986, 247-279.*

Schwertmann, U., Bigham, J.M. and Murad, E., "The first occurrence of Schwertmannite in a natural stream environment", *Eur. J. Mineral., 7*, 1995, 547-552.

Schwertmann, U. and Cornell R.M., *Iron Oxides in the Laboratory: Preparation and Characterisation, VCH Weinheim and VCH New York*, 1991, 137p.

Stevens, J.G., Khasanov, A.M., Miller, J.W., Pollak, H. & Li, *Z., Mossbauer Mineral Handbook, Mossbauer Effect Data Centre*, 1998.

Stumm. W, "Chemistry of the solid-water interface", *John Wiley & Sons, Inc., New York*, 1992, 428p.

Sylva, R.N., "The Hydrolysis of Iron(III)", *Pure Appl. Chem.*, *22*, 1972, 115 – 132.

Tainton, U.C. and Leyson, L.T., "Electrolytic zinc from complex ores", *Trans. AIME (LXX)*, 1924, 486 – 522.
Takala, H.,"Leaching of Zinc Concentrates at Outokumpu Kokkola Plant", *ERZMETALL, 52, 1*, 1999, 37-42.

Torfs, K.J., "The Union Miniere goethite process: plant practice and future prospects", *Proceedings of the Second International Symposium on Iron Control in Hydrometallurgy, Ottawa 1996, J.E. Dutrizac and G.B. Harris, Eds., The Canadian Institute of Mining, Metallurgy and Petroleum, Canada*, 1996, 135 – 146.

Tsunoda, S., Maeshiro, I., Ewi, M. and Sekine, K., "The construction and Operation of the Iijima Electrolytic Zinc Plant", *AIME T.M.S. Paper No. A73 – 65*, Chicago, 1973.

US Patent, *Patent No. 3,656,941*, Hydrometallurgical treatment of siliceous zinc ores, April 18, 1972, [Matthew et al].

US Patent, *Patent No. 3,954,937*, Process for the treatment of material containing zinc and silica for the recovering of zinc by hydrometallurgical way, May 4, 1976, [Bodson, F.J.J.].

US Patent, *Patent No. 4,148,862*, Hydrometallurgical treatment of soluble silicate-bearing zinc material, May 4, 1979, [Fugleberg et al].

Uusipaavalniemi, E., and Karlman, S.G., "Handling of iron at the zinc plant in Kokkola", *Proceedings of the Second International Symposium on Iron Control in Hydrometallurgy, Ottawa 1996, J.E. Dutrizac and G.B. Harris, Eds., The Canadian Institute of Mining, Metallurgy and Petroleum, Canada*, 1996, 101 – 115.

Varret, F., Gerard, A. and Imbert, P., "Magnetic Field Distribution Analysis of the Broadened Mössbauer Spectra of Zinc Ferrite", *Phys. Stat. (b), 43,* 1971, 723.

Van Niekerk, C.J., and Begley, C.C., "Zinc in South Africa", *J. S. Afr. Inst. Min. Metall., 91, 7*, Jul. 1991, 233 – 248.

Walter-Levy, L. and Quemeneur, E., "On the hydrolysis of ferric sulphate at 100°C", *C. R. Acad. Sc., Paris, 258*, 1964, 3028 – 3031.

Wang Qian-kun, Ma Rong-jun and Tan Zhi-zheng, "The Jarosite Process – Kinetic Study", *Zinc '85: International Symposium on Extractive Metallurgy of Zinc, Tokyo 1985, K. Tozawa, Ed., The Mining and Metallurgical Institute of Japan, Tokyo*, 1985, 675 – 690.

Yakovlev, Y.B., Kul'ba, F.Y., Pus'ko, A.G. and Gerchikova, M.N., "Hydrolysis of Iron(III) Sulphate in Zinc Sulphate Solutions at 25, 50 and 80°C", *Russ. J. Inorg. Chem., 22, 1*, 1977, 27 – 29.